Ex Vivo Protein Post Translational Modifications in Poorly Stored Blood Plasma and Serum and their use as Markers of Biospecimen Integrity

by

Joshua W. Jeffs

A Dissertation Presented in Partial Fulfillment
of the Requirements for the Degree
Doctor of Philosophy

Approved October 2018 by the
Graduate Supervisory Committee:

Chad R. Borges, Chair
Wade Van Horn
Peter Williams

ARIZONA STATE UNIVERSITY

December 2018

ABSTRACT

Exposure of blood plasma/serum (P/S) to thawed conditions, greater than -30°C, can produce biomolecular changes that misleadingly impact measurements of clinical markers within archived samples. Reported here is a low sample-volume, dilute-and-shoot, intact protein mass spectrometric assay of albumin proteoforms called "ΔS-Cys-Albumin" that quantifies cumulative exposure of archived P/S samples to thawed conditions. The assay uses the fact that S-cysteinylation (oxidation) of albumin in P/S increases to a maximum value when exposed to temperatures greater than -30°C. The multi-reaction rate law that governs this albumin S-cysteinylation formation in P/S was determined and was shown to predict the rate of formation of S-cysteinylated albumin in P/S samples—a step that enables back-calculation of the time at which unknown P/S specimens have been exposed to room temperature. To emphasize the capability of this assay, a blind challenge demonstrated the ability of ΔS-Cys-Albumin to detect exposure of individual and grouped P/S samples to unfavorable storage conditions. The assay was also capable of detecting an anomaly in a case study of nominally pristine serum samples collected under NIH-sponsorship, demonstrating that empirical evidence is required to guarantee accurate knowledge of archived P/S biospecimen storage history.

The *ex vivo* glycation of human serum albumin was also investigated showing that P/S samples stored above their freezing point leads to significant increases in glycated albumin. These increases were found to occur within hours at room temperature, and within days at -20 °C. These increases continued over a period of 1-2 weeks at room temperature and over 200 days at -20 °C, ultimately resulting in a doubling of glycated albumin in both healthy and diabetic patients. It was also shown that samples stored at

lower surface area-to-volume ratios or incubated under a nitrogen atmosphere experienced less rapid glucose adduction of albumin—suggesting a role for oxidative glycation in the *ex vivo* glycation of albumin.

DEDICATION

To my beautiful wife and the mother of our children, Brittany, who has been by my side through the ups and downs. Without her I would be lost, she is my beacon in the storm.

To my dad and mom, Ron and Terrie, who taught me that I can do anything through hard work and dedication.

To my family, whose love and support is always with me.

ACKNOWLEDGMENTS

I would like to express my sincere appreciation to my advisor, Dr. Chad R. Borges, for his extraordinary guidance and support during my graduate research and study career at Arizona State University. Without his mentorship and counsel, it would not have been possible to accomplish all that I have.

I would also like to thank my committee members, Dr. Wade Van Horn and Dr. Peter Williams for their guidance and helpful insights over the years and all the other Arizona State University professors and instructors that have helped along the way.

I thank the School of Molecular Sciences and the Biodesign Institute Center for Personalized Diagnostics at Arizona State University for providing the opportunity to work with a great group of scientists and state of the art facilities.

In addition, I would like to thank my current and former lab mates and friends, Shadi Ferdosi, Yueming Hu, Stephanie Thibert, Erandi Kapuruge, Jesus Aguilar, and Sally Jensen; as well as members of Biodesign Institute Center for Molecular Biomarkers, Olgica Trenchevska and Dobrin Nedelkov, for their valuable insights and counsel when facing problems in my research and studies, and for keeping me motivated through it all.

TABLE OF CONTENTS

Page

CHAPTER Page

CHAPTER Page

CHAPTER Page

LIST OF TABLES

LIST OF FIGURES

Figure Page

LIST OF ABBREVIATIONS

AFIP	Armed Forces Institute of Pathology
AlbSH	Native (Reduced) Albumin
Cys	Cysteine
Cys-Cys	Cystine
EDTA	Ethylenediaminetetraacetic Acid
ESI	Electrospray Ionization
GA	Glycated Albumin
GC	Gas Chromatography
HbA1c	Glycated Hemoglobin
HBS	HEPES Buffered Saline
HPLC	High Pressure Liquid Chromatography
IEC	Institutional Ethics Committee
IRB	Institutional Review Board
LC	Liquid Chromatography
Lys	Lysine
Met	Methionine
mRNA	Messenger RNA
MS	Mass Spectrometry
MSTFA	N-Methyl-N-Trimethylsilyl Trifluoroacetamide
MWCO	Molecular Weight Cut-Off
NCI	National Cancer Institute

NIH	National Institutes of Health
P/S	Plasma and Serum
pcT2D	Poorly-Controlled Type 2 Diabetic
PTMs	Post Translational Modifications
QA	Quality Assurance
QC	Quality Control
Q-TOF	Quadrupole Time of Flight
RMSD	Root Mean Squared Deviation
S-Cys-Alb	S-Cysteinylated (Oxidized) Albumin
SD	Standard Deviation
SOPs	Standard Operating Procedures
SPE	Solid Phase Extraction
TFA	Trifluoracetic Acid
WAG	Weighted Albumin Glycation
XIC	Extracted Ion Chromatograph

CHAPTER 1

INTRODUCTION

1.1 The biological function, and importance of proteins

Proteins are the macromolecules that accomplish most of the genetically instructed plans and tasks inside and outside of cells and tissues. Proteins vary in size from about 70 amino acids up to as large as ~30,000 amino acids. The primary sequence of amino acid residues enables specific functions of proteins through directing the folding of the native proteins into three-dimensional architectures. The sequence of the amino acid monomers found in proteins is encoded in the nucleotide triplet code of the DNA in every gene, this information is passed from DNA to protein through the messenger RNA pathway. The information pathway, DNA to RNA to protein, was discovered by molecular biologists in the 1960s (1, 2). This discovery showed how information stored in the stable DNA sequence of genes is transcribed into RNA molecules. RNA is then translated from nucleotide code to amino acid-based code in proteins, which are the major players that accomplish the functions of life.

Scientists have recently discovered that the human proteome is vastly more complex than the human genome. It is estimated that the human genome comprises between 20,000 and 25,000 genes, the total number of proteins in the human proteome is estimated at over 1 million. These estimations demonstrate that multiple proteins can be encoded by a single gene. Genomic recombination, transcription initiation at alternative promoters, differential transcription termination, and alternative splicing of the transcript

are mechanisms that generate different RNA transcripts from a single gene leading to the diversity of the proteome.

Proteins are polymers made up from 20 different standard (canonical) amino acids. Each amino acid consists of a carbon atom bonded to a carboxyl group (COO^-), an amino group (NH_3^+) and a distinctive side chain. The specific chemical properties of the different amino acid side chains determine the roles each amino acid will have in protein structure and function. The amino acids can be grouped into four broad categories according to the properties of their side chains (nonpolar, polar, basic, and acidic). The side chains of two amino acids, cysteine (Cys) and methionine (Met), are unique in that they contain sulfur atoms. Cys however contains a free sulfhydryl (SH) group, as will be discussed later, the sulfhydryl group of Cys plays an important role in protein structure because it allows the formation of disulfide bonds between the side chains of different Cys residues.

1.2 Post Translational Modifications of Proteins

The increase in complexity from the level of the genome to the proteome is further facilitated by protein post-translational modifications (PTMs). PTMs of proteins refers to the chemical change proteins may undergo after translation. PTMs play a key role in the proteome because they regulate activity, localization, and interaction with other cellular molecules such as proteins, nucleic acids, lipids and cofactors. Recent developments in mass-spectrometry (MS) methods have enabled the identification of thousands of PTM sites. Hundreds of diverse types of PTMs are currently known (3, 4).

Most, if not all, proteins are modified extensively after their synthesis by specific cuts, proteolytic cleavages in the peptide chain, chemical modification of certain amino

acid residues, or by the addition of one or more non-amino acid prosthetic groups, such as sugar, lipid or phosphate residues. PTMs are important to the overall structure-function characteristics of proteins and extend the range of functions of the protein either by attaching biochemical functional groups (e.g., phosphate, acetate, or carbohydrates) or by making structural changes, such as protein oxidation (e.g., formation of disulfide bridges, sulfoxides) to the amino acids present in the protein (5-9). These modifications, in turn, effect the overall functional properties of proteins (10, 11).

PTMs come in a wide variety of types and are mostly catalyzed by enzymes that recognize specific target sequences in specific proteins. The most common modifications are the specific cleavage of precursor proteins; formation of disulfide bonds; or covalent addition or removal of low-molecular-weight groups, thus leading to modifications such as acetylation, amidation, biotinylation, cysteinylation, deamidation, glutathionylation, glycation (nonenzymatic conjugation with carbohydrates), glycosylation (enzymatic conjugation with carbohydrates), hydroxylation, methylation, oxidation, phosphorylation, or sulfation.

PTMs play a fundamental role in regulating the folding of proteins, their targeting to specific subcellular compartments, their interaction with ligands or other proteins, and their functional state, such as catalytic activity in the case of enzymes or the signaling function of proteins involved in signal transduction pathways. Some PTMs (e.g., phosphorylation) are readily reversible by the action of specific deconjugating enzymes. The relationship between modifying and demodifying enzymes allows for rapid and economical control of protein function. A similar control by protein degradation and de novo synthesis would take much longer time and cost much more bioenergy.

As mentioned earlier PTMs are typically mediated by enzymes, but there are several reported cases of protein modifications thought to occur via spontaneous chemical reactions. Although the regulation of enzymatic modifications is quite distinct from that of non-enzymatic modifications, the two processes are not mutually exclusive and, in some instances, can occur in parallel, as in the case of lysine (Lys) acetylation (12). Non-enzymatic PTMs can be viewed as the result of a reaction between a reactive metabolite and a nucleophilic or redox-sensitive amino acid side chain. The oxidation of Cys to sulfenic acid by hydrogen peroxide provides an example of this type of reaction. Variations in the concentration of hydrogen peroxide can be sensed by distinct Cys residues that are reactive toward this oxidant and located at an accessible site. A subsequent change in the redox environment can result in reduction of sulfenic acid moieties by antioxidants such as glutathione, and regeneration of free Cys (13).

A protein of interest is the multifunctional plasma protein, human serum albumin, which is the most abundant plasma protein (about 60% of total protein content). It is a medium globular protein of 66k Da that accounts for both antioxidant functions, such as reactive oxygen species (ROS) scavenging, extracellular redox balance, and transport functions for many molecules. Among its 585 amino acids it contains 35 Cys residues, 34 of which form structural disulfide bonds, leaving one free Cys (Cys34) that is prone to oxidation through disulfide-bond formation via exchange with free cystine (Cys-Cys) and oxidation of free Cys from the blood, resulting in S-cysteinylated (oxidized) albumin (S-Cys-Alb)—both *in vivo* and *ex vivo* (14). Cys34 accounts for over 80% of the total free thiols (R-SH) in plasma and 70-90% of circulating albumin contains Cys34 in the reduced state (15), which is highly susceptible to oxidative PTM.

1.2.1 Cysteine Oxidation

Oxidative PTM of Cys residues is an important mechanism that regulates protein structure and ultimately function. The unique properties of a Cys side chain permit a variety of oxidative PTMs, which potentially result in diverse regulatory effects (16). The side chain of a Cys residue contains a terminal thiol (R-SH) functional group. The sulfur atom at the core of the thiol is electron rich and its d-orbitals allow for multiple oxidation states (17, 18), which influences the formation of a varied range of oxidative PTMs. Thiol oxidation is among the most ubiquitous reactions in biology, playing key roles in protein folding, redox homeostasis, signal transduction, and the regulation of gene expression (19).

Thiol oxidation leads to the formation of various reversible and irreversible products. Among the products of Cys oxidation, sulfenic acids and disulfides are of interest given the roles that they play in redox cycling and/or regulation of enzymes and transcription factors involved in cell signaling processes. One basic chemical reaction that is well understood is the oxidation of Cys to Cys-Cys. This oxidation occurs through a simple disulfide exchange (inter- or intra-molecular) mechanism or through a disulfide formation mechanism where, in the presence of oxygen and trace metals, two thiols can form a disulfide bond (13, 20). There are multiple routes in which Cys thiols can form disulfides as seen in Fig. 1.1. The simplest method is through a disulfide-based exchange forming intramolecular and intermolecular disulfides. However, free thiols (R-SH) can form thiolates ($R\text{-}S^-$) through simple acid-base chemistry which can then either be oxidized by hydroperoxides in a two-electron oxidation process that yields sulfenic acid (R-S-OH) or a one-electron process that forms thiyl radicals ($R\text{-}S^\bullet$) through the reaction

of thiols with enzymes such as ribonucleotide reductase (21). Sulfenic acid can either react with free thiols to form disulfides or be further oxidized to sulfinic/sulfonic acids. The thiyl radicals can react directly with free thiols to form disulfides or react with molecular oxygen/superoxide to yield sulfinic acid. Ultimately, this process leads to the oxidation of susceptible proteins such as albumin.

1.2.2 Protein Glycation

Human serum albumin can also be glycated *in vivo* and *ex vivo*. Glycation is a non-enzymatic process in which proteins react with reducing sugar molecules and may change the characteristics of the proteins. The reaction occurs between the α amino group of the N-terminal amino acid or the ε amino groups of Lys and the aldehyde or keto group of the reducing sugar (22). Sugars (e.g., glucose) can react with amino groups directly leading to protein glycation. However, sugars may also go through an autoxidative type reaction that makes the sugar molecule more reactive toward protein amino groups, which ultimately promotes excess protein glycation (23). The first step in this autoxidative type reaction is the formation of an unstable Schiff base, which rearranges to form a more stable Amadori product. The Amadori product can then react further to form irreversible cross-linked products called advanced glycation end products (AGEs) (Fig. 1.2).

1.3 The Effects of *Ex Vivo* Protein modifications

It has been previously shown that protein modifications (e.g., oxidation and glycation) occur *ex vivo* in blood plasma and serum (P/S) under common but suboptimal storage/handling conditions, which can potentially lead to false conclusions regarding physiological oxidative stress in clinical research (14, 24-26).

When plasma or serum (P/S) is exposed to air, the dissolved oxygen concentration [$O_2(aq)$] can increase up to approximately 0.25 mM (27, 28)—an $O_2(aq)$ concentration that is much higher than that found in the P/S compartment of blood *in vivo*, this initiates the process of certain oxidative PTMs. Within proteins, such oxidative insults typically occur at the sulfur atoms of Cys and Met residues. Oxidative alteration of these amino acids changes the biochemical properties of affected proteins in a manner like amino acid substitution. This process may quite literally be considered unnatural amino acid substitution. Viewed in this manner, it is not surprising that even a minor alteration, such as oxidation of Met into Met sulfoxide, is an established means by which protein-protein binding interactions may be disrupted. Reviewing some of the literature available on this topic reveals that Met oxidation has been documented to disrupt a large variety of biomolecular interactions including Met oxidized (MetOx) antibody binding to protein A/G and Fc receptors (29-31), MetOx calmodulin binding to its receptor (32, 33), the activity of MetOx parathyroid hormone (34-37), MetOx antigenic peptide binding to the MHC and subsequent recognition by the T cell receptor (38), the binding of a MetOx C-type natriuretic peptide analog to its receptor (39), and the binding of the MetOx prion protein (PrP) to antibodies against its Helix-3 region (40).

When looking at how this could possibly affect the outcome of clinical research. Gaza-Bulseco et al. showed that when the methionine on a monoclonal antibody is oxidized, there is a decrease in the binding affinity between the antibody and the protein of interest. The study used ELISA and surface plasmon resonance, both of which rely on protein interaction, to show that the binding affinity between antibody and protein is disrupted by methionine oxidation. This oxidation-induced decrease in the binding

affinity led to a lower apparent abundance of the protein, ultimately resulting in an apparent quantitative loss of the protein being measured (29). Thus, it is evident that protein oxidation in improperly handled clinical samples should not be dismissed as an unimportant event that has no possible bearing on the outcome of clinical assays that rely on protein interactions.

1.4 Storage and Handling of Plasma and Serum Samples

There are many clinically important P/S biomolecules used as biomarkers that are unstable *ex vivo*, and susceptible to *ex vivo* modifications (13, 41-44). *Ex vivo* storage and handling conditions have the potential to impact measurements of these molecules as much or more than the *in vivo* conditions of interest (13, 32, 45, 46). Many biological samples, especially those used for long term research or archived for future research, are stored in freezers raising the question, "Have these samples been stored properly to give a correct assessment for a particular study?"

There are many reasons in why researchers are interested in storing samples for long period of times, one of the main reasons is that samples are extremely valuable, both financially and scientifically. The cost, financially, that goes into the process of collecting samples is expensive, which leads primary investigators into wanting to get as much in return as they can out of their samples. One way in which they can recoup some of the initial cost of collecting samples is to sell the samples to other secondary investigators or receive grant subcontracts from other investigators. When this is done, not only does this help the primary investigator financially, but it also helps the entire scientific community by being able to address a separate scientific question beyond the ones of the primary study. This is a good thing but can create problems when the integrity of the samples

comes into question. Comprehensive and well-maintained biobanks are becoming prevalent to help mitigate some of these concerns.

1.4.1 Biobanking

Biobanks are repositories that assemble, store, and manage collections of human specimens and related data. Biobanks are one of the major sources used when investigators procure stored or archived samples. One of the first biobanks in the United States was the Armed Forces Institute of Pathology (AFIP). The AFIP was established in 1862 as the Army Medical Museum and later evolved, over the span of a century, into a joint military-civilian organization. The AFIP has procured and developed, over the last 150 years, a repository of samples from over 3 million clinical cases, 10 million tissue specimens, and 50 million paraffin blocks that cover the entire spectrum of human and animal disease (47). Currently there are more than 160 biobank repositories in the United States and many more throughout the world, all of which contain millions of stored samples (48).

Biobanks have been around for many years in some form or another. However, recently there has been increased attention on the way that researchers and organizations manage them and the way in which samples are being stored. This increased attention has led to an increase in the number of biobanks (59% have been established since 2001) and in effect, the number of samples that are being stored has increased as well (49-51). Biobanks are useful in that studies don't need comprehensive Institutional Review Board (IRB) or Institutional Ethics Committees (IEC) approvals for the use of biobanked samples, due to the fact this was performed during sample collection.

Academic and epidemiological research forms an important foundation of the need for biobanks. Biobanking facilities can range from large global-scale repositories for collaborative research to smaller stores employed by service industries, academic departments and pharmaceutical companies (52). There are also various purposes of biobanks, such as diagnostic, therapeutic, or research which all have different standard operating protocols (SOPs), meaning not all samples are stored the same way. Thus, the decision on what type, processing protocol, and volume of biospecimens to include in a biobank for specific purposes may affect all other downstream analyses and logistical processes.

Biobanks in the United States have on average around 500,000 specimens stored at any given time, biobanks can range from very small (less than 100 specimens) to very large (more than 50 million) (49). Henderson et al. reports that around 75% of biobanks receive their specimens from direct contributions by individual donations, 57% of biobanks receive residual specimens that were previously acquired from hospitals and other clinical settings and 13% of biobanks receive specimens from research studies. Approximately, 76% of biobanks receive specimens that come primarily from individuals with some type of disease and approximately, 77% of biobanks store serum or plasma (49). With so many different samples being collected and the logistics that go into storage and handling, investigators need to be aware that sample integrity may be a major concern when it comes time to distribute these samples for future clinical research.

1.4.2 Plasma and Serum Integrity of Stored/Archived Samples

Blood P/S proteins are not intrinsically stable. For example, pre-analytical sample handling and storage conditions can dramatically impact proteolytic enzyme activity and subsequent protein concentration measurements, potentially rendering assay results invalid. While acceptable pre-analytical handling and storage conditions are generally well defined for FDA-approved clinical protein assays, they cannot always be optimally pre-defined for clinical research studies where samples are to be archived indefinitely for future research. This creates a need for quality control tools (e.g., markers and assays) that allow for retrospective assessment of sample integrity (45, 46). Such tools are becoming more important as the practice of biobanking continues to rise worldwide.

The varying quality of the existing biospecimens in biobanks has been identified as one of the major concerns inhibiting scientific progress (53-55). Oftentimes sample integrity is overlooked, to expand this point further, there are currently no universally accepted reference markers of biospecimen integrity. Identifying and standardizing quality control (QC) markers that are easy to monitor, represents an important objective of biobanking related research. This has created an urgent and growing demand to minimize *ex vivo* changes to P/S samples and to accurately identify those changes when they do occur (45). Most markers currently proposed for retrospective analysis of P/S specimen integrity are based on an apparent quantitative loss (or ‘paradoxical’ increase) in a particular target molecule without consideration of the molecular root cause (45).

Preanalytical variables can introduce modifications, either systematically or randomly, that adversely affect results. When the result of a test deviates from that which is expected, the analytical integrity of the results is often questioned rather than the

preanalytical integrity of the samples. Ultimately, the test analysis can be perfect, but still the result could be inaccurate. Most errors in a clinical chemistry laboratory are due to preanalytical errors which can account for 32%-75% of laboratory errors (56-58). These errors can have a significant impact on laboratory results and it is imperative that laboratory personnel are able to spot these erroneous results, rather than falsely attributing them to an underlying medical cause. When these preanalytical errors are not accounted for in the clinical research settings it is not the patients that are impacted, but rather the scientific community. These errors mislead researchers into pursuing research based on incorrect results that have been published in the literature.

Preanalytical variables can be grouped into three categories: sample collection, sample processing, and sample storage and handling. In both clinical and research settings, blood collection has the advantage of being minimally invasive. However, in clinical settings specimens are often quickly analyzed, whereas in research settings these samples can be stored anywhere from hours to months, possibly years, before they are analyzed, making sample collection protocols important to ensuring sample processing can be expedited and samples stored properly (59). As an example, there is an increased risk of hemolysis in P/S samples associated with the amount of time a tourniquet is in place (60), in other words, red blood cell lysis will introduce components into the P/S sample that are not representative of the *in vivo* condition, which may interfere with downstream analytical conclusions. Another factor to take into consideration during sample collection are the type of collection tubes. Each tube must be filled in a specific order to prevent cross contamination of blood additives within the collection tubes (61). One must also worry about how old the collection tubes are. The vacuum contained

within the tube determines how much blood will be collected to fill the tube completely. The closer to the expiration date, the weaker the vacuum may be within the tube, causing the tubes to not be fully filled. This may reduce the reproducibility of downstream analysis.

After collection, the manner in which specimens are processed plays a critical role in the quality of samples obtained. Centrifugation speeds, duration and temperature can affect the quality of the sample as speeds that are too fast, too long or not at the correct temperature will damage cell components, introducing an environment that may not represent the actual *in vivo* conditions, reducing the reliability and reproducibility of results between samples. Not only will the process of centrifugation affect the quality of samples, but also the time, or delay, for samples to be centrifuged. A delay in the separation of plasma and serum from whole blood has been shown to decrease the consistency of analytes, such as cytokines (62), even a delay in centrifugation as short as 4 hours when samples are stored at 4 °C has an apparent effect on the concentration of different analytes that are found in plasma and serum (63).

Laboratory staff are trained to pick up obvious problems in samples such as hemolysis or abnormal coagulation, but what about the problems that aren't obvious or even visible? To illustrate this point, consider a cut apple that is left out on the table, there is an oxidation reaction that occurs and causes the apple to turn brown. However, if a P/S sample is left out there is no visible change, but it would be naïve to think that similar oxidative processes occurring in the apple would not occur in a P/S sample, the only difference being there is no visual change that will inform the analyst the sample has been mistreated.

SOP's are in place to maximize reproducibility (decrease the amount of error) in biospecimen collection and processing. However, the preanalytical variable of storage and handling remains as the main source of error in clinical research carried out on P/S samples. After sample collection and processing, the way in which samples are stored and handled has a dramatic effect on the outcome of analysis. This is seen in multiple unstable analytes that are of clinical interest in P/S (64-67).

There are many ways in which samples can be stored after collection and processing; the best way is to have the P/S samples directly placed in a -80 °C freezer. However, not all collection sites may have a -80 °C freezer available for storage of samples leading to samples being stored at -20 °C or 4 °C for a short time. Whether it is overnight or for a couple days, the concern that the first collected sample may not be as "fresh" as the last sample collected becomes a valid question to contemplate. Another handling condition to consider is the transport of samples, whether it is going from across the hall or across the country, samples need to stay frozen. Samples are typically shipped with dry ice to keep them frozen, but delays (e.g., rerouted or canceled flights, delays in delivery) could possibly lead to samples thawing partially or completely. These are conditions that are sometimes uncontrollable and are not always documented.

Many preliminary studies have suggested that PTMs of albumin (e.g., oxidation and glycation) are promising markers to evaluate the progression of oxidative stress-related diseases, (68-70), though no definitive marker has been established. An example on how these suggested PTMs might be misrepresented is to look at the properties of stored albumin. A recent study has shown that albumin that is not completely frozen will have an increase in the amount of oxidation present (14). Consider a group of samples

where half of the samples were stored properly, and the other half were delayed in transport allowing them to partially thaw. If these studies, that suggest the use of albumin PTMs as markers of oxidative stress, were to use the group of samples just described, they may unknowingly attribute the increase in albumin oxidation/glycation to an oxidative stress-related disease, even though the increase comes from the preanalytical variable of storage and handling. In conclusion, suboptimal storage and handling conditions can potentially lead to false conclusions regarding physiological oxidative stress (14). Preanalytical variables, albeit seemingly minor, can impact the success of an assay or study.

As mentioned, S-Cys-Alb has been previously identified as a protein-representative oxidative molecular modification that results from poor sample storage and handling (14). To utilize this known oxidation as a biospecimen integrity marker, a simple, low sample consumption, high-throughput method that *directly* measures the molecular modification has been developed (14). The goal of this research is to develop a model that will allow for subsequent prediction of the rate and extent to which oxidative S-Cys-Alb occurs *ex vivo*, when samples are exposed to thawed conditions (e.g., temperatures > -30 °C). Then using this information, develop an assay to measure the integrity of long-term stored P/S samples rapidly and efficiently.

P/S samples that are not stored properly may have many modifications occur *ex vivo* that will change or alter the results of research studies (45). As has been shown previously and will be shown further in this work, protein PTMs (e.g., oxidation and glycation) may affect the quality and outcome of stored samples, leading to false or misleading results in clinical research studies. It is imperative that the samples collected

and stored today are suitable for the future. The work described below will help ensure that future researchers can have confidence in the quality of their plasma and serum samples and ultimately, the quality of their research.

Figures

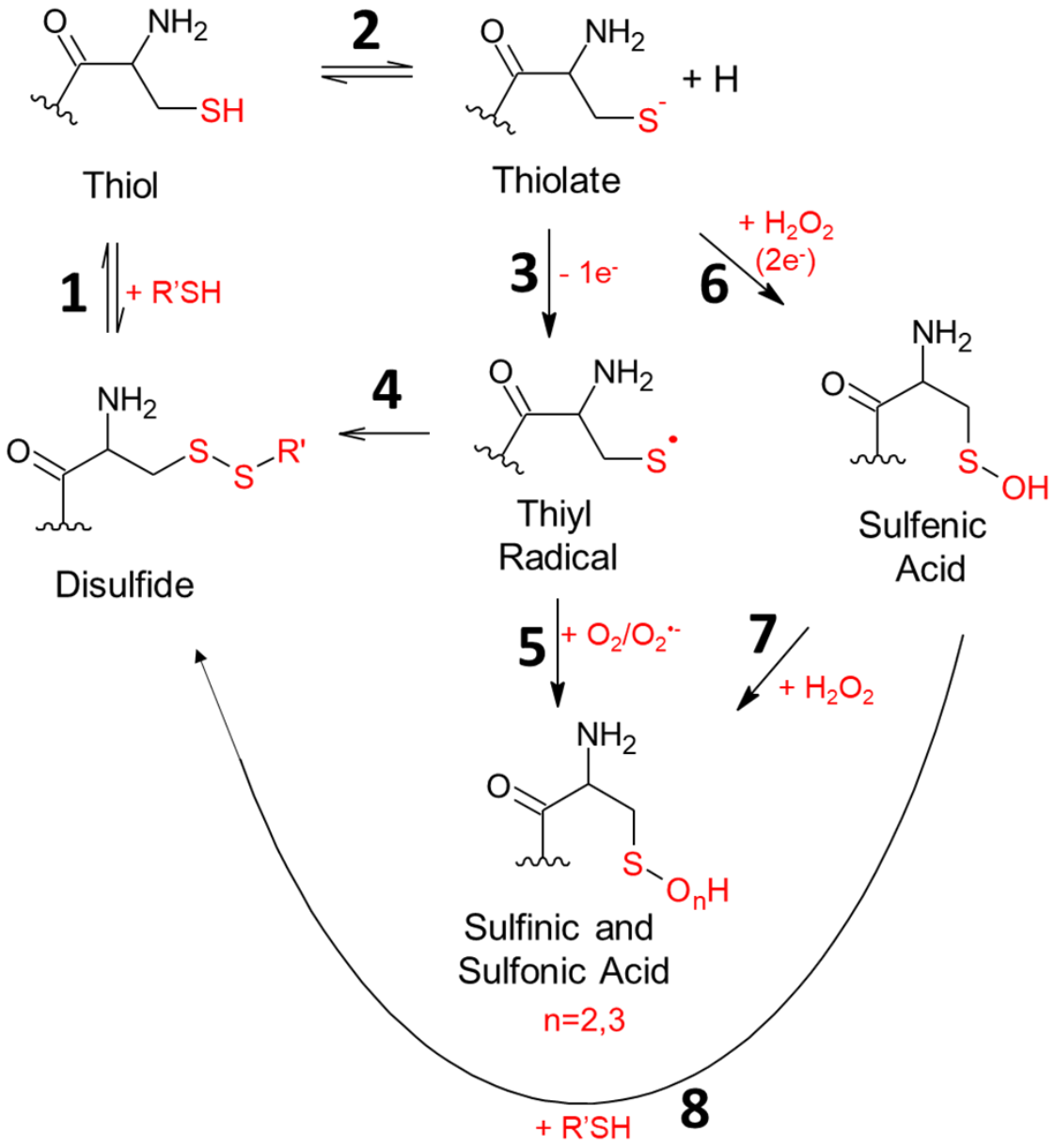

Figure 1.1. Thiol/Disulfide Redox Reaction Pathway. Thiol-disulfide exchange (1). Thiol acid-base behavior (2). One-electron oxidation of thiolates to thiyl radicals (3). Thiyl radicals can react with molecular oxygen/superoxide or other thiols, yielding sulfinic acid and disulfides as final products (4 and 5). Thiolates can react through a two-electron oxidation process yielding sulfenic acid (6). Sulfenic acid can be further oxidized to sulfinic and sulfonic acids (7). Inter- and intramolecular disulfides are formed from the reaction of sulfenic acid with other thiols (8).

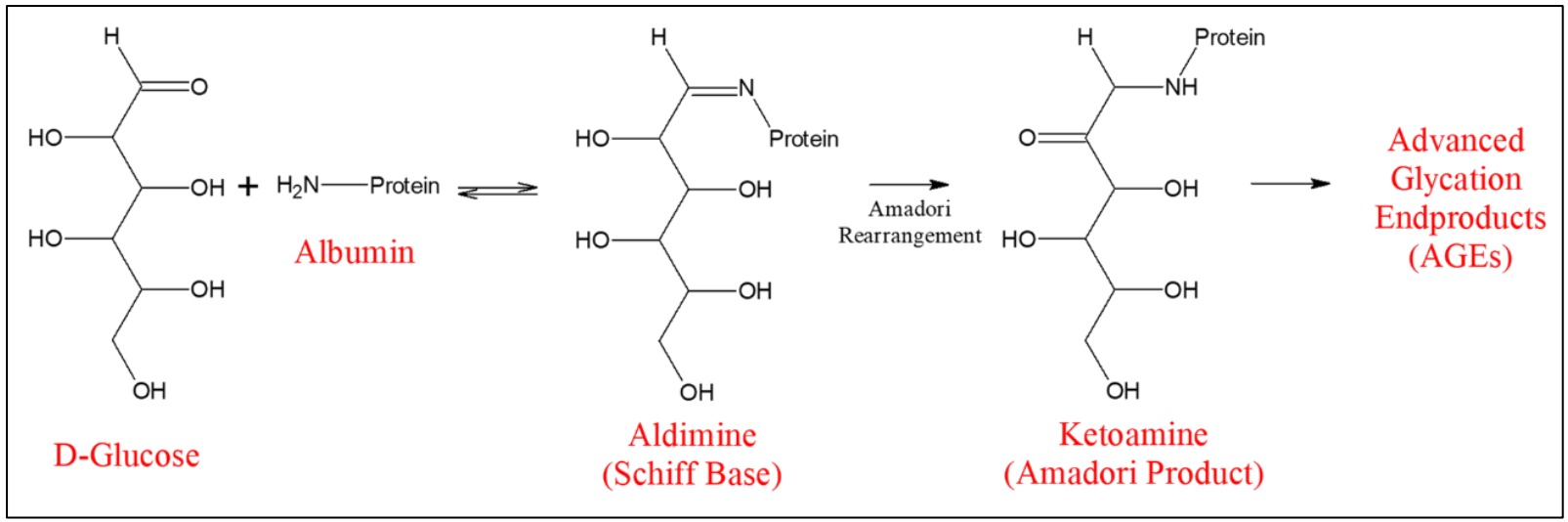

Figure 1.2. Reaction scheme for the formation of glycated albumin. The non-enzymatic reaction between glucose and albumin starts with formation of a Schiff base. This is followed by an intramolecular rearrangement that leads to an Amadori product, which can ultimately lead to advanced glycation end products (AGEs).

CHAPTER 2

KINETIC RATE MODEL OF *EX VIVO* S-CYSTEINYLATION (OXIDATION) OF HUMAN SERUM ALBUMIN

2.1 Introduction

The rate of reaction is important to predict how quickly a reaction mixture approaches equilibrium and helps lead to an understanding of the mechanisms behind the reaction. Reactions can be broken down into a sequence of elementary steps and then analyzed to determine the rates of each of these steps. Such studies lead to an empirical rate law that relates the reaction rate to the concentrations of reactants, products, and intermediates at any point in time.

When it is possible to measure the reaction that is occurring, there are two methods in which to determine the rate law, either by the isolation method or the method of initial rates. The isolation method uses the concept of increasing, in excess, all the reactants present in the reaction except for one, in this case all reactants except for the one being measured can be considered constant. This will produce the appearance of a first-order rate law, or in other words a pseudo first-order rate law, which is much easier to analyze and identify the rate law regarding the one reactant not in excess. The dependence of the rate on the concentration of each of the reactants may be found by isolating them in turn (by having all the other reactants present in large excess), and so constructing a picture of the overall rate law.

In the method of initial rates, the initial rate is measured at the beginning of the reaction for several different initial concentrations of each reactant. For a series of initial concentrations, a plot of the logarithms of the initial rates against the logarithms of the

initial concentrations of the reactant should produce a straight line, with the slope of the line equal to the order of reaction. The rate constants for the given rate law can then be determined by using non-linear regression, using all initial rates and concentrations of the reactants in the calculation. Once the rate constants and the order of reaction have been determined the overall rate law can then be solved by integrating the reaction equations, using differential equations, that will give the concentration as a function of time. An advantage of using the method of initial rates compared to the isolation method is it does not require the assumption that a pseudo first order reaction has been achieved.

Recent studies have shown that under thawed conditions albumin oxidation in P/S samples increases in a regular pattern (14). When considering the reactions that govern this albumin oxidation, shown in Reactions 1 and 2, a simple disulfide exchange mechanism is observed, where AlbSH is the native reduced form of albumin, Cys-Cys is cystine, SCysAlb is S-cysteinylated albumin, and Cys is cysteine. With the determination of these reactions it is possible to use the method of initial rates to determine the rate constants and order of reaction for the oxidation and reduction of albumin, and ultimately determine the overall rate law of the reaction. With the determination of the overall rate law a predictive kinetic rate model for albumin oxidation can be established.

$$AlbSH + Cys\text{-}Cys \underset{k_2}{\overset{k_1}{\rightleftharpoons}} SCysAlb + Cys \quad (1)$$

$$2Cys + O_2 \xrightarrow[k_3]{Cu(II)} Cys\text{-}Cys + H_2O_2 \quad (2)$$

An established rate law of this reaction would allow the measurement of albumin oxidation at any given time to be linked to the amount of time a P/S sample has spent at

room temperature like conditions. This would represent an unprecedented achievement in biospecimen science and would lay the groundwork for linking any clinical biomarker of interest to albumin oxidation without necessarily having to measure the two markers simultaneously in the same sample.

Shown here is the use of the method of initial rates combined with intact protein mass spectrometry to determine the kinetic rate law for the *ex vivo* oxidation of human serum albumin at room temperature. The determination of this rate law makes it possible to model and predict the *ex vivo* oxidation of human serum albumin and facilitates its use as a predictive marker in clinical biospecimen integrity.

2.2 Materials and Methods

2.2.1 Materials and Reagents

Highly purified human serum albumin (Cat. No. A3782), L-cysteine (C7352), trifluoroacetic acid (TFA, 299537), L-Cystine (30200), L-Cystine dihydrochloride (C2526), L-Cysteine-2,3,3,-D3 (701424), Amicon Ultra-4 centrifugal filter, MWCO = 50 kDa (Z740191), ammonium hydroxide (320145), ammonium bicarbonate (A6141), sodium sulfate (S9627), deferoxamine mesylate salt (D9533), HEPES (H3375) and NaCl (S7653) for preparation of HEPES-buffered saline solution (HBS buffer) were purchased from Sigma-Aldrich (St. Louis, MO). LC-MS grade Acetonitrile (TS-51101), LC-MS grade water (TS-51140), hydrochloric acid (50-878-166), Pierce BCA protein assay kit (23227), and methanol (A456) were purchased from ThermoFisher Scientific (Waltham, MA). Chelex 100 resin (1421253) was purchased from Bio-Rad Laboratories (Hercules, CA). SPE cartridges (SPE-P0005-03BB) purchased from Silicycle (Quebec, Canada). L-Cystine-3,3,3’,3’-D4 (DLM-9812-PK) was purchased from Cambridge Isotope

Laboratories, Inc. (Andover, MA). N-Methyl-N-Trimethylsilyl Trifluoroacetamide (MSTFA) (24589-78-4) was purchased from Regis Technologies (Morten Grove, IL). All non-LC-MS solvents were of HPLC grade.

Section 2.2.2 Plasma and Serum Samples

Fasting EDTA plasma and serum samples were collected from healthy volunteers, via venipuncture, under IRB approval at Arizona State University. The samples were collected according to the National Institute of Health's (NIH) Early Detection Research Network blood collection SOPs (71, 72). Within 35 minutes of collection, plasma samples were processed, aliquoted, and placed in -80 °C freezer; serum samples were placed at -80 °C within 95 minutes of collection. One or more of these P/S specimens were used for all experiments described below. Unless otherwise noted, aliquot volumes were 50 μL.

2.2.3 Quantitative Model Development

The rate law for formation of S-cysteinylated or oxidized albumin (S-Cys-Alb) in the P/S environment is governed by the chemical reactions listed in Reactions 1 and 2. The rate law for Reaction 2 has been previously determined by Kachur et al. (20). Thus in order to obtain a complete combined rate law for formation of S-Cys-Alb, the rate laws for the forward and reverse reactions described in Reaction 1 were determined using the method of initial rates (73). Briefly, this approach entailed measuring the initial rate of the forward (and, separately, reverse) reaction by plotting S-Cys-Alb (or the reduced form of albumin (AlbSH)) concentration in molar units (M) vs. time (s). The initial phase of these plots was linear. From this initial linear phase, the slope was obtained and

recorded as the initial rate (v_o). This process was repeated for multiple starting concentrations of reactants in which none of the products were initially present.

This latter requirement made it necessary to create and isolate AlbSH in which no S-Cys-Alb was present and, for the reverse reaction, S-Cys-Alb in which essentially no AlbSH was present. Pure AlbSH was prepared starting with a 1 mM concentration of commercially prepared albumin in HBS buffer (pH 7.4). The sample was aliquoted into 500 µL volumes and mixed with 300 µL of 10 mM Cys, followed by incubation for 1 hour at room temperature. After the incubation period, 1 µL of sample was diluted in 600 µL of 0.1% TFA and analyzed to verify complete reduction of albumin. The aliquots were then split into 200 µL aliquots in Amicon Ultra-4 centrifugal spin filters (MWCO 50K). Each sample had 4 mL of HBS buffer added and then was centrifuged for 10 minutes at 4,000 x g to a final volume of approximately 200 µL, this process was repeated 7 times, facilitating Cys removal and protein concentration. All aliqouts were then combined and albumin concentration was determined with a BCA protein assay, following the manufacturer's protocol. To verify that no structural disulfide bonds were reduced and only the free Cys residue (Cys34) was reduced, 5 µL of AlbSH was incubated with 5 µL of 50 mM maleimide in ammonium acetate buffer (pH 5). This was incubated at 50 °C for 15 minutes and then 1 µL of sample was mixed with 500 µL of 0.1% TFA and analyzed by LCMS (Fig. 2.1). Pure S-Cys-Alb was obtained by following the same protocol but instead incubating 0.5 mM commercially prepared albumin with 1 mM Cys-Cys. All samples were stored at -80 °C until further analysis.

To eliminate interference from Reaction 2 during the rate law determinations, trace quantities of copper and other transition metals were minimized by pre-treating all

buffers with Chelex 100 resin per the manufacturer's batch-wise instructions. Desferrioxamine (0.2 mM) was also added to the buffers employed in rate law determinations. To determine initial rates, pure AlbSH at concentrations ranging from 30-60 µM or pure S-Cys-Alb (30-90 µM) were incubated with free Cys-Cys or Cys (300-900 µM) at 23 °C, respectively (Tables 2.1 and 2.2). A control sample with no added Cys-Cys or Cys was also prepared to ensure that no artifactual oxidation or reduction occurred. Time courses for albumin oxidation and reduction were acquired by diluting 0.5 µL of a sample into 0.1% TFA to a final concentration of 1 µM albumin at various time points, which was then analyzed by LC-MS to provide time point concentrations of S-Cys-Alb and AlbSH. Time points were taken more frequently during the initial linear portion which yielded a slope that was used to determine the initial rate of reaction for each of the varying concentrations (Tables 2.1 and 2.2). The method of initial rates was then used to determine the reaction orders and rate constants for the disulfide-exchange oxidation and reduction of albumin (73). Slopes of log v_o vs. log reactant concentration (at several concentrations of the second reactant) were used to determine reaction orders and non-linear regression of the entire forward-reaction dataset and reverse reaction dataset was employed to determine the forward and reverse rate constants, respectively.

2.2.4 Quantitative Model Verification

Immediately following collection, matched serum and K_2EDTA plasma from a healthy donor were each split into two 95-µL portions: One portion was spiked with Cys and Cys-Cys (in 5 µL of HBS buffer, pH 7.4) to increase the concentration of Cys by 12 µM and the concentration of Cys-Cys by 62 µM; the second portion was diluted by the same amount of buffer but without added Cys or Cys-Cys. These specimens were then

incubated at 23 °C for 4 days, with numerous measurements of S-Cys-Alb collected initially and then at least once a day after Day 1. The data were then fit with the predictive model (using Wolfram Mathematica 10.2 or MatLab 2016), using the empirically determined initial concentrations of all species, determined as follows.

2.2.4.1 Measurement of Initial Reactant/Product Concentrations

Fresh aliquots of matched P/S samples were sent to ARUP Laboratories to determine concentrations of albumin (total), free copper and total copper. Initial fractions of S-Cys-Alb and AlbSH were determined using the S-Cys-Alb assay described above. These fractions were then converted to actual concentrations by multiplying by the total albumin concentration.

Cys-Cys concentration was determined from quadruplicate aliquots of serum and, separately, plasma using solid phase extraction (SPE) and gas chromatography-mass spectrometry (GC-MS) using procedures adapted from (74-76). Calibration curve samples were prepared in 40 mg/ml albumin in HBS buffer (pH 7.4) with the addition of 0, 15, 30, 45, 60, or 90 µM of Cys-Cys. Three microliters of 2 mM Cys-Cys-d_4 internal standard in 1 M ammonium hydroxide and 1 M ammonium bicarbonate (pH 9.4) were combined with 96.5 µL of P/S and calibration curve samples, followed by 0.5 µL of 1 mM Cys-d_3 internal standard in 1 M ammonium hydroxide and 1 M ammonium bicarbonate (pH 9.4). Proteins were then immediately precipitated by first adding 200 µL of acetonitrile and then 200 µL of 0.2 M HCl which lowered the sample pH, minimizing disulfide exchange reactions. Samples were incubated on ice for 30 minutes and then centrifuged for 2 minutes at 13,000xg to remove protein precipitate. Sample supernatant was then stored on ice until ready for cation exchange SPE. The SPE cartridges were

conditioned with 2 mL acetonitrile and then equilibrated with 2 mL of 0.1 M HCl. The entire sample was then loaded onto the cartridge and washed with 2 mL methanol. Samples were then eluted with 2 mL of 5% ammonium hydroxide in methanol into silanized glass test tubes and then dried using a Savant SC250EXP SpeedVac Concentrator. After samples were dry, 50 µL of acetonitrile and 50 µL of N-methyl-N-(trimethylsilyl)trifluoroacetamide (MSTFA) were added and then incubated for 30 minutes at 85 °C. Samples were then loaded into GC-MS autosampler vials and injected onto the GC-MS.

2.2.4.2 GC-MS

GC-MS analysis was carried out on an Agilent Model A7890 gas chromatograph (equipped with a CTC PAL autosampler) coupled to a Waters GCT (time-of-flight) mass spectrometer. One microliter of the sample was injected in split mode onto an Agilent split-mode liner that contained a small plug of silanized glass wool. The injector temperature was set at 280 °C and the split ratio was 5:1. The carrier gas was regulated in constant flow mode at 0.8 mL/min. The capillary column was a 30-m fused silica DB-5MS with a 0.25 µM film thickness and 0.250 mm inner diameter. The temperature program was started at 100 °C with initial holding for 1 minute and was increased at the rate of 10 °C/min to 300 °C and held for 3 minutes. The temperature was then increased 30 °C/min to 325 °C, with final holding of 3 minutes. The temperature of the transfer line to the MS was 280 °C. Mass spectra were obtained by standard (70 eV) electron ionization scanning from *m/z* 40 to 800 at a spectral accumulation rate of 0.09 seconds/spectrum.

2.2.4.3 Data Analysis GC-MS

Quantification was done by integrating summed extracted ion chromatogram (XIC) peak areas, using QuanLynx software. The peaks were integrated automatically and verified manually. The extracted ions (± 0.15 *m/z* units) used for quantification were: Cys-Cys (*m/z* 411.1 and 232.1), Cys-Cys-d_4 (*m/z* 415.1 and 234.1), Cys (*m/z* 220.1, 232.1, and 322.1), Cys-d_2 (which results from reduction of Cys-Cys-d_4 during derivatization as described below; *m/z* 222.1, 234.1, and 324.1) and Cys-d_3 (*m/z* 223.1, 235.1, and 325.1). All summed XIC peak integrals were exported to a spreadsheet for further analysis.

Cys-Cys is partially reduced to Cys during the derivatization step that is necessary to facilitate analysis by GC-MS. As such, Cys ions were used in the quantification of Cys-Cys. However, to use Cys in this quantification scheme it was necessary to subtract out any signal that was due to the endogenous Cys. This was done by spiking in 5 µM Cys-d_3 into each sample, which is equivalent to the concentration of endogenous Cys in P/S samples (as explained in the next paragraph and illustrated in Fig. 2.2). The magnitude of the summed XIC areas from Cys-d_3 was then assumed to represent the magnitude of the summed XIC areas from endogenous Cys. Thus, the total area of the summed XICs from Cys-d_3 was subtracted from the summed XIC areas of endogenous Cys. All residual summed XIC peak area from Cys ions was then considered to be derived from Cys-Cys. Prior to making this calculation, however, isotopic overlap between natural forms of Cys ions and their d_2-labeled internal standard counterparts was corrected for based on the known isotopic distribution of each fragment ion employed for

quantification. This isotope correction procedure was analogous to that which has previously been employed and widely used elsewhere (77, 78).

Given the initial concentrations of AlbSH, S-Cys-Alb, free and total copper, and Cys-Cys determined above, all rate law models with initial Cys concentrations anywhere within the physiologically observed range (79, 80) revealed that by the time plasma and serum were separated from whole blood, the concentration of Cys in P/S had equilibrated to a steady state concentration of ~ 5 μM (Fig. 2.2). Given this information and the fact that, relative to Cys-Cys, Cys contributes ≤ 5% of the total Cys equivalents in P/S, an initial Cys concentration of 5 μM was assumed in all kinetic models.

2.2.5 Data Analysis LC-MS

As previously described (14), approximately 1 minute of recorded spectra were averaged across the chromatographic peak apex of albumin. The electrospray ionization charge-state envelope was deconvoluted with Bruker DataAnalysis v3.4 software to a mass range of 1000 Da on either side of any identified peak. Deconvoluted spectra were baseline subtracted, and all peak heights were calculated, tabulated and exported to a spreadsheet for further analysis. Peak heights were used for quantification as opposed to peak areas, because of the lack of baseline resolution for some of the peaks.

2.2.6 LC-ESI-MS

Relative quantification of intact albumin proteoforms was done by liquid chromatography-electrospray ionization-mass spectrometry (LC-ESI-MS) on a Dionex Ultimate 3000 HPLC equipped with a 1:100 flow splitter connected to a Bruker maXis 4G quadrupole-time-of-flight (Q-TOF) mass spectrometer. A trap-and-elute form of LC-MS was carried out in which 5 μL of sample was loaded via a loading pump at 10 μl/min

in 80% water containing 0.1% formic acid (Solvent A) / 20% acetonitrile (Solvent B) onto an Optimize Technologies protein captrap configured for uni-directional flow on a 10-port diverter valve. The trap was then rinsed at this solvent composition with the HPLC loading pump at 10 µl/min for 3 minutes. The flow over the captrap was then switched to the micro pump, which was set at a flow rate of 3 µL/min and composition of 65/35 A/B. This composition was held until 4.5 min. From 4.5-4.6 min. the composition was ramped to 55/45 A/B then held. From 7.5-7.6 min. the composition was ramped to 20/80 A/B then held. Then from 9.4-9.5 min. the composition was ramped back to 65/35 A/B in preparation for the next injection. Following the valve switch at 3 minutes, the captrap eluate was directed to the mass spectrometer operating in positive ion, TOF-only mode, acquiring spectra in the m/z range of 300 to 3000. ESI settings for the Agilent G1385A capillary microflow nebulizer ion source were as follows: End Plate Offset -500 V, Capillary -4500 V, Nebulizer nitrogen 3 Bar, Dry Gas nitrogen 3.0 L/min at 225°C. Data were acquired in profile mode at a digitizer sampling rate of 4 GHz. Spectra rate control was by summation at 1 Hz.

2.3 Results

2.3.1 Rate Law Determination of *Ex Vivo* Formation of S-Cys-Alb

The major reactions that govern the ex vivo formation of S-Cys-Alb in P/S include:

$$AlbSH + Cys\text{-}Cys \underset{k_2}{\overset{k_1}{\rightleftharpoons}} SCysAlb + Cys \quad (1)$$

$$2Cys + O_2 \xrightarrow[k_3]{Cu(II)} Cys\text{-}Cys + H_2O_2 \quad (2)$$

Where AlbSH is the native reduced form of albumin, Cys-Cys is cystine, SCysAlb is S-cysteinylated albumin, and Cys is cysteine.

With the average initial starting concentrations of each reactant and product in P/S known and with the knowledge of the rate law governing the formation of S-Cys-Alb, it may be possible, in theory, to provide an estimate of the time spent by P/S samples at the temperature in which the rate law was determined. The rate law (including k_3) for Reaction 2 was previously determined by Kachur et al. (20); the forward and reverse reaction rate laws for Reaction 1 were determined here at 23 °C.

Reaction 1 is initially linear in both the forward and reverse directions (Fig. 2.3). Thus in order to be able to model a simultaneous system of chemical reactions comprised of Reactions 1 and 2, the forward and reverse rate laws for Reaction 1 were determined using the method of initial rates (73). To obtain albumin in fully reduced or fully oxidized form, high purity human serum albumin was fully reduced with Cys or fully oxidized with Cys-Cys, then spin-filtered to purify and concentrate the protein. Verification of complete reduction and oxidation was carried out by LC-MS of the intact protein following alkylation with maleimide to verify that no structural disulfide bonds were reduced (Fig. 2.1). Starting conditions for all incubations employed to determine the forward and reverse rate laws for Reaction 1 are provided in Tables 2.1 and 2.2, respectively. The slopes of plots of log v_o (initial rate) vs. log [*reactant concentration*] (for several different co-reactant concentrations) revealed that the reaction order for all species in Reaction 1 was 1 (Fig. 2.4). Subsequently, the data in Table 2.1 were fit to the equation:

$$v_o = k_1[\text{AlbSH}][\text{Cys-Cys}] \qquad (3)$$

(where v_o is the initial reaction rate in M/s) and non-linear regression was used to determine that $k_1 = 0.095 \pm 0.017\ M^{-1}\ s^{-1}$. Likewise, the data in Table 2.2 were fit to the equation:

$$v_o = k_2[\text{SCysAlb}][\text{Cys}] \qquad (4)$$

and non-linear regression was used to determine that $k_2 = 3.37 \pm 0.44\ M^{-1}\ s^{-1}$. Given that k_1 and k_2 were determined at 23 °C, their values are consistent with the values of $0.6 \pm 0.1\ M^{-1}\ s^{-1}$ and $6.6 \pm 0.4\ M^{-1}\ s^{-1}$, respectively, that were just recently determined by Bocedi et al. at 37 °C (81).

Once the forward and reverse rate laws for Reaction 1 had been determined, a series of differential equations that simultaneously consider Reactions 1 and 2 and their respective rate laws were assembled:

$$\frac{d[AlbSH]}{dt} = -k_1[AlbSH][Cys\text{-}Cys] + k_2[SCysAlb][Cys] \quad (5)$$

$$\frac{d[Cys\text{-}Cys]}{dt} = -k_1[AlbSH][Cys\text{-}Cys] + k_2[SCysAlb][Cys] + \frac{k_3[Cu(II)][Cys]}{K_z\left(1 + \frac{K_y}{[Cys]}\right) + [Cys]} \quad (6)$$

$$\frac{d[SCysAlb]}{dt} = k_1[AlbSH][Cys\text{-}Cys] - k_2[SCysAlb][Cys] \quad (7)$$

$$\frac{d[Cys]}{dt} = k_1[AlbSH][Cys\text{-}Cys] - k_2[SCysAlb][Cys] - 2\left(\frac{k_3[Cu(II)][Cys]}{K_z\left(1 + \frac{K_y}{[Cys]}\right) + [Cys]}\right) \quad (8)$$

In Equations 5-8, [Cu(II)] is the total concentration of copper (which stays constant), and K_y and K_z represent the first and second equilibrium dissociation constants pertaining to

Cys complexation of Cu(II) that are involved in the copper-catalyzed oxidation of Cys to Cys-Cys at pH 7.4 as described by Kachur et al. (20). Equations 5-8 cannot be solved explicitly, but numerical solutions at any point in time can be obtained once all constants and starting concentrations are supplied.

2.3.2 Quantitative Model Verification in Serum and Plasma

To evaluate the ability of the combined rate law model (Equations 5-8) to predict formation of S-Cys-Alb in actual plasma and serum, matched plasma and serum were collected from a healthy donor. Serum was collected into trace metal-free tubes to facilitate quantification of copper. Initial concentrations of S-Cys-Alb, AlbSH, Cys-Cys and free and total copper for use in the predictive model were made as described in Materials and Methods. Measurement of Cys was deemed unnecessary because according to the model, by the time serum or plasma are processed from whole blood the concentration of Cys drops to a steady state at about 5 µM—regardless of whether or not the initial concentration starts at the low or high end of physiological Cys concentrations observed in human plasma (Fig. 2.2)—and which, in terms of Cys equivalents, is within the error of Cys-Cys quantification.

Immediately following collection serum and plasma were each split into two portions: One portion was spiked with Cys and Cys-Cys (in a minimal volume of HBS buffer, pH 7.4) to increase the concentration of Cys by 12 µM and the concentration of Cys-Cys by 62 µM; the second portion was left unmodified. A 100-µL aliquot of each specimen in a closed 1.5-mL snap-cap tube was then incubated at 23 °C for 4 days on a rotating vortex mixer (200 RPM), with numerous measurements of S-Cys-Alb collected initially and then at least once a day after Day 1. The data were then fit with the

predictive model, using the empirically determined initial concentrations of all species along with rate and equilibrium constants pertinent to the model, determined as described above (k_1 and k_2; Reaction 1 at 23 °C) or as previously determined (k_3, K_y and K_z; Reaction 2 at 37 °C (20)) (Fig. 2.5). To best approximate the latter three parameters at the actual temperature of the experiment (23 °C), a value of -50 kJ/mol was estimated as the enthalpy of reaction per Cys ligand binding to Cu(II) based on the known enthalpy of Cys binding to other divalent cations (82) (binding to Cu(II) is unknown). Integration of the van't Hoff equation provides the following formula to estimate the change in an equilibrium association constant (K) with temperature (T) given the estimated change in enthalpy (ΔH°) (83):

$$\ln K_2 = \ln K_1 - \frac{\Delta H^\circ}{R}\left(\frac{1}{T_2} - \frac{1}{T_1}\right) \qquad (9)$$

where R is the ideal gas constant. Application of this formula to K_y and K_z resulted in a 2.5-fold decrease in each value to 2.0 x 10^{-6} M and 3.5 x 10^{-4} M, respectively. The same factor was applied to estimate k_3 as 0.13 s^{-1} as well—a factor in the middle of the range of the fold-change expected for a 14 °C decrease in temperature (73)[1]. All plasma copper was assumed to be catalytically available and half of serum copper (95% of which is bound to ceruloplasmin (85)) was assumed to be catalytically available since only about

[1] In a simple system consisting of only buffer, Cu^{2+}, and Cys, Reaction 2 exhibits two different kinetics phases—the first of which is faster and runs until the molar concentration of Cys is equal to that of Cu^{2+}. (20. Kachur, A. V., Koch, C. J., and Biaglow, J. E. (1999) Mechanism of copper-catalyzed autoxidation of cysteine. *Free Radic Res* 31, 23-34). In the absence of a second co-reaction (i.e., Reaction 1) that generates fresh free thiol-containing Cys, all Cys is then bound to copper; hydrogen peroxide then accumulates in the absence of free Cys and subsequently drives the second reaction phase, the rate constant for which, at 37 °C, is 4.25-fold lower than the rate constant of the first phase. In P/S, Reaction 1 continually generates fresh Cys; moreover, the catalase concentration in P/S is about 50 U/mL (84. Goth, L. (1991) A simple method for determination of serum catalase activity and revision of reference range. *Clin Chim Acta* 196, 143-151)—a quantity sufficient to prevent accumulation of hydrogen peroxide and therefore the second reaction phase)—as such, only the rate constant for phase 1 of Reaction 2 was considered in the models presented here.

40% of ceruloplasmin-bound copper resides in the Cu(II) oxidation state (86). Models in which only free copper, only the ~5% of copper not bound to ceruloplasmin, or all copper in serum were assumed to be catalytically available show that a major portion of bound copper must be catalytically available (Fig. 2.6). Additional models in which K_y, K_z, and k_3 are run at their 37 °C-values and 10-fold below these values are also provided for illustrative purposes, see *Appendix A.*

RMSD fit (expressed as %CV) for unfortified serum was 6.1% and that for unfortified K_2EDTA plasma was 6.3% (Fig. 2.5). The observed S-Cys-Alb trajectory in the matched serum and plasma samples, that were fortified with 62 µM Cys-Cys and 12 µM Cys, however, did not match the model predictions (Fig. 2.5). Considering that the rate law established for Reaction 2 (20) assumed that dissolved oxygen concentration [O_2(*aq*)] would not be rate limiting (i.e., did not take it into account)—in conjunction with the fact that dissolved oxygen demand would be substantially higher in P/S fortified with extra Cys-Cys and Cys—it was reasoned that the observed lower-than-predicted S-Cys-Alb formation rate may have been due to [O_2(*aq*)] becoming rate limiting at the unnaturally high Cys-Cys and Cys concentrations fortified into P/S. Simulation results from a more complex (but currently speculative) model than that provided by Equations 5-8 support this explanation, see *Appendix B.*

To evaluate the practical effect on S-Cys-Alb of processing plasma normally then storing samples under an inert atmosphere in sealed vials, parallel incubations of freshly collected plasma in air and under a nitrogen atmosphere (using a Spilfyter "Hands-in-a-Bag" artificial atmospheric chamber) were conducted. Initial rates of S-Cys-Alb formation under the two atmospheres were nearly identical, but eventually deviated and

resulted in a modestly lower maximum concentration of S-Cys-Alb in the sample incubated under nitrogen (Fig. 2.7). These experimental results compare favorably with the [O_2(*aq*)]-dependent model in which a modest concentration of O_2(*aq*) (70 µM) is assumed at the outset but no further O_2 can enter the unfortified sample over time (see *Appendix B, part B, panel n*).

2.4 Discussion

The chemical reactions that contribute to S-Cys-Alb formation in P/S *ex vivo* are known (Reactions 1 and 2). This made it possible to actually determine rate laws and develop a mathematical model to facilitate: First, predict how albumin oxidation will behave across a wide range of reactant and product starting concentrations and second, back-calculate the approximate time at which an "average" P/S specimen has been exposed to the temperature(s) at which the rate law has been determined.

The initial rate law model developed here assumes that the concentration of dissolved oxygen, [O_2(*aq*)], in P/S is not rate limiting. This appeared to hold true in samples that contained a physiologically normal concentration of Cys and Cys-Cys (Fig. 2.5). Two observations, however, suggested that the [O_2(*aq*)] in P/S was very close to becoming rate limiting: First, storage of unfortified plasma under nitrogen after initial processing was found to limit the overall formation of S-Cys-Alb (Fig. 2.7). And second, the rate at which S-Cys-Alb forms in unfortified P/S samples was accurately predicted by the model that does not take [O_2(*aq*)] into account while the rate at which S-Cys-Alb forms in P/S samples fortified with extra Cys and Cys-Cys is significantly overestimated by this model (Fig. 2.5). Yet the rate at which S-Cys-Alb forms in both unfortified and fortified P/S can be predicted using a model that takes [O_2(*aq*)] into account (*Appendix*

B). Thus, the present model based on Equations 5-8 should only be employed under two conditions: First, when P/S samples are known to have been stored under air, and second, in patient populations without kidney disease requiring hemodialysis.

The rate and equilibrium constants associated with Reaction 2 were determined for Cu(II) in a 40 mM sodium phosphate buffer (20)—a solution wherein the copper ions would be complexed to the various protonated forms of phosphate ions present. In serum, however, 95% of copper is bound to ceruloplasmin (85) and in K_2EDTA plasma essentially all of the copper is bound to the ~5 mM EDTA present. As such, the values of k_3, K_y and K_z used here—while appear to be reasonably accurate empirically (Fig. 2.5; *Appendix A*)—are not necessarily accurate representations of these values as they exist in actual P/S. Transition metals besides copper—most prominently iron—may also play some role in catalyzing Reaction 2 in P/S. "Free" or non-transferrin bound iron is typically in the nM range in serum (87). It has also been previously observed that Cu(II) ions are a far more efficient catalyst of intramolecular disulfide bond formation than is Fe(III) ions (13). As such, "free" iron in serum likely contributes negligibly to Reaction 2. In plasma, however, Fe(III)-EDTA may play a significant role in this reaction—potentially accounting for the higher-than-predicted initial rate of S-Cys-Alb formation (Fig. 2.5; *Appendix A*). Efforts are underway to develop a comprehensive rate model that takes [O_2(*aq*)] and all relevant metals within their P/S-liganded context into account across the range of temperatures likely to be encountered by P/S samples. Regarding the different temperatures, and the effect they will have on the rate constants used in the rate law, a group has recently been able to determine the rate constants for the thiol disulfide exchange reaction of albumin at 37 °C (81). Using the rate constants determined at 37 °C

and the determined rate law developed here, it was possible to accurately model the S-Cys-Alb formation at 37 °C (*Fig. 3.2b*). Showing that the rate model developed here is capable of accurately predicting the formation of S-Cys-Alb at other temperatures, once the rate constants have been determined.

It has previously been shown that the degree of air headspace above P/S samples stored at -20 °C does not significantly impact the overall rate of S-Cys-Alb formation (14). However, dissolved oxygen is involved in the oxidation of Cys to Cys-Cys (Reaction 2) and its potential range in an aqueous solution such as P/S is 0 - 250 μM (88, 89), which lies in the range of the total concentration of Cys equivalents in P/S (~150 μM). As such, the impact of nitrogen as a headspace gas (relative to air) on the formation profile of S-Cys-Alb in plasma was evaluated. The results (Fig. 2.7) suggest that once P/S samples are exposed to air, storing them under an inert atmosphere may provide a modest but significant ability to mitigate oxidative biomolecular damage.

2.5 Conclusion

The goal of this research was to determine the rate and the conditions associated with the occurrence of the spontaneous oxidation of albumin *ex vivo*. By using the method of initial rates and quantitatively monitoring the degree of oxidation (S-Cys-Alb formation) via analysis of the intact protein by electrospray ionization-mass spectrometry the disulfide-exchange oxidation rate constants, k_1 and k_2 (Reaction 1), for the reaction of *ex vivo* albumin oxidation in P/S were determined to be 0.095 ± 0.017 s^{-1} and 3.37 ± 0.44 s^{-1}, respectively.

Using these two rate laws along with the rate law already determined for Cys oxidation (20), the reaction for *ex vivo* albumin oxidation was accurately modeled (Fig.

2.5), with CV values of 6.1% and 6.3% for unfortified serum and plasma samples, respectively. The apparent deviation in the fit of the fortified serum and plasma samples is possibly explained by the increased consumption of oxygen, in which, oxygen becomes rate limiting (*Appendix B*). In validating this disulfide-exchanged based model of *ex vivo* albumin oxidation it facilitates the use of albumin oxidation as a metric of blood P/S integrity.

Figures

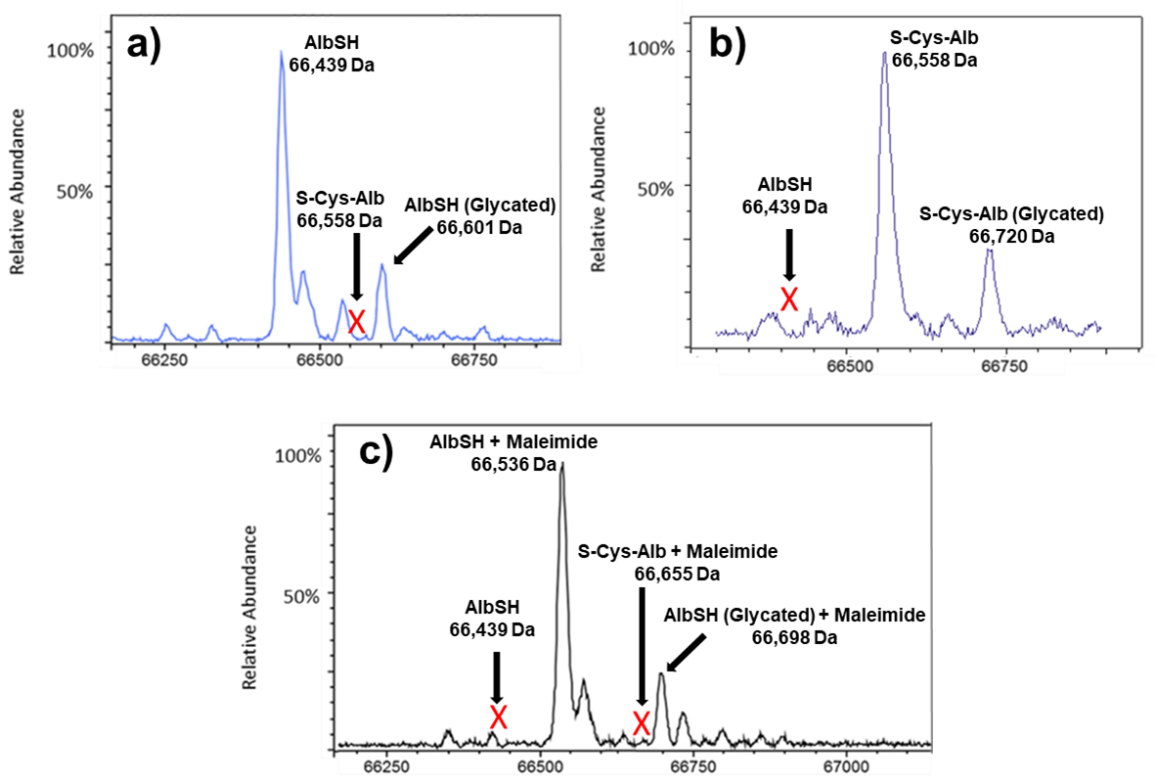

Figure 2.1: Charge deconvoluted ESI-mass spectra of the a) fully reduced and b) fully oxidized (S-cysteinylated) albumin employed for determination of the forward and reverse rate laws of the reactions shown in Reaction 1. c) To verify that no structural disulfide bonds were reduced in the former case, the sample was alkylated with maleimide. The mass shift of exactly +97 Da, with no peaks at +2*97 Da or higher indicate that the reduced albumin possessed only a single free Cys residue as expected.

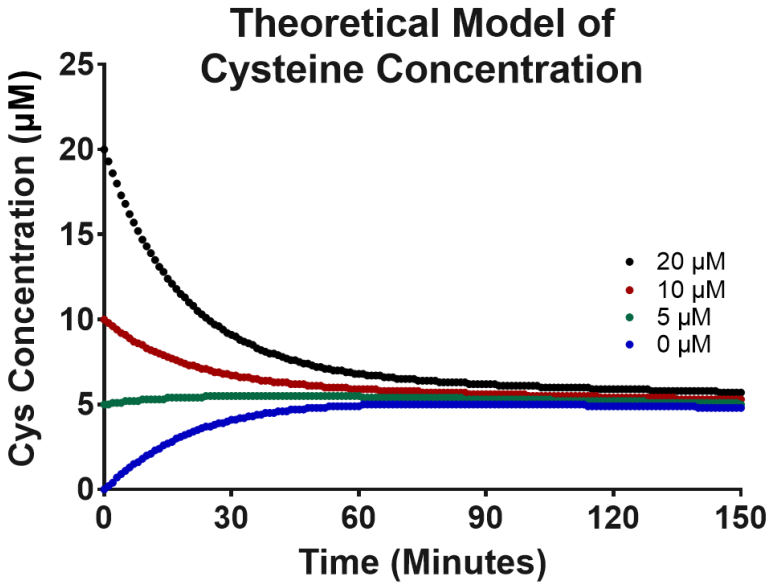

Figure 2.2: Reaction kinetics models based on the empirically determined rate law (**Eqns. 5-8**) illustrating that by the time serum or plasma were processed from whole blood, the concentration of Cys drops to a near steady-state concentration of about 5 µM—regardless of whether or not the initial concentration started at the low or high end of physiological Cys concentrations observed in human plasma.

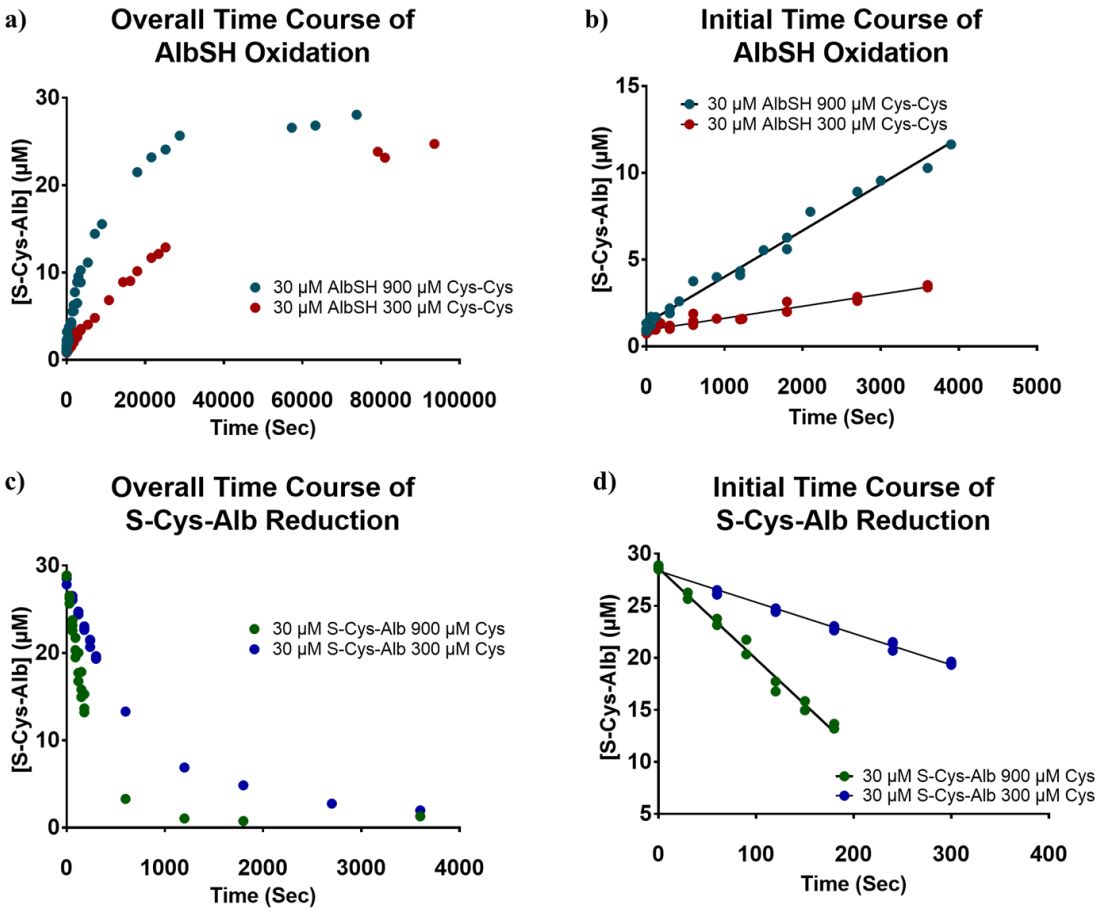

Figure 2.3: Rates of albumin oxidation (S-cysteinylation) and reduction at 23 °C. a) Overall time course for albumin S-cysteinylation (oxidation) and b) initial rate for albumin S-cysteinylation starting with 30 μM AlbSH and 300 or 900 μM Cys-Cys. c) Overall time course for reduction of S-Cys-Alb and d) initial rate for reduction of S-Cys-Alb starting with 30 μM S-Cys-Alb and 300 or 900 μM Cys.

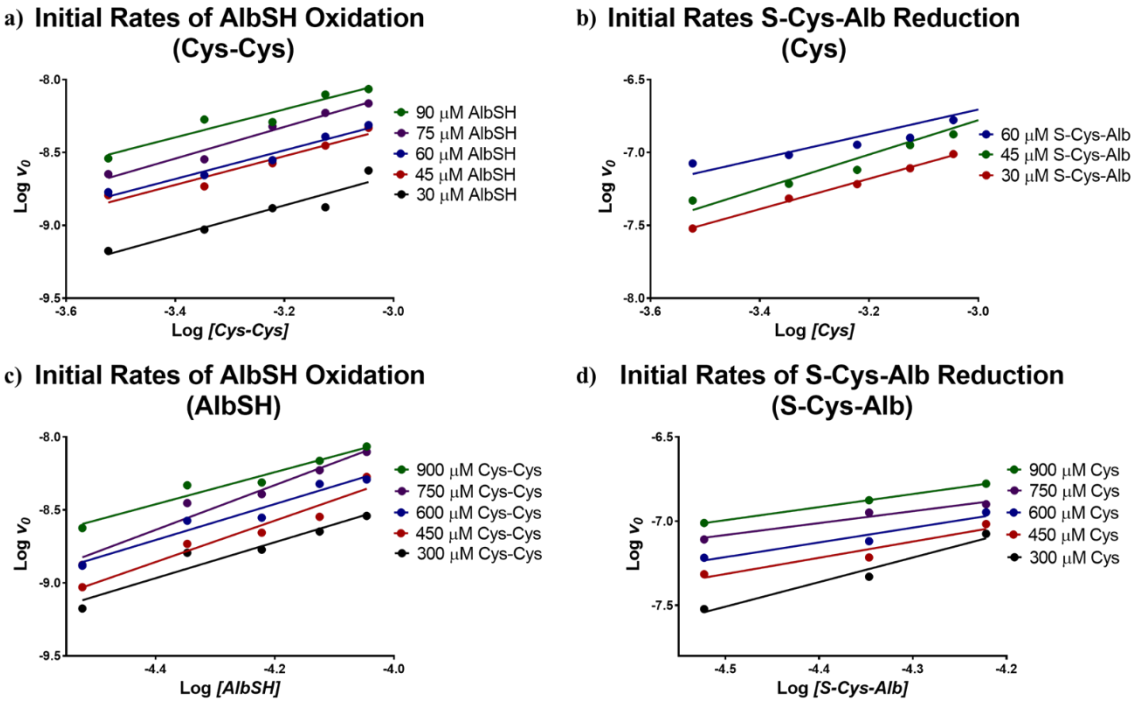

Figure 2.4: Log-log plots employed to determine the reaction order for all species in the reversible oxidation (S-cysteinylation) of AlbSH by Cys-Cys (Reaction 1). The average slopes for **a**, **b**, **c**, and **d** were 1.01 ± 0.05, 0.87 ± 0.25, 1.30 ± 0.17 and 0.96 ± 0.30, respectively. Thus, both the forward and reverse reactions were determined to be first order with respect to each reactant.

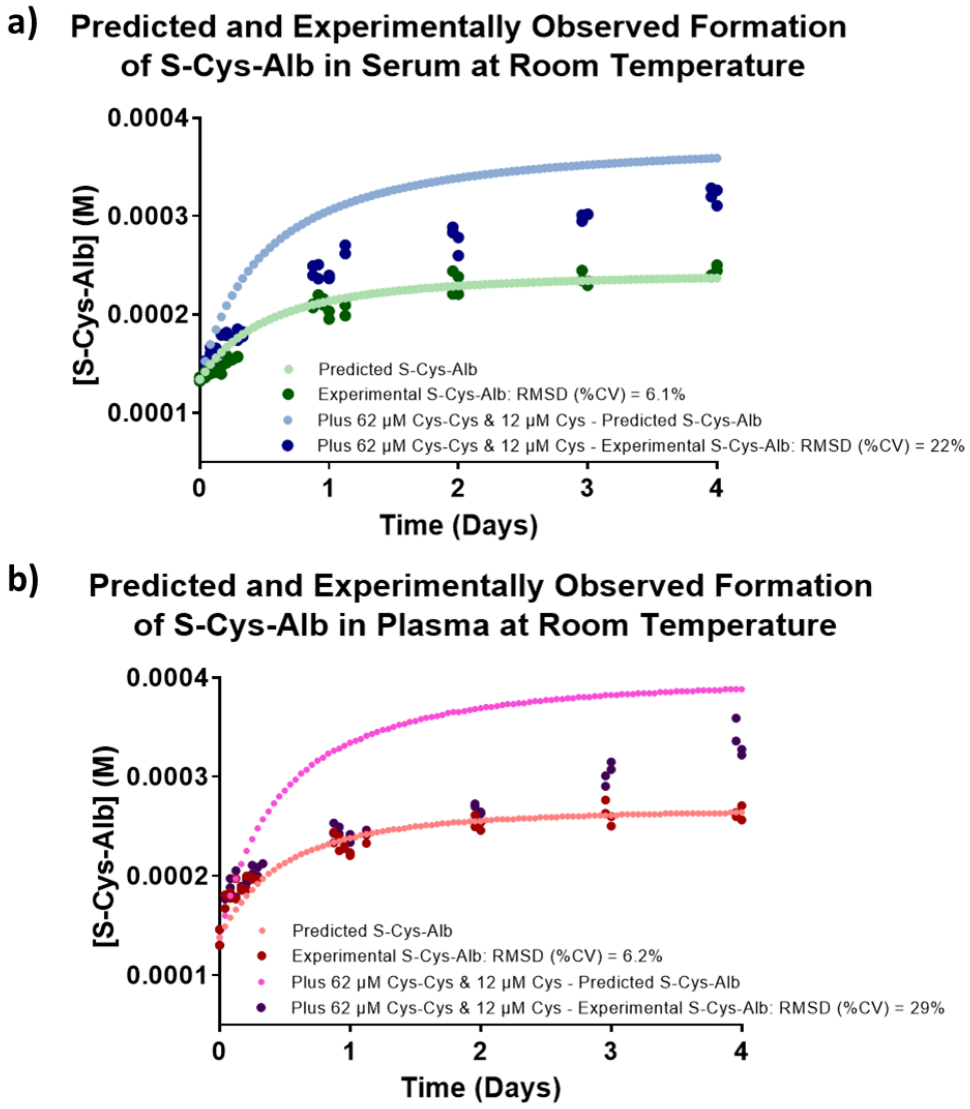

Figure 2.5: Observed and rate law model-predicted formation of S-Cys-Alb in matched a) serum and b) K_2EDTA plasma from a healthy donor. Green (serum) and red (plasma) circles represent natural, unfortified serum or plasma containing initially measured concentrations of AlbSH = 609 µM (serum) or 605 µM (plasma); S-Cys-Alb = 134 µM (serum) or 138 µM (plasma); Cys-Cys = 52 µM (serum) or 58 µM (plasma); Cys = 5 µM (inferred, not measured, see Fig. 2.2); and Cu(II) = 12.6 µM. Blue (serum) and purple (plasma) cirlces represent aliquots of the same samples into which extra Cys-Cys and Cys were fortified, bringing the final concentration of Cys-Cys to 114 µM (serum) or 120 µM (plasma) and Cys to 17 µM (serum & plasma). Dashed lines represent rate model-predicted trajectories for S-Cys-Alb formation based on numerical solutions to Equations 5-8 employing the rate and equilibrium constant parameters described in the main text. The poor model fit for samples fortified with extra Cys-Cys and Cys appears to be due to the concentration of dissolved oxygen, [O_2(*aq*)], becoming rate limiting under these fortified conditions (*Appendix B*).

a) Serum: Only free Cu(II) catalytically available (0.4 μM)

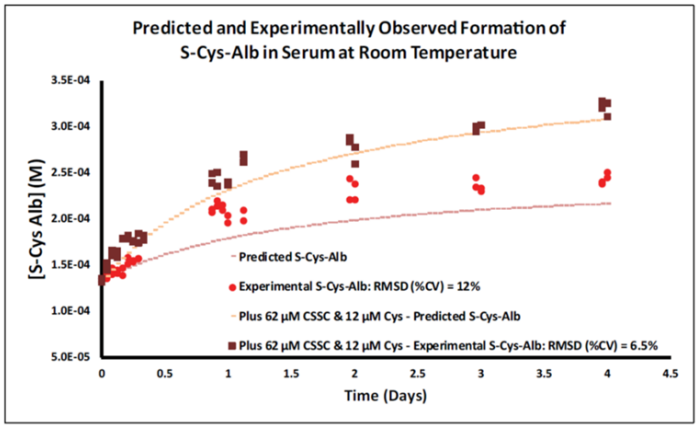

b) Serum: Only the ~5% of serum Cu(II) not bound to ceruloplasmin catalytically available (0.63 μM)

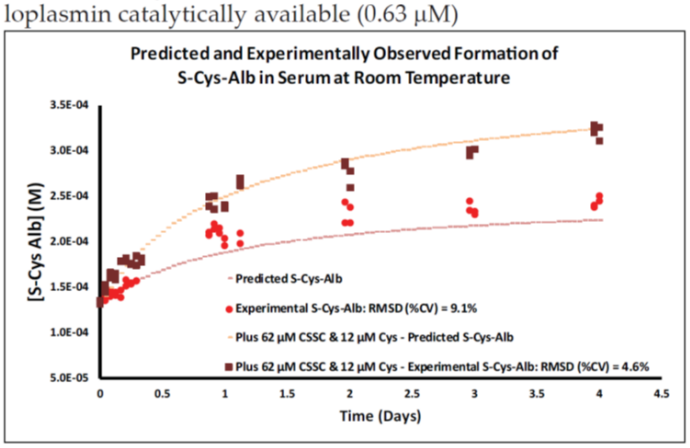

c) Serum: All serum Cu(II) catalytically available (12.6 μM)

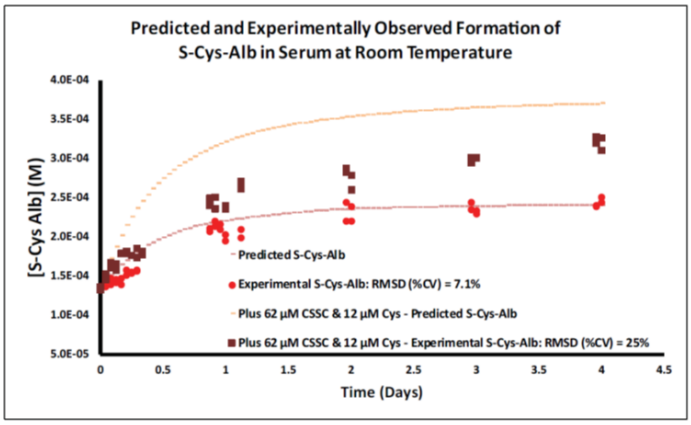

Figure 2.6: Kinetics simulations in which a) only free serum Cu(II) (0.4 μM), b) the ~5% of serum Cu(II) not bound to ceruloplasmin (0.63 μM), and c) all Cu(II) in serum (12.6 μM) is assumed to be catalytically available. Cys-Cys is abbreviated as CSSC in the legends.

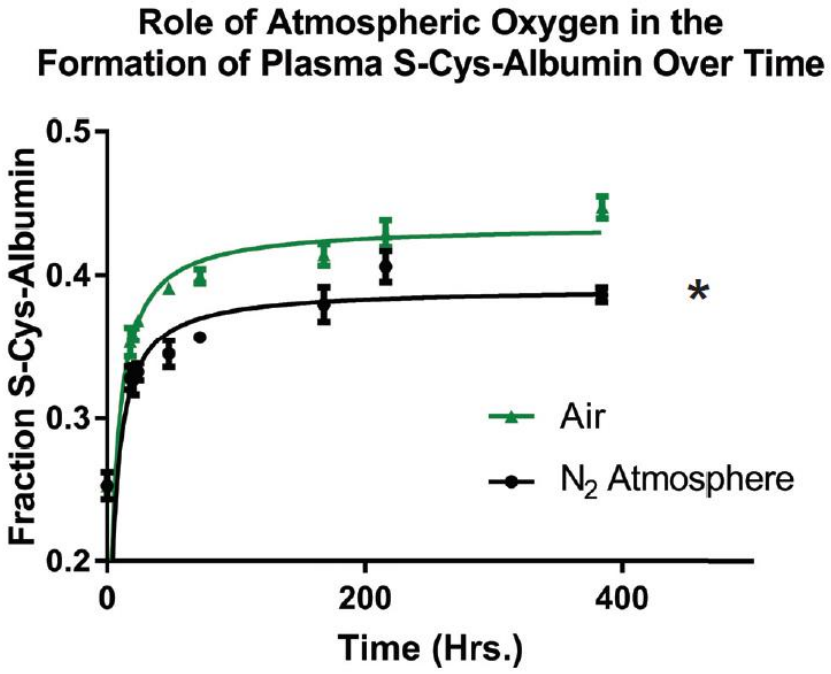

Figure 2.7: Formation of S-Cys-Alb over time in aliquots of the same plasma incubated at 23 °C in air (green triangles) or under a nitrogen atmosphere (black circles). The nitrogen atmosphere modestly but significantly lowered the total fraction of S-Cys-Alb formed (* $p < 0.01$; Wilcoxon matched pairs signed-rank test. n = 4 per time point; error bars represent SD.)

Tables

Table 2.1: Initial concentrations employed for determining the rate law for S-cysteinylation (oxidation) of albumin (AlbSH) by cystine (Cys-Cys). Values listed inside the pivot table are initial rates in units of M/s.

	$[Cys\text{-}Cys]_0$ (M)				
$[AlbSH]_0$	0.0003	0.00045	0.0006	0.00075	0.0009
0.00003	6.68E-10	9.35E-10	1.31E-09	1.33E-09	2.38E-09
0.000045	1.61E-09	1.85E-09	2.67E-09	3.52E-09	4.67E-09
0.00006	1.69E-09	2.21E-09	2.8E-09	4.06E-09	4.88E-09
0.000075	2.25E-09	2.84E-09	4.77E-09	5.92E-09	6.87E-09
0.00009	2.88E-09	5.33E-09	5.12E-09	7.9E-09	8.61E-09

Table 2.2: Initial concentrations employed for determining the rate law for reduction of S-cysteinylated albumin (S-Cys-Alb) by cysteine (Cys). Values listed inside the pivot table are initial rates in units of M/s.

	$[Cys\text{-}Cys]_0$ (M)				
$[AlbSH]_0$	0.0003	0.00045	0.0006	0.00075	0.0009
0.00003	6.68E-10	9.35E-10	1.31E-09	1.33E-09	2.38E-09
0.000045	1.61E-09	1.85E-09	2.67E-09	3.52E-09	4.67E-09
0.00006	1.69E-09	2.21E-09	2.8E-09	4.06E-09	4.88E-09
0.000075	2.25E-09	2.84E-09	4.77E-09	5.92E-09	6.87E-09
0.00009	2.88E-09	5.33E-09	5.12E-09	7.9E-09	8.61E-09

CHAPTER 3

DELTA S-CYSTEINYLATED ALBUMIN AS A MARKER OF BIOSPECIMEN INTEGRITY

3.1 Introduction

Collection, processing, storage and handling expose clinical biospecimens to pre-analytical variables that, when unaccounted for, have the potential to produce misleading results in downstream clinical research (90-94). For blood plasma and serum (P/S) samples, numerous pre-analytical variables such as the type of collection tube, degree of tube filling, number of tube inversions, degree of hemolysis, and pre-centrifugation delay can quantitatively impact clinical measurements (95-98). Arguably, exposure to the thawed state (i.e., temperatures above -30 °C (46, 99)) is the most difficult pre-analytical variable to track and control over the lifetime of a P/S biospecimen—particularly at the individual aliquot level.

There is widespread agreement regarding the need for robust biospecimen quality control (QC) / quality assurance (QA) checks in biomarker discovery and validation work. Yet relatively little research effort focuses on this arena. P/S specimens are among the most commonly employed biospecimens in biomarker-related research but, to date, no gold standard marker of P/S integrity has been identified and put into widespread, routine use. This is evidenced by the fact that despite the recent emphasis on robustness and reproducibility, the U.S. National Cancer Institute (NCI, part of the National Institutes of Health (NIH)) does not currently require any empirical evidence-based QA thresholds be met before pre-existing P/S specimens are employed in NCI-sponsored research. This QC/QA problem is widespread. For example, in 2014, 287 out of 455 NCI-

sponsored extramural grants (63%) relied on pre-existing biospecimens; 107 of these sponsored projects employed pre-existing P/S (100).

Written documentation that includes the types of specimens analyzed and the specimen storage conditions is now required for manuscript submissions to leading clinical research journals (101-103), but as experienced—and as described here—paper trails are insufficient to guarantee disclosure of incidents that may compromise specimen integrity. The possible reasons for this are rarely discussed but may range from poor note taking to conflicts of interest about disclosing incidents that may have resulted in biospecimen damage. Moreover, paper trails lack the ability to thoroughly quantify the molecular integrity of specimens that may have experienced minor "exposure" incidents, that are either not captured in the documentation or, if they were, cannot be precisely assigned to individual samples or aliquots. Yet if temperature-unstable or even potentially temperature-unstable markers are to be analyzed in a set of P/S samples, it is critically important to know the biomolecular integrity of every individual sample.

This line of reasoning implies that a gold standard metric of P/S integrity should involve some form of empirical, quantitative biomolecular analysis that, if necessary, could be applied to every sample in a clinical study (whether the sample was collected for immediate analysis or is to be analyzed retrospectively)—even if the study employed thousands of P/S samples. As such, the ideal assay would focus on endogenous analyte(s), require a very low sample volume, require minimal sample preparation, be automatable from the point of fully frozen P/S to the point of generating the final report, and be inexpensive. Moreover, the majority, if not all, of the representative molecular alterations caused by the most unavoidable (bio)chemical processes that occur upon P/S

exposure to the thawed state should be captured by the integrity marker. Such processes include: 1) drifting toward an equilibrium state that is never observed *in vivo*, 2) *ex vivo* oxidation, due to P/S samples taking on a dissolved oxygen concentration of up to 0.25 mM (88, 89) – a concentration that is orders of magnitude higher than that observed in the P/S compartment *in vivo*, 3) enzyme-mediated biomolecular degradation, and 4) macromolecular denaturation. Additionally, changes in the QA marker(s) should occur in the same time frame in which some of the most "fragile", time-sensitive biomolecules within the P/S sample are altered beyond their original *in vivo* status. And finally, if intended as generally representative, thawed-state sensitive changes in QA marker(s) should neither be inhibited nor accelerated by stabilization practices that focus on a single mechanism of *ex vivo* alteration such as protease inhibitors or heat-based "inactivation".

Together, these characteristics are quite stringent and are unlikely to be met by a single QA analyte or assay. As such, it should at least be possible to link changes in the QA marker to changes in specific analytes of interest by analyzing both in parallel. When linked empirically, this is possible for most imaginable QA markers. However, the best QA markers will be those for which a (bio)chemical rate law can be determined, making it possible for the marker(s) to serve as a molecular stopwatch for the timespan of thawed-state exposure—i.e., making it possible to effectively place an exposure time stamp on every single sample. With the rate law for the QA marker established, it would be possible for any investigator to link their assay(s) of interest to the QA marker by simply following good assay development guidelines and conducting a stability time course with their analyte(s) of interest.

In 2014 it was reported that two of the most abundant P/S proteins, albumin and apolipoprotein A-I, are susceptible to *ex vivo* oxidation events that occur over two non-overlapping time segments in P/S specimens exposed to temperatures above -30 °C. These proteins were measured in a single dilute-and-shoot LC-MS assay of the intact proteins that required less than 1 µL of P/S (14). It was clear that albumin oxidation (S-cysteinylation of its single free cysteine residue) would meet most of the ideal QA marker specifications described above, but the *in vivo* reference range for the fraction of albumin in the oxidized state and the multi-reaction rate law for the formation of S-cysteinylated albumin were not known. Subsequently (and as reported here), measurements were made that provided a conservative estimate of the population reference range for the fraction of albumin in its S-cysteinylated form (S-Cys-Alb), but found that it was too close to the maximum degree of S-cysteinylation obtained by some samples *ex vivo*—i.e., once albumin had consumed all of the free cysteine (Cys) and cystine (Cys-Cys) equivalents present. This limited, in theory, the useable dynamic range of S-Cys-Alb as a P/S QA marker. Nevertheless, the population reference range for albumin in P/S is known (104) and those for Cys and Cys-Cys in plasma are well estimated (79, 80). Thus assuming that albumin is the only significant oxidative consumer of Cys equivalents, it is possible to calculate that if S-Cys-Alb is measured in a fresh plasma sample and then intentionally driven to its maximum possible value *ex vivo* (14), over 99% of the human population under age 60 should experience a *change* in S-Cys-Alb between these two measurements (ΔS-Cys-Alb) of 11-30%. (This range increases in persons over age 60 to 16-39% because albumin concentrations decrease (105) and Cys-Cys concentrations increase with age (79)). Charge deconvoluted ESI-mass spectra of albumin that illustrate the ΔS-Cys-

Alb phenomenon are provided in Fig. 3.1. Given that the inter-assay precision for measurement of S-Cys-Alb (on this scale) is 1.2% (14), ΔS-Cys-Alb as a QA marker for exposure of P/S samples to the thawed state was intentionally pursued.

Reported here are the development of an assay for ΔS-Cys-Alb, estimates for the population reference ranges for S-Cys-Alb and ΔS-Cys-Alb, insights into the role of dissolved oxygen in driving S-Cys-Alb formation, the results of a blind challenge of the ability of ΔS-Cys-Alb to detect exposures of both group and individual P/S samples to the thawed state (i.e., temperatures above -30 °C), and an actual case study in which ΔS-Cys-Alb detected and subsequently prompted disclosure of a biospecimen integrity discrepancy in a set of nominally pristine serum samples collected under NIH sponsorship.

3.2 Materials and Methods

3.2.1 Materials and Reagents

Trifluoroacetic acid (TFA, 299537), HEPES (H3375) and NaCl (S7653) for preparation of HEPES-buffered saline solution (HBS buffer) were purchased from Sigma-Aldrich (St. Louis, MO). LC-MS grade Acetonitrile (TS-51101), LC-MS grade water (TS-51140) were purchased from ThermoFisher Scientific (Waltham, MA). All non-LC-MS solvents were of HPLC grade.

3.2.2 Plasma and Serum Samples

Fasting K_2EDTA plasma and serum samples from healthy volunteers were collected, via forearm venipuncture, under IRB approval at Arizona State University. The samples were collected according to the NIH's Early Detection Research Network blood collection standard operating procedures (71, 72). All tubes were filled to the proper level

and inverted the proper number of times (8 times for EDTA plasma and 5 times for serum). Within 30 minutes of collection, plasma samples were processed, aliquoted, and placed in a -80 °C freezer; serum samples were allowed to clot for ~ 40 minutes, then immediately centrifuged, aliquoted, and placed at -80 °C within 70 minutes of collection.

Matched K_2EDTA plasma and serum samples were collected under IRB approval from non-acute cardiac patients presenting with chest pain suggestive of coronary artery disease and undergoing coronary angiogram, cardiac stress test and/or coronary computed tomography angiography at Maricopa Integrated Health Systems. None of these patients had severe or end-stage renal disease (i.e., estimated glomerular filtration rate, eGFR < 30 mL/min*1.73 m^2) and none were on hemodialysis; only 6 had eGFR values < 60 mL/min*1.73 m^2. Patient age range was 34-83 years (mean ± SD was 59 ± 8.5 years). Samples were collected and processed as described above for healthy volunteers. Times of draw, centrifugation and placement at -80 °C were recorded for every individual sample. Sample hemolysis was noted by visual comparison to a color chart, resulting in placement of samples into categories of minimal, mild, and moderate-and-above hemolysis—corresponding to < 20 mg hemoglobin/dL, 20-50 mg/dL and > 50 mg/dL, respectively.

Serum specimens for the case study of pre-existing samples were collected under IRB approval from stage I lung cancer patients and corresponding age, gender and smoking-status matched controls. These samples were collected under NIH-sponsorship by seasoned investigators with well-defined, matched standard operating procedures. Briefly, serum samples were collected into red top tubes (BD Vacutainer catalog no. 366430). These were allowed to sit upright at room temperature for 30-60 minutes after

blood was drawn to allow the clot to form. If the blood was not centrifuged immediately after the clotting time, the tubes were refrigerated at 4 °C for no longer than 24 hours. After clotting, samples were centrifuged at 1,200 RCF for 20 minutes at room temperature. Aliquots were then placed into 2-mL cryovials and stored at -80 °C. Most case and control samples were processed and placed at -80 °C within 2-3 hours of collection. Cancer patients were 69% female / 31% male and controls were 71% female / 29% male. The average age (mean ± SD) of the cancer patients and controls was 71.9 ± 9.2 yrs and 68.4 ± 8.1 yrs, respectively. Cancer patients had a slightly lower average number of smoking pack years (33.9 pack yrs) compared to the controls (37.3 pack yrs).

All P/S samples were coded and de-identified prior to transfer to the analytical laboratory. All human subject experiments were conducted according to the principles expressed in the Declaration of Helsinki.

3.2.3 S-Cys-Alb and ΔS-Cys-Alb Assay Sample Preparation

P/S samples were prepared for injection onto the LC-MS by 1000x dilution in 0.1% (v/v) TFA. Typically, 0.5 or 1µL was mixed with 500 or 1000 µL of 0.1% TFA. Once diluted, S-Cys-Alb measurements are stable for over 16 hrs at 10 °C (14). For measurement of ΔS-Cys-Alb, 9 µL of residual P/S sample was then placed into a 0.6-mL Eppendorf snap-cap polypropylene test tube and incubated in an oven set at 37 °C for 18 hrs. Following this period, the sample was diluted 1000x in 0.1% TFA then injected onto the LC-MS. The *difference* in S-Cys-Alb before and after this 18-hr incubation at 37 °C constitutes ΔS-Cys-Alb.

3.2.4 Blind Challenge

P/S samples were acquired from a single healthy donor on three different draw dates. These samples were divided into 120 aliquots of 50 µL each and were evenly distributed to the grouped and individual treatment sets. Each sample was marked with an identifier code to enable clear distinction between samples by the mediator, but the key to the identifier codes was not disclosed to the analyst until completion of the experiments and data interpretation had occurred. The sixty samples in each set were divided into ten groups consisting of three serum and plasma samples (one serum and plasma sample from each blood draw), and each group was assigned a treatment condition (Table 3.1). The samples present in the grouped set were given distinct labels consisting of a number (1-10) and a letter (A-F), with the number denoting samples in each grouped treatment condition. The role of the number on each of these samples was disclosed to the analyst, giving knowledge on the samples present in each group, but the treatment condition for each group and the letter distinction were not revealed. The labels used to distinguish samples in the individual set were created using a 4-digit random number generator to inhibit the analyst from identifying samples present in the same treatment condition. After completion of the assigned treatment condition, all samples were stored at - 80 °C until further analysis was completed.

The analyst then used the ΔS-Cys-Alb assay by using 10 µL of the P/S sample, of which 1 µL was used to measure the initial oxidation of albumin, the remaining 9 µL was incubated overnight at 37 °C to intentionally drive it to maximum oxidation. Oxidation was again measured, the difference in these measurements, called ΔS-Cys-Alb was calculated.

3.2.5 Case Vs. Control Real Life Samples

The samples were collected under NIH-sponsorship by seasoned investigators with well-defined standard operating procedures. Samples were analyzed using the ΔS-Cys-Alb assay by using 10 µL of the P/S sample, of which 1 µL was used to measure the initial oxidation of albumin, the remaining 9 µL was incubated overnight at 37 °C to intentionally drive it to maximum oxidation. Oxidation was again measured, the difference in these measurements, ΔS-Cys-Alb was calculated.

3.2.6 Data Analysis

3.2.6.1 LC-ESI-MS Analysis

Relative quantification of intact albumin proteoforms was done by liquid chromatography-electrospray ionization-mass spectrometry (LC-ESI-MS) on a Dionex Ultimate 3000 HPLC equipped with a 1:100 flow splitter connected to a Bruker maXis 4G quadrupole-time-of-flight (Q-TOF) mass spectrometer. A trap-and-elute form of LC-MS was carried out in which 5 µL of sample was loaded via a loading pump at 10 µl/min in 80% water containing 0.1% formic acid (Solvent A) / 20% acetonitrile (Solvent B) onto an Optimize Technologies protein captrap configured for uni-directional flow on a 10-port diverter valve. The trap was then rinsed at this solvent composition with the HPLC loading pump at 10 µl/min for 3 minutes. The flow over the captrap was then switched to the micro pump, which was set at a flow rate of 3 µL/min and composition of 65/35 A/B. This composition was held until 4.5 min. From 4.5-4.6 min. the composition was ramped to 55/45 A/B then held. From 7.5-7.6 min. the composition was ramped to 20/80 A/B then held. Then from 9.4-9.5 min. the composition was ramped back to 65/35 A/B in preparation for the next injection. Following the valve switch at 3 minutes, the

captrap eluate was directed to the mass spectrometer operating in positive ion, TOF-only mode, acquiring spectra in the m/z range of 300 to 3000. ESI settings for the Agilent G1385A capillary microflow nebulizer ion source were as follows: End Plate Offset -500 V, Capillary -4500 V, Nebulizer nitrogen 3 Bar, Dry Gas nitrogen 3.0 L/min at 225°C. Data were acquired in profile mode at a digitizer sampling rate of 4 GHz. Spectra rate control was by summation at 1 Hz.

3.2.6.2 Data Analysis

As previously described (14), approximately 1 minute of recorded spectra were averaged across the chromatographic peak apex of albumin. The electrospray ionization charge-state envelope was deconvoluted with Bruker DataAnalysis v3.4 software to a mass range of 1000 Da on either side of any identified peak. Deconvoluted spectra were baseline subtracted, and all peak heights were calculated, tabulated and exported to a spreadsheet for further analysis. Peak heights were used for quantification as opposed to peak areas, because of the lack of baseline resolution for some of the peaks.

3.3 Results

3.3.1 Development of the ΔS-Cys-Alb Assay

The highest temperature to which human P/S is exposed in its normal *in vivo* environment is 37 °C; as such, this temperature was chosen as the incubation temperature for the ΔS-Cys-Alb assay. To determine the time required to maximize S-Cys-Alb, as well as the impact of blood collection type and the effect of varying Cys and Cys-Cys concentrations on the time required to reach a maximum value of S-Cys-Alb, a matched collection of K_2EDTA plasma, sodium heparin plasma, and serum from a healthy donor was obtained and S-Cys-Alb was measured in the freshly processed samples. Portions of

each specimen were then fortified with an additional 1 µM Cys and 10 µM Cys-Cys or 2 µM Cys and 20 µM Cys-Cys. These added concentrations represent approximately 1-2 standard deviations (SDs) of the mean values of ~ 10 µM Cys and ~ 62 µM Cys-Cys seen in the plasma of typical donors (79, 80). Nine-microliter aliquots of each unique P/S sample were then incubated in sealed 0.6-mL tubes at 37 °C and S-Cys-Alb was measured at 4, 18, 24 and 30-hr time points (three separate 9-µL aliquots were made for each time point). Differences between matched serum and plasma were negligible, with all specimens reaching their maximum value of S-Cys-Alb by 18 hrs. Addition of Cys and Cys-Cys to the samples resulted in a higher maximum value of S-Cys-Alb but did not alter the time required to reach it (Fig. 3.2).

3.3.2 ΔS-Cys-Alb in Fresh Samples from Cardiac Patients

Non-acute cardiac patients presenting with chest pain, suggestive of coronary artery disease, undergoing coronary angiogram cardiac stress test and/or coronary computed tomography angiography at the recommendation of a cardiologist are likely to be individuals under continual low to moderate levels of systemic oxidative stress—a situation that could potentially raise their endogenous levels of S-Cys-Alb above that of nominally healthy individuals. As such, these cardiac patients represented a clinical population that could potentially pose a challenge to the theoretically usable dynamic range of the ΔS-Cys-Alb assay. To estimate the typical values of S-Cys-Alb and ΔS-Cys-Alb observed in fresh samples from these patients, matched K_2EDTA plasma and serum samples were collected from 30 of them. P/S specimens were collected under rigorous guidelines to ensure the highest possible sample quality. Fresh K_2EDTA plasma and serum were found to have similar but significantly different values of S-Cys-Alb (paired

t-test, $p < 0.001$; Fig. 3.3). Following incubation of 9-µL aliquots at 37 °C for 18 hrs, S-Cys-Alb was measured again and the difference between the two measurements was recorded as ΔS-Cys-Alb. Both the maximum value of S-Cys-Alb and ΔS-Cys-Alb were found to be significantly higher in plasma than serum (paired t-test, $p < 0.001$; Fig. 3.3). All distributions were Gaussian (D'Agostino & Pearson normality test; $p > 0.05$). The mean value of ΔS-Cys-Alb in cardiac patient plasma (± SD) was 0.22 ± 0.039 and in serum was 0.17 ± 0.030 (when plasma and serum data are combined, the mean ± SD is 0.20 ± 0.041). Empirically, these values suggest that ΔS-Cys-Alb values in 95% of fresh cardiac patient plasma and serum samples will fall in the ranges of 14% - 30% and 11% - 23%, respectively.

3.3.3 Blind Challenges of ΔS-Cys-Alb

Two separate challenges were conducted for ΔS-Cys-Alb as a marker of P/S exposure to thawed conditions in which the analyst was blinded to sample identities. The first study was a group-wise challenge wherein discrete groups of samples were either exposed to thawed conditions or properly stored at -80 °C *as groups*. The second blind challenge involved proper storage or mistreatment of discrete, individual samples. Prior to unblinding, the analyst was only aware that there would be a group-wise challenge and an individual sample challenge; the analyst was unaware of any other aspect of the experimental design described below.

3.3.3.1 Group-wise Blind Challenge

Matched plasma and serum were collected from the same individual on three separate days, all spaced at least six days apart. This produced six unique but not highly different samples. Ten 50-µL aliquots were created from each sample, creating ten

groups, each of which contained one aliquot each of the original six specimens. These groups were then randomly assigned: two groups were kept continually at -80 °C, and one group was subjected to each of the following eight conditions: 23 °C for 2 hrs, 23 °C for 4 hrs, 23 °C for 6 hrs, 23 °C for 8 hrs, 4 °C for 8 hrs, 4 °C for 16 hrs, -20 °C for 24 hrs, and -20 °C for 48 hrs (Table 3.1). The samples were then given to the analyst with only a coded identifier on each sample that corresponded to its unique group. ΔS-Cys-Alb was then measured in each sample (Fig. 3.4a). The distributions of all data sets overlapped to some degree, indicating that it would likely be difficult to distinguish control group(s) from mistreated group(s). As such, data were analyzed using a statistical approach designed to limit type II errors (i.e., one-way ANOVA followed by uncorrected Fisher's LSD with $p < 0.1$ serving as the cutoff for statistical significance). Based on this analysis, it was clear that Groups 1 and 3 had higher mean values of ΔS-Cys-Alb than all other groups, except for Group 7, whose status was unclear. Moreover, the ΔS-Cys-Alb values in Groups 1 and 3 were consistent with fresh samples or those kept at -80 °C (cf. Fig. 3.3). Thus Groups 1 and 3 were named by the analyst as control groups. Group 7 could not be definitively categorized but was guessed/presumed to also be a properly handled control group. All other groups were assigned as having been exposed to thawed conditions of some sort. Upon unblinding it was revealed that all assignments except for Group 7 had been made correctly (Fig. 3.4a).

3.3.3.2 Individual Blind Challenge

Ten additional 50-µL aliquots were made from the six samples described in the preceding paragraph, producing a total of 60 specimens. These aliquots were made at the same time as the others to avoid an additional freeze-thaw cycle. Twelve of these

specimens (n = 2 aliquots of each of the original six P/S samples) were kept at -80 °C. One aliquot each of the original six P/S samples was then subjected to each of the following eight conditions: 23 °C for 24 hrs, 23 °C for 48 hrs, 23 °C for 72 hrs, 23 °C for 7 days, 4 °C for 7 days, 4 °C for 14 days, -20 °C for 60 days, -20 °C for 90 days (Table 3.1). Each individual test tube had only a single, completely unique coded identifier on it. The analyst was then given the samples and ΔS-Cys-Alb was measured in each sample. Since statistical analysis cannot be conducted on single samples, a ΔS-Cys-Alb integrity cutoff had to be assigned. Based on the Gaussian distribution of ΔS-Cys-Alb in P/S from nominally unhealthy patients that have been collected to date (Fig. 3.3), it can be predicted that 99% of fresh P/S samples have ΔS-Cys-Alb values in the range of 9% to 30%. This range was determined based on the mean ± 2.58 SDs of the combined plasma and serum samples represented in Fig. 3.3b. Thus, a ΔS-Cys-Alb value of 0.090 (or 9.0%) was set as the cutoff for this individual sample-level blind challenge. Using this cutoff, all 60 individual specimens were categorized correctly (Fig. 3.4b).

3.3.4 Case Study: Application of ΔS-Cys-Alb

Following development of the ΔS-Cys-Alb assay, an occasion arose in the laboratory in which it was needed. In short, a set of serum samples from stage I lung cancer patients and corresponding age, gender and smoking-status matched controls were undergoing glycan "node" analysis (106-110) as part of an unrelated project. The samples were collected under NIH-sponsorship by seasoned investigators with well-defined SOPs and, on paper, there should not have been any specimen integrity problems. As part of the glycan "node" assay, relative blood glucose concentrations were (unintentionally) determined. The relative blood glucose concentrations in these samples indicated

unexpectedly elevated levels of blood glucose in the cases. It has been previously observed that albumin glycation increases significantly over time in P/S samples exposed to thawed conditions (*Chapter 4*); as such, even though there was a pristine paper trail associated with these samples, it was decided to measure ΔS-Cys-Alb in them. The mean values of ΔS-Cys-Alb were significantly different between the cases and controls ($p < 1 \times 10^{-20}$; student's t-test) and there was nearly no overlap in their ΔS-Cys-Alb distributions (Fig. 3.5). Since ΔS-Cys-Alb is not a marker of stage I lung cancer, these data indicated an integrity discrepancy between the two sets of serum samples. Upon showing these data to the clinical investigators who had provided the samples, it was ultimately disclosed that the -80 °C freezers in which the control samples had been stored had experienced a power outage for about 3-4 days during a natural disaster. Using the combined rate law model described in (*Chapter 2 Equations 5-8*) in combination with average population values for total albumin, AlbSH, S-Cys-Alb, Cys, Cys-Cys and total copper in fresh serum, it was estimated that the control serum samples had been exposed to the equivalent of room temperature (~ 23 °C) for an average of ~ 1.2 days—an estimate that aligns with the fact that despite losing power for 3-4 days, the freezers had not been opened.

3.4 Discussion

The fraction of albumin in the S-cysteinylated form, S-Cys-Alb, increases to a maximum value over time when P/S samples are exposed to temperatures above -30 °C (14). As shown here, S-Cys-Alb, rarely exceeds 40% in fresh P/S samples from cardiac patients (Fig. 3.3a). The range of S-Cys-Alb observed in fresh samples, however, overlaps with the range of maximum values of S-Cys-Alb observed after samples have

been intentionally incubated in the thawed state (Fig. 3.3a). These facts undermine the utilization of S-Cys-Alb as a biomarker of oxidative stress unless extreme care is taken to rigorously document specimen exposure to thawed conditions prior to measurement; they also preclude the use of S-Cys-Alb as a self-contained marker of P/S integrity.

Nevertheless, as also illustrated here, ΔS-Cys-Alb values are above 11% in most fresh plasma and serum samples (Fig. 3.3b; range: 12.1% - 29.2%; mean ± SD: 0.20 ± 0.04). This observed range of ΔS-Cys-Alb in P/S lies in-line with the theoretical range (11 – 39%) of ΔS-Cys-Alb that can be predicted based on the average plasma concentrations of albumin, Cys-Cys and Cys observed in the human population (79, 80, 104). This predicted range of ΔS-Cys-Alb does not consider the possibility that other P/S proteins, such as alpha-1-antitrypsin (111) may consume Cys-Cys/Cys equivalents in thawed P/S—potentially accounting for slightly lower mean values of ΔS-Cys-Alb than predicted in both plasma and serum.

The major source of the discrepancy in ΔS-Cys-Alb between matched plasma and serum samples was not the initial value of S-Cys-Alb but was rather the maximum value reached following incubation for 18 hrs at 37 °C (Fig. 3.3). This discrepancy is not observed in all samples; yet the source of the discrepancy is unclear as it is not related to the difference in pre-centrifugation delay between the matched serum and plasma samples, nor is it related to serum clotting time (Fig. 3.6). Neither is it related to the visually documented degree of hemolysis or the difference in degree of hemolysis between plasma and serum. Clotting factors such as Factor XIII contain free Cys residues and may consume some free Cys and/or Cys-Cys equivalents during the clotting process—which in some, but not necessarily all cases (Fig. 3.6) may consume a

significant portion of available free Cys and/or Cys-Cys equivalents, making these equivalents unavailable for reaction with albumin during serum storage. Regardless of the source of the modest difference between plasma and serum, the facts that 1) ΔS-Cys-Alb inevitably falls from the ranges in the preceding paragraph to zero once the relevant reactions (*Section 2.3.1.1 Reactions 1 and 2*) in *ex vivo* P/S samples have reached equilibrium (i.e., 18 hrs at 37 °C (Fig. 3.2), ~4 days at 23 °C (14) (*Figs. 2.5 and 2.7*), and ~ 60 days at -20 °C (14) (Fig. 3.7)), and 2) the S-Cys-Alb assay is highly precise (1.2% inter-assay precision on this scale) (14), support the utilization of ΔS-Cys-Alb as a marker of P/S exposure to thawed conditions.

Two other known potential assay confounders place only minor limits on such use of ΔS-Cys-Alb. First, patients with poor kidney function who require hemodialysis are susceptible to abnormally elevated levels of circulating Cys and Cys-Cys (112); they may also have elevated levels of S-Cys-Alb (113-116)—though these studies did not explicitly consider the possible *ex vivo* formation of S-Cys-Alb. Elevated S-Cys-Alb *in vivo* does not impact ΔS-Cys-Alb, but elevated circulating Cys and Cys-Cys may account for ΔS-Cys-Alb levels above 40%. Such samples would take slightly longer periods of time to reach the lower values of ΔS-Cys-Alb considered to represent samples exposed to thawed conditions. However, if the samples are known to come from kidney failure patients, this fact can be considered vis-à-vis the rate law established in *Chapter 2*. Second, human albumin mutations represent the only qualitative ΔS-Cys-Alb assay confounder. These are rare in most populations (with average rates of 0.001 – 0.03% (117))—but even if such samples were measured, the highly accurate mass spectrometry measurements of the

intact protein on which the ΔS-Cys-Alb assay is based would detect all but the inconsequential isobaric protein variants.

Conceptually, the development of a low-volume, inexpensive P/S integrity marker that is based on known chemical reactions and their established rate laws (i.e., mathematical model—*Chapter 2*) and can be used to forensically approximate the amount of time a specimen has spent at the equivalent of room temperature, represents a critical waypoint in biobanking QA. Yet its development does not represent a fix-all QA remedy: Ultimately, setting a ΔS-Cys-Alb cutoff that defines samples as "bad" depends on the intended use(s) of the samples. Moreover, prioritizing the tradeoff between keeping/using "bad" samples and throwing away "good" samples will always involve economic as well as scientific considerations. This means that functionally clarifying the meaning of QA marker measurements will always be context-dependent. However, because the kinetic behavior of ΔS-Cys-Alb has been well defined (at least at 23 °C), the only "added ingredient" necessary to link clinically important biomarkers of interest to ΔS-Cys-Alb is to *independently* characterize their empirical stability in P/S at room temperature—which is often done as part of careful analytical method development. Once this has been done, the time point at which initial instability occurred can be mapped to a clinical marker-specific ΔS-Cys-Alb cutoff vis-à-vis the kinetics model established in *Chapter 2*. This will allow the rapid, inexpensive, low-volume measurement of ΔS-Cys-Alb in unknown samples to provide direct insights into the validity of clinical biomarker measurements in any archived P/S specimen—regardless of their presumed storage and handling history.

Rate laws and mathematical modeling aside, the blind challenges conducted provide an empirical sense of the ability of ΔS-Cys-Alb to detect P/S exposures to thawed conditions. They also underscore the fact that very minor exposures to thawed conditions (e.g., 2 hrs at 23 °C; Fig. 3.4) can be detected. However, as would be the case with any QA marker, only in the context of distinct groups of samples that have been stored or handled separately—a scenario which is actually quite common amongst archived specimens that are brought together for a discovery or validation study. Assuming the averages and SDs observed here (Fig. 3.3) are representative of clinical biospecimens in general, measurement of ΔS-Cys-Alb in three P/S specimens from a questionable group will provide greater than 90% power to detect a value of ΔS-Cys-Alb that is significantly lower than 2 SDs below the mean values of ΔS-Cys-Alb found in the fresh P/S of cardiac patients here ($\alpha = 0.05$). That stated, testing all samples within a questionable group is the only way to ensure that only pristine samples that have experienced minimal exposure to temperatures above -30 °C are employed in clinical studies. Mistreatment of one-off, individual P/S specimens can also be detected—but this must be done based on absolute terms—i.e., detection of a ΔS-Cys-Alb value below a pre-established absolute threshold.

To set an optimal balance between type I and type II errors, the integrity threshold for ΔS-Cys-Alb in individual samples was established at 9.0%, which is 2.58 standard deviations below the mean value observed in combined fresh plasma and serum samples from nominally unhealthy patients (Fig. 3.3). The distribution of these values was Gaussian; thus, in theory, 99% of pristine samples would fall above this cutoff, while most samples that were moderately mistreated (e.g., 24 hrs at 23 °C or 7 days at 4 °C)

would fall below the cutoff. This proved to be true in practice (Fig. 3.4b), resulting in zero sample mischaracterizations in the individual-sample blind challenge. Clearly the chosen mistreatment conditions played a role in defining the success or failure of the blind challenge studies. The specific mistreatment conditions were chosen, however, because they represented realistic mild-to-moderate thawed-state conditions to which "real life" P/S samples may be exposed to during their lifetimes.

The realistic nature of thawed-state exposure conditions that result in ΔS-Cys-Alb values above zero but below the 9.0% threshold was proven in the case study of serum samples presented (Fig. 3.5). This case not only demonstrated the ability of ΔS-Cys-Alb to detect integrity problems in clinical samples that were considered on paper to be pristine, but also illustrated the ability of the associated rate law model to back-calculate the approximate time frame over which the samples were exposed to the equivalent of room temperature conditions. Age-weighted population averages of initial reactant and product concentrations were employed in this estimate. If ever deemed necessary however, age range-specific *in vivo* concentrations of albumin (105), Cys and Cys-Cys (79, 80) are available and can be employed in conjunction with the rate law. Rate law-based calculations of ΔS-Cys-Alb values vs. *ex vivo* time at 23 °C in persons under 60 (Table 3.2), over 60 (Table 3.3) and in U.S. population age-weighted group (Table 3.4) are provided for reference.

3.5 Conclusions

ΔS-Cys-Albumin, measured via a low-volume (≤ 10 μL), dilute-and-shoot, LC/MS assay, is an effective biomolecular oxidation-based QC/QA marker for P/S exposure to thawed conditions (i.e., > -30 °C). Though in need of fine tuning vis-à-vis

determination of the rate law for oxidation of Cys to Cys-Cys under conditions highly specific to *ex vivo* plasma and serum, the multi-reaction rate law governing the formation of S-Cys-Alb has been determined and empirically shown to be capable of accurately predicting S-Cys-Alb formation in P/S (*Chapter 2*); thus when population averages of the relevant reactants are assumed, the combined rate law facilitates estimation of the time frame over which P/S samples with unknown storage & handling histories have been exposed to the equivalent of room temperature conditions. As such, the stability of any clinical biomarker of interest can readily be linked to ΔS-Cys-Alb by conducting a room temperature stability study of the marker—regardless of the mechanism by which it exhibits its own instability. When P/S samples are grouped, ΔS-Cys-Alb can detect room temperature exposures as little as 2 hrs—yet ~3-4 days at room temperature are required for P/S samples to reach the ΔS-Cys-Alb minimum value of zero. Based on the survey of fresh, matched plasma and serum from cardiac patients reported here, as little as 3 representative samples from an unknown group are required to provide greater than 90% power to detect a ΔS-Cys-Alb value that is significantly lower than 2 SDs below the mean values of ΔS-Cys-Alb observed in fresh samples from cardiac patients ($\alpha = 0.05$). Mistreatment of individual samples can also be detected when their ΔS-Cys-Alb values are 2.5 SDs below these means (i.e., < 9%). ΔS-Cys-Alb identifies poor-quality P/S specimens and will, when properly deployed, prevent their inclusion in clinical research studies.

Figures

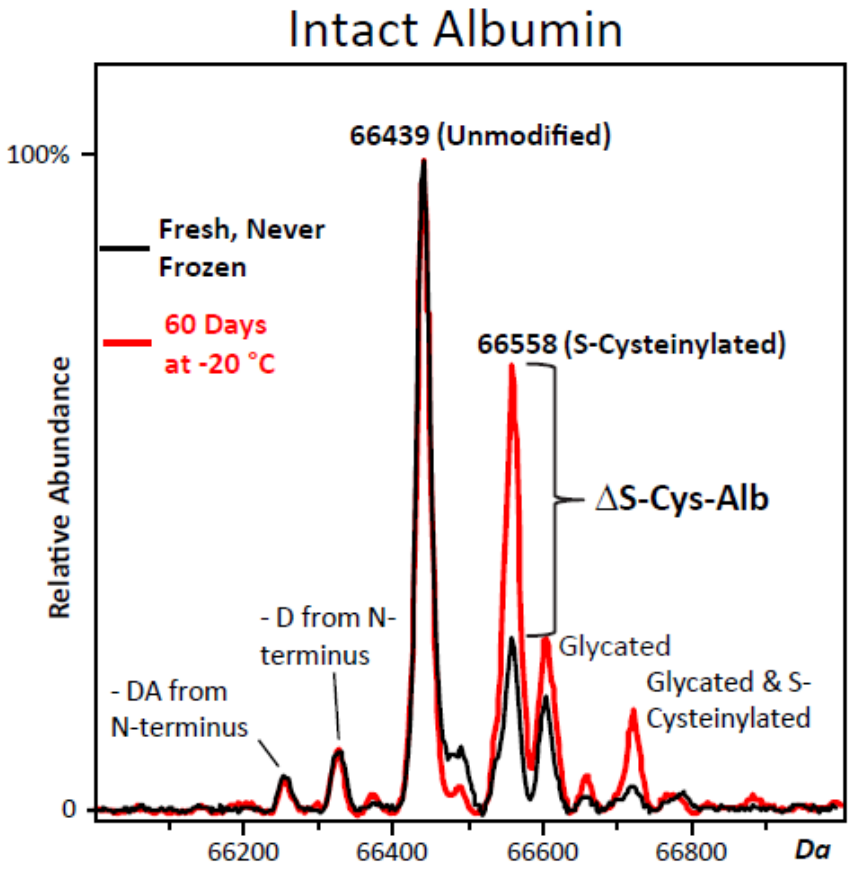

Figure 3.1: Charge deconvoluted ESI-mass spectra of albumin that illustrate ΔS-Cys-Alb. The black spectrum is from a fresh sample obtained immediately after centrifugation. The red spectrum is from the same sample stored for 60 days at -20 °C. As indicated, small fractions of albumin are N-terminally truncated, and both the native and S-cysteinylated forms may be glycated.

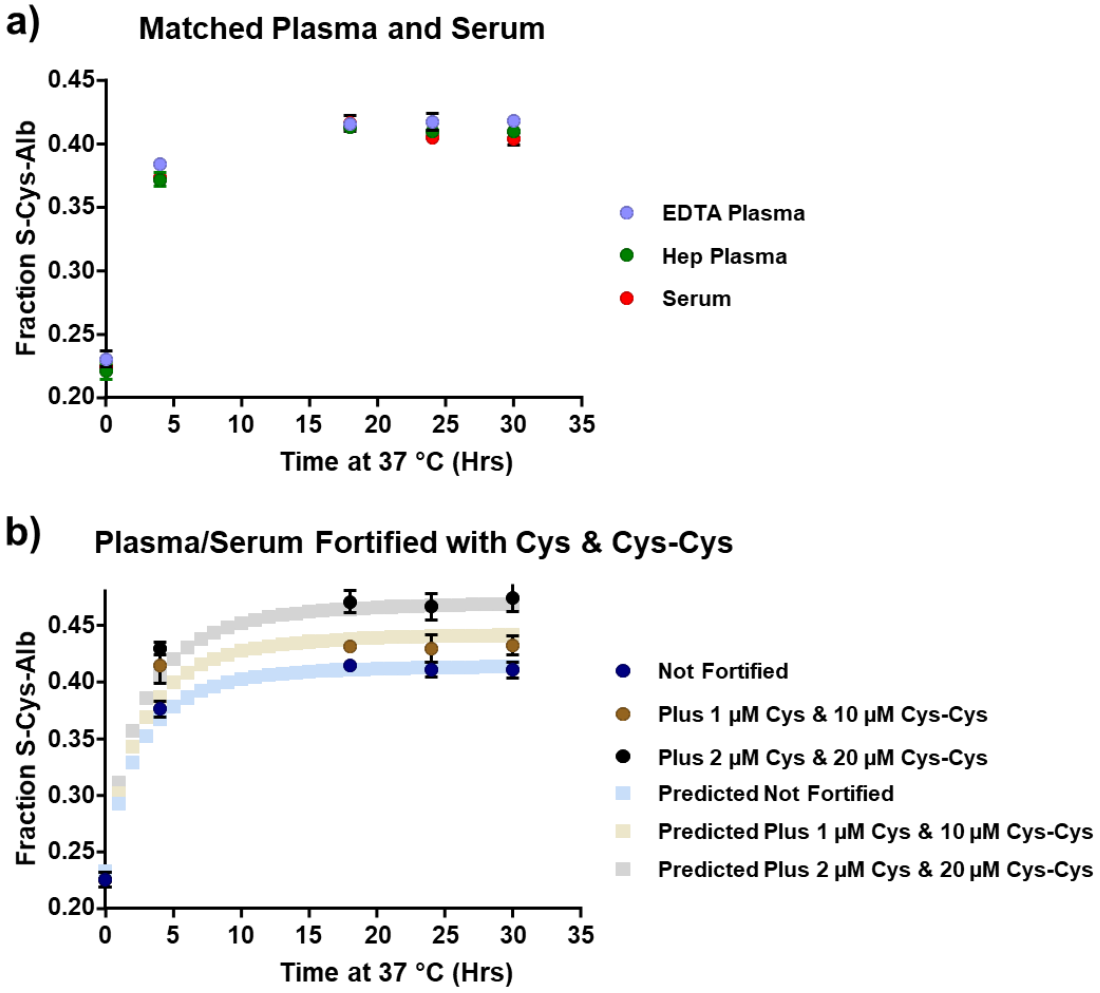

Figure 3.2: Determination of the time required at 37 °C to maximize S-Cys-Alb in P/S samples. a) Nine-microliter aliquots of matched K_2EDTA plasma, sodium heparin plasma, and serum from a healthy donor were incubated in closed vials at 37 °C for up to 30 hrs. No significant differences were found between plasma and serum or between the two types of plasma. No changes were observed after 18 hrs at 37 °C. n = 3 per data point; error bars represent SD. b) Each P/S sample was divided into 3 portions; one was left unmodified, to the second was added 1 µM Cys and 10 µM Cys-Cys, and to the third was added 2 µM Cys and 20 µM Cys-Cys. The addition of Cys and Cys-Cys results in an increase in the maximum value of S-Cys-Alb observed, but does not increase the time frame required to reach the maximum obtainable value of S-Cys-Alb at 37 °C. Obtained data agrees with the predicted data obtain using the determined rate law and the rate constants at 37 °C previously determined (81). Data from both types of plasma and serum were pooled and are displayed together as mean ± SD (n = 9 per data point).

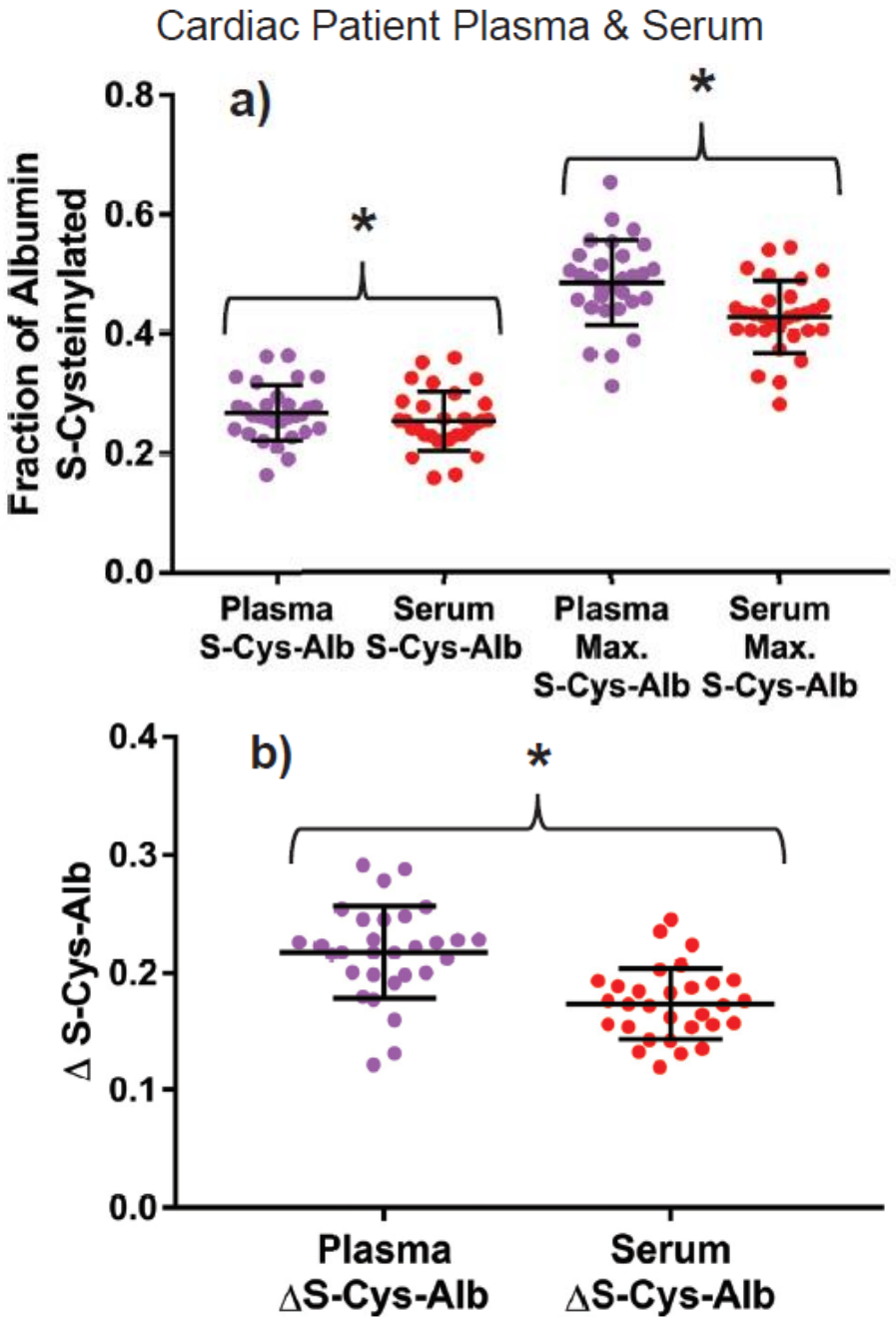

Figure 3.3: S-Cys-Alb and ΔS-Cys-Alb in fresh, rapidly processed samples from cardiac patients. a) S-Cys-Alb and maxed-out S-Cys-Alb observed in fresh samples from matched K_2EDTA plasma and serum samples from cardiac patients undergoing coronary angiogram, cardiac stress test and/or coronary computed tomography angiography. b) ΔS-Cys-Alb, calculated from panel a) by taking individual sample differences between maxed-out S-Cys-Alb and S-Cys-Alb. Error bars represent mean ± SD; n = 30 per group; * indicates a significant difference between means of indicated groups with $p < 0.0001$, paired t-tests.

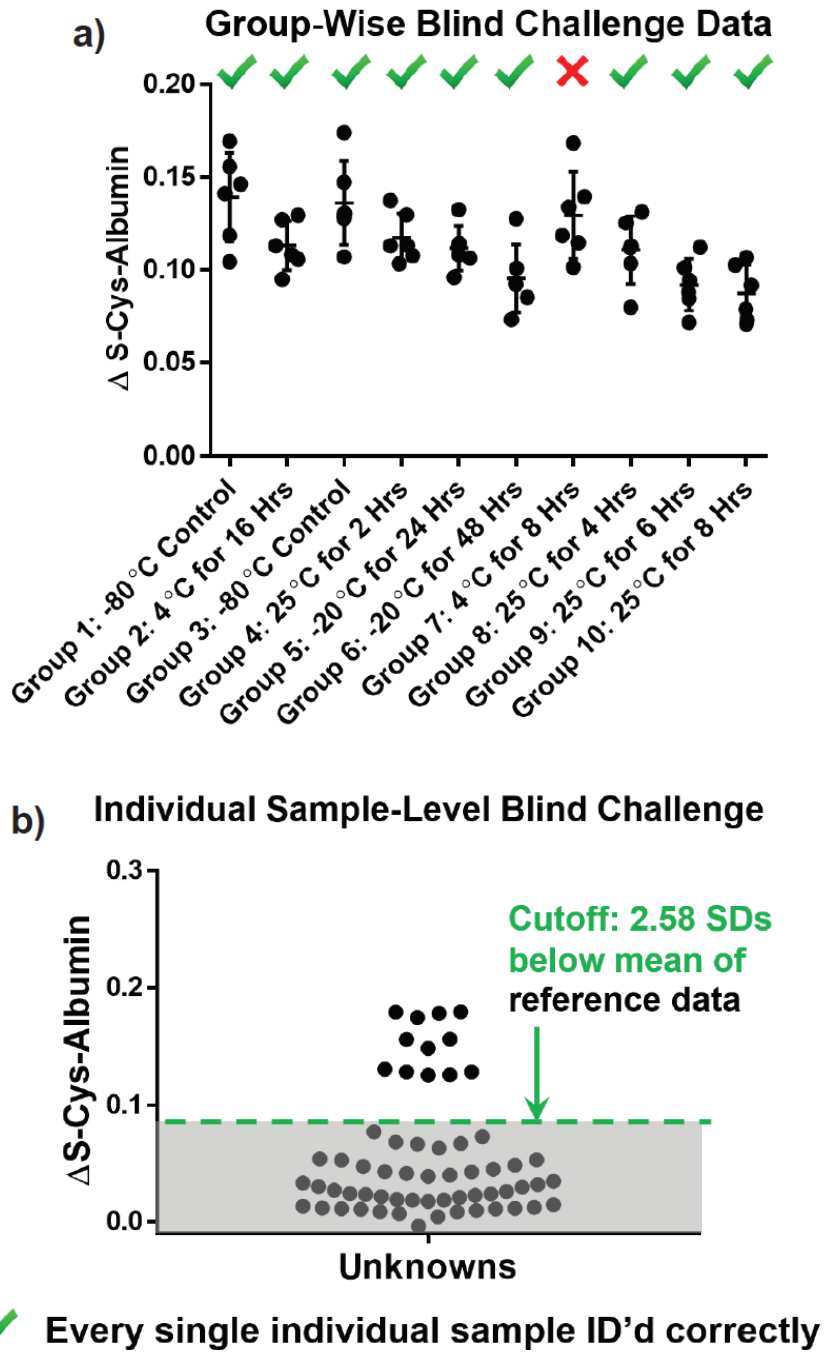

Figure 3.4: Results from blinded challenges of the ability of ΔS-Cys-Alb to distinguish a) *groups* of samples exposed to various thawed conditions (listed below each group), and b) *individual* samples exposed to various thawed conditions including 23 °C for 24 hrs, 23 °C for 48 hrs, 23 °C for 72 hrs, 23 °C for 7 days, 4 °C for 7 days, 4 °C for 14 days, -20 °C for 60 days, -20 °C for 90 days; controls kept at -80 °C.

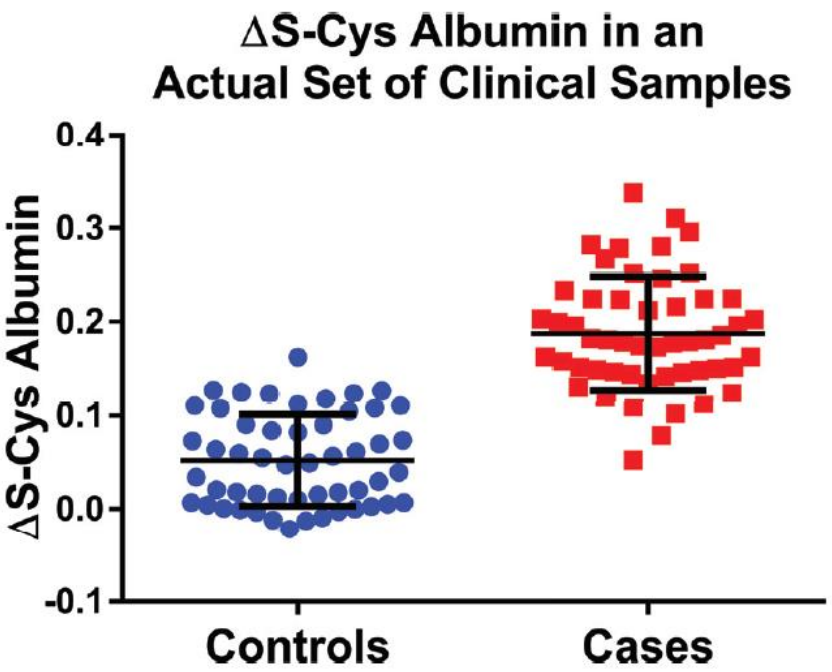

Figure 3.5: ΔS-Cys-Alb results from a case study of serum samples with an excellent pedigree but in which an integrity discrepancy was suspected (see main text for details). The values of ΔS-Cys-Alb in the controls barely overlapped with those of the cases (receiver operating characterisitic curve c-statistic = 0.96) and the mean value of ΔS-Cys-Alb was strongly significantly lower in the controls than it was in the cases ($p < 1$ x 10-20; two-tailed student's t-test). ΔS-Cys-Alb in the stage I lung cancer cases was essentially the same as it was in *fresh* samples from cancer free patients (cf. Figs. 3.3 and 3.4), meaning that the difference in ΔS-Cys-Alb between the cases and controls in this set cannot be due to the presence of cancer—leaving variable exposure to the thawed state as the only reasonable explanation for the difference observed. This was subsequently confirmed by the sample providers. Notably, the initial measurement of S-Cys-Alb revealed a clear (albeit less robust) separation between the controls and cases, but the maximum degree of S-Cys-Alb observed following the intentional incubation at 37 °C for 18 hrs did not vary between the controls and cases.

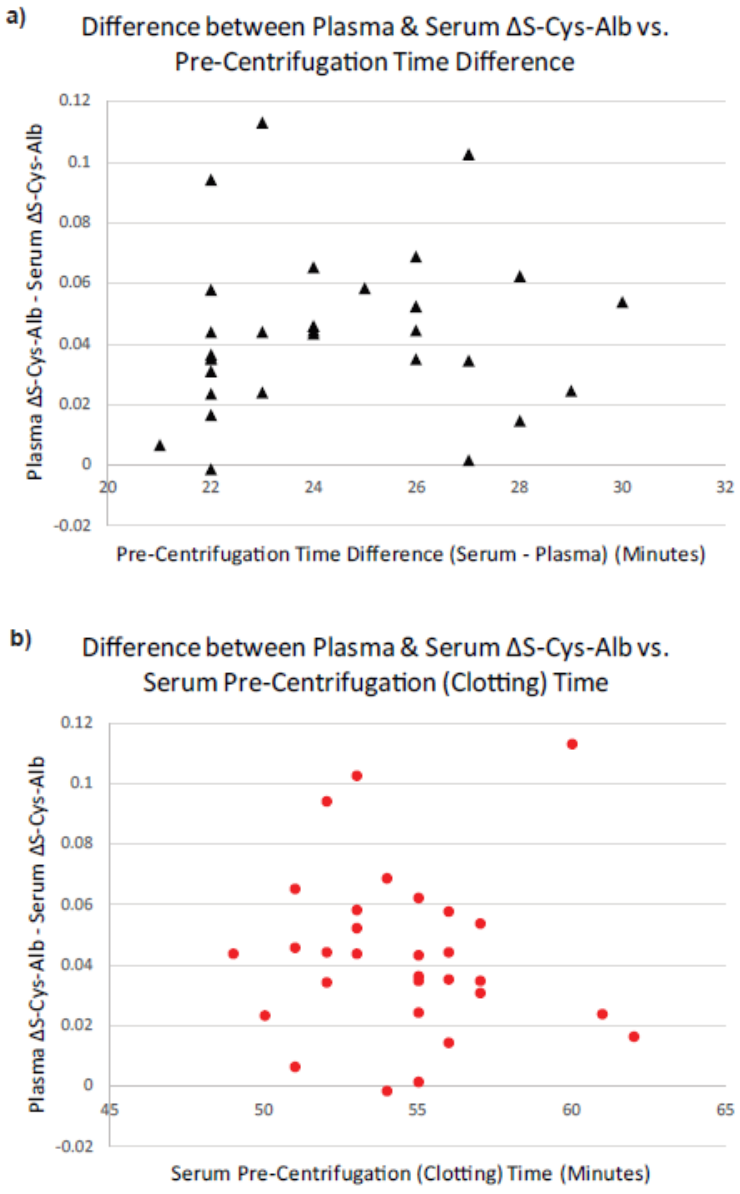

Figure 3.6: The *difference* between *matched* plasma and serum sample ΔS-Cys-Alb values was not correlated to a) the pre-centrifugation time difference between plasma and serum or b) serum pre-centrifugation (clotting) time. ($p > 0.5$ in both cases; Pearson correlation).

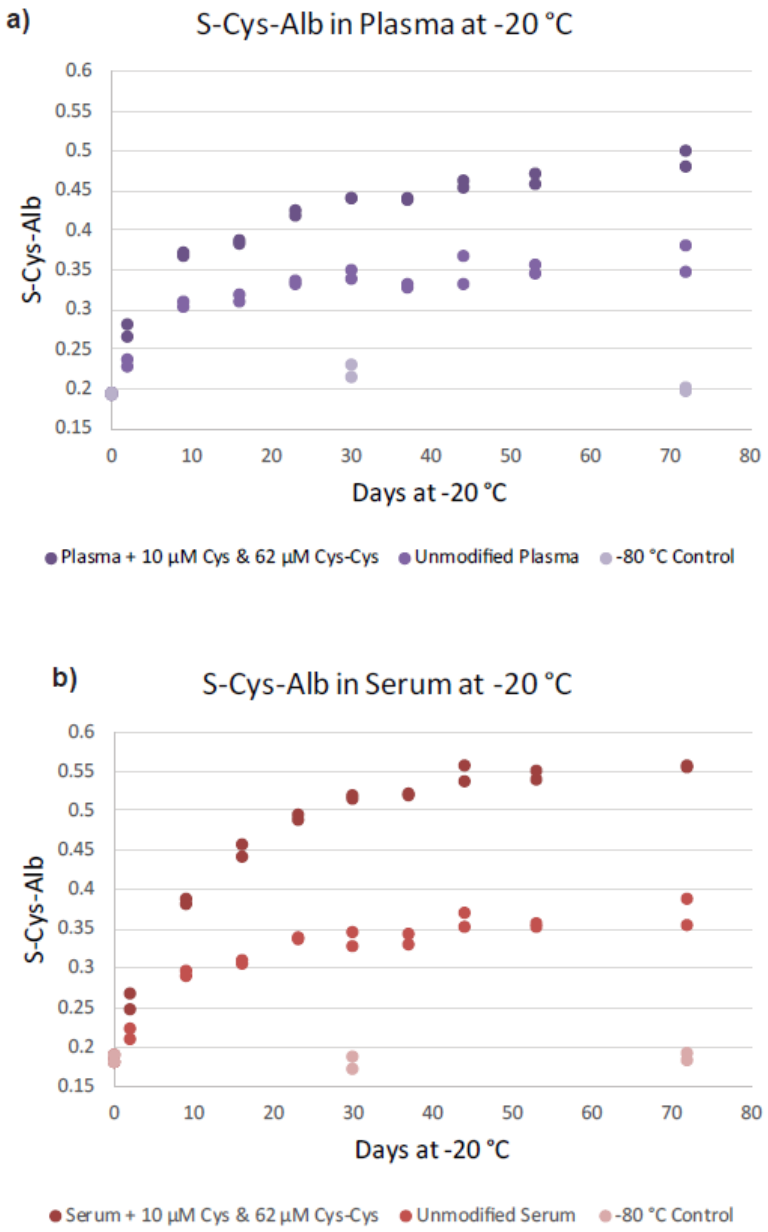

Figure 3.7: Time courses of S-Cys-Alb formation at -20 °C in matched a) plasma and b) serum with and without fortification with an extra 62 µM Cys-Cys and 12 µM Cys. Time points from unfortified control aliquots stored at -80 °C are shown for comparison.

Tables

Table 3.1: Assigned treatment conditions for the Individual and Group Blind challenge.

Individual Challenge	
Group	Treatment
1	-80°C
2	4° C for 7 days
3	-80°C
4	25°C for 24 hours
5	-20°C for 60 days
6	-20°C for 90 days
7	4°C for 14 days
8	25°C for 48 hours
9	25°C for 72 hours
10	25°C for 7 days

Group Challenge	
Group	Treatment
1	-80°C
2	4°C for 16 hours
3	-80°C
4	25°C for 2 hours
5	-20°C for 24 hours
6	-20°C for 48 hours
7	4°C for 8 hours
8	25°C for 4 hours
9	25°C for 6 hours
10	25°C for 8 hours

Table 3.2: Oxygen-independent rate law-based calculations of ΔS-Cys-Alb over time at 23 °C for people under 60 years. [a]

Under 60 Years Old [b]

	Serum	Plasma		Serum	Plasma
Time at Room Temperature (Hrs)	ΔS-Cys-Alb	ΔS-Cys-Alb	Time at Room Temperature (Hrs)	ΔS-Cys-Alb	ΔS-Cys-Alb
0	19.3	19.5	49	2.5	2.1
1	18.2	18.2	50	2.4	2.0
2	17.0	17.0	51	2.3	1.9
3	16.0	15.9	52	2.3	1.9
4	15.1	15.0	53	2.2	1.8
5	14.2	14.1	54	2.1	1.8
6	13.4	13.2	55	2.1	1.7
7	12.7	12.5	56	2.0	1.7
8	12.0	11.8	57	2.0	1.6
9	11.4	11.1	58	1.9	1.6
10	10.9	10.5	59	1.9	1.5
11	10.3	10.0	60	1.8	1.5
12	9.8	9.4	61	1.8	1.4
13	9.4	9.0	62	1.7	1.4
14	8.9	8.5	63	1.7	1.3
15	8.5	8.1	64	1.6	1.3
16	8.1	7.7	65	1.6	1.3
17	7.8	7.3	66	1.5	1.2
18	7.4	7.0	67	1.5	1.2
19	7.1	6.7	68	1.5	1.2
20	6.8	6.4	69	1.4	1.1
21	6.6	6.1	70	1.4	1.1
22	6.3	5.8	71	1.4	1.1
23	6.0	5.6	72	1.3	1.0
24	5.8	5.3	73	1.3	1.0
25	5.6	5.1	74	1.3	1.0
26	5.4	4.9	75	1.2	1.0
27	5.2	4.7	76	1.2	0.9
28	5.0	4.5	77	1.2	0.9
29	4.8	4.3	78	1.1	0.9
30	4.6	4.1	79	1.1	0.9
31	4.4	4.0	80	1.1	0.8
32	4.3	3.8	81	1.1	0.8
33	4.1	3.7	82	1.0	0.8
34	4.0	3.5	83	1.0	0.8
35	3.9	3.4	84	1.0	0.7
36	3.7	3.3	85	1.0	0.7
37	3.6	3.1	86	0.9	0.7
38	3.5	3.0	87	0.9	0.7
39	3.4	2.9	88	0.9	0.7
40	3.3	2.8	89	0.9	0.7
41	3.2	2.7	90	0.8	0.6
42	3.1	2.6	91	0.8	0.6
43	3.0	2.5	92	0.8	0.6
44	2.9	2.4	93	0.8	0.6
45	2.8	2.4	94	0.8	0.6
46	2.7	2.3	95	0.8	0.6
47	2.6	2.2	96	0.7	0.5
48	2.5	2.1			

[a] All initial concentrations are based on population averages, the sources of which are provided in the main text. Parameters common to all models: $k_3 = 0.13\ M^{-1}\ s^{-1}$, $K_y = 2.0 \times 10^{-6}$ M, $K_z = 3.5 \times 10^{-4}$ M, Cu(II) in plasma = 18.7×10^{-6} M (104), Cu(II) in serum = 9.35×10^{-6} M (half of plasma as per main text)

[b] $[Cys\text{-}Cys]_0 = 62 \times 10^{-6}$ M, $[Cys]_0 = 5 \times 10^{-6}$ M, Serum:$[AlbSH]_0 = 487 \times 10^{-6}$ M, $[SCysAlb]_0 = 166 \times 10^{-6}$ M, Plasma:$[AlbSH]_0 = 478 \times 10^{-6}$ M, $[SCysAlb]_0 = 175 \times 10^{-6}$ M. $[AlbSH]_0$ and $[SCysAlb]_0$ differ slightly in serum and plasma based on results shown in Fig. 3.3.

Table 3.3: Oxygen-independent rate law-based calculations of ΔS-Cys-Alb over time at 23 °C for people over 60 years. [a]

Over 60 Years Old [c]

	Serum	Plasma		Serum	Plasma
Time at Room Temperature (Hrs)	ΔS-Cys-Alb	ΔS-Cys-Alb	Time at Room Temperature (Hrs)	ΔS-Cys-Alb	ΔS-Cys-Alb
0	25.7	25.9	49	3.7	3.2
1	24.1	24.3	50	3.6	3.1
2	22.7	22.8	51	3.5	3.1
3	21.3	21.4	52	3.4	3.0
4	20.1	20.1	53	3.3	2.9
5	19.0	19.0	54	3.2	2.8
6	18.0	17.9	55	3.1	2.7
7	17.1	16.9	56	3.0	2.6
8	16.2	16.0	57	3.0	2.6
9	15.4	15.2	58	2.9	2.5
10	14.7	14.4	59	2.8	2.4
11	14.0	13.7	60	2.7	2.4
12	13.3	13.0	61	2.7	2.3
13	12.7	12.4	62	2.6	2.2
14	12.2	11.9	63	2.5	2.2
15	11.7	11.3	64	2.5	2.1
16	11.2	10.8	65	2.4	2.1
17	10.7	10.3	66	2.3	2.0
18	10.3	9.9	67	2.3	1.9
19	9.9	9.5	68	2.2	1.9
20	9.5	9.1	69	2.2	1.8
21	9.1	8.7	70	2.1	1.8
22	8.8	8.3	71	2.1	1.8
23	8.4	8.0	72	2.0	1.7
24	8.1	7.7	73	2.0	1.7
25	7.8	7.4	74	1.9	1.6
26	7.5	7.1	75	1.9	1.6
27	7.3	6.8	76	1.8	1.5
28	7.0	6.6	77	1.8	1.5
29	6.8	6.3	78	1.8	1.5
30	6.6	6.1	79	1.7	1.4
31	6.3	5.9	80	1.7	1.4
32	6.1	5.7	81	1.6	1.4
33	5.9	5.5	82	1.6	1.3
34	5.7	5.3	83	1.6	1.3
35	5.6	5.1	84	1.5	1.3
36	5.4	4.9	85	1.5	1.2
37	5.2	4.8	86	1.5	1.2
38	5.1	4.6	87	1.4	1.2
39	4.9	4.5	88	1.4	1.1
40	4.8	4.3	89	1.4	1.1
41	4.6	4.2	90	1.3	1.1
42	4.5	4.0	91	1.3	1.1
43	4.4	3.9	92	1.3	1.0
44	4.2	3.8	93	1.2	1.0
45	4.1	3.7	94	1.2	1.0
46	4.0	3.6	95	1.2	1.0
47	3.9	3.5	96	1.2	0.9
48	3.8	3.3			

[a] All initial concentrations are based on population averages, the sources of which are provided in the main text. Parameters common to all models: $k_3 = 0.13\ M^{-1}\ s^{-1}$, $K_y = 2.0 \times 10^{-6}$ M, $K_z = 3.5 \times 10^{-4}$ M, Cu(II) in plasma = 18.7×10^{-6} M (104), Cu(II) in serum = 9.35×10^{-6} M (half of plasma as per main text)

[c] $[\text{Cys-Cys}]_0 = 79 \times 10^{-6}$ M, $[\text{Cys}]_0 = 5 \times 10^{-6}$ M, Serum: $[\text{AlbSH}]_0 = 460 \times 10^{-6}$ M, $[\text{SCysAlb}]_0 = 157 \times 10^{-6}$ M, Plasma: $[\text{AlbSH}]_0 = 452 \times 10^{-6}$ M, $[\text{SCysAlb}]_0 = 165 \times 10^{-6}$ M. $[\text{AlbSH}]_0$ and $[\text{SCysAlb}]_0$ differ slightly in serum and plasma based on results shown in Fig. 3.3.

Table 3.4: Oxygen-independent rate law-based calculations of ΔS-Cys-Alb over time at 23 °C for US average age weighted population. [a]

Age-Weighted Population Average [d]					
	Serum	Plasma		Serum	Plasma
Time at Room Temperature (Hrs)	ΔS-Cys-Alb	ΔS-Cys-Alb	Time at Room Temperature (Hrs)	ΔS-Cys-Alb	ΔS-Cys-Alb
0	20.6	20.7	49	2.6	2.3
1	19.3	19.4	50	2.5	2.2
2	18.1	18.1	51	2.5	2.1
3	17.0	17.0	52	2.4	2.1
4	16.0	15.9	53	2.3	2.0
5	15.1	15.0	54	2.3	1.9
6	14.3	14.1	55	2.2	1.9
7	13.5	13.3	56	2.1	1.8
8	12.8	12.6	57	2.1	1.8
9	12.1	11.9	58	2.0	1.7
10	11.5	11.3	59	2.0	1.7
11	10.9	10.7	60	1.9	1.6
12	10.4	10.1	61	1.9	1.6
13	9.9	9.6	62	1.8	1.5
14	9.5	9.1	63	1.8	1.5
15	9.0	8.7	64	1.7	1.4
16	8.6	8.3	65	1.7	1.4
17	8.2	7.9	66	1.6	1.4
18	7.9	7.5	67	1.6	1.3
19	7.6	7.2	68	1.6	1.3
20	7.2	6.9	69	1.5	1.2
21	6.9	6.6	70	1.5	1.2
22	6.7	6.3	71	1.4	1.2
23	6.4	6.0	72	1.4	1.1
24	6.1	5.7	73	1.4	1.1
25	5.9	5.5	74	1.3	1.1
26	5.7	5.3	75	1.3	1.1
27	5.5	5.1	76	1.3	1.0
28	5.3	4.9	77	1.2	1.0
29	5.1	4.7	78	1.2	1.0
30	4.9	4.5	79	1.2	1.0
31	4.7	4.3	80	1.1	0.9
32	4.6	4.1	81	1.1	0.9
33	4.4	4.0	82	1.1	0.9
34	4.2	3.8	83	1.1	0.9
35	4.1	3.7	84	1.0	0.8
36	4.0	3.6	85	1.0	0.8
37	3.8	3.4	86	1.0	0.8
38	3.7	3.3	87	1.0	0.8
39	3.6	3.2	88	0.9	0.8
40	3.5	3.1	89	0.9	0.7
41	3.4	3.0	90	0.9	0.7
42	3.3	2.9	91	0.9	0.7
43	3.2	2.8	92	0.9	0.7
44	3.1	2.7	93	0.8	0.7
45	3.0	2.6	94	0.8	0.6
46	2.9	2.5	95	0.8	0.6
47	2.8	2.4	96	0.8	0.6
48	2.7	2.3			

[a] All initial concentrations are based on population averages, the sources of which are provided in the main text. Parameters common to all models: $k_3 = 0.13\ M^{-1}\ s^{-1}$, $K_y = 2.0 \times 10^{-6}$ M, $K_z = 3.5 \times 10^{-4}$ M, Cu(II) in plasma = 18.7×10^{-6} M (104), Cu(II) in serum = 9.35×10^{-6} M (half of plasma as per main text)

[d] $[Cys\text{-}Cys]_0 = 65.4 \times 10^{-6}$ M, $[Cys]_0 = 5 \times 10^{-6}$ M, Serum: $[AlbSH]_0 = 482 \times 10^{-6}$ M, $[SCysAlb]_0 = 164 \times 10^{-6}$ M, Plasma: $[AlbSH]_0 = 473 \times 10^{-6}$ M, $[SCysAlb]_0 = 173 \times 10^{-6}$ M. $[AlbSH]_0$ and $[SCysAlb]_0$ differ slightly in serum and plasma based on results shown in Fig. 3.3.

CHAPTER 4

EX VIVO GLYCATION OF HUMAN SERUM ALBUMIN

4.1 Introduction

Many of the naturally occurring (bio)chemical reactions in the plasma and serum (P/S) compartment of blood are not at equilibrium when blood exits the body (118). In addition, exposure of P/S to air results in a dissolved oxygen concentration that is much higher than that found in the P/S compartment of blood *in vivo*. Introduction of this relatively high dissolved oxygen concentration into P/S establishes numerous additional redox disequilibria that did not exist *in vivo*. As such, proper storage and handling conditions are critical for maintaining the quality of P/S samples (i.e., maintaining P/S in a state that accurately represents blood chemistry *in vivo*). Exposure to the thawed state permits (bio)chemical reactions to run toward equilibrium—a state that, for many reactions, does not represent biomolecular status *in vivo*. The thermodynamic melting of ice in plasma commences at -27 °C (119, 120). According to the European Pharmacopoeia, plasma is not completely frozen until -30 °C. (46, 99) (The 3 °C discrepancy is probably due to the fact that plasma does not exhibit simple eutectic behavior) (119, 121). Thus, storage and handling of P/S samples for prolonged periods above their melting point of -30 °C may compromise sample integrity, producing inaccurate and, in turn, misleading results in clinical research.

Numerous studies have demonstrated molecular alterations associated with inadequate sample handling and storage (14, 24-26, 45, 122). In a recent study, Pasella et al. found that plasma samples stored at various temperatures above -30 °C, including -20 °C, 4 °C, and room temperature (20-25 °C), showed an apparent variation in the

abundance of certain plasma proteins over a two-week period (24). A metabolomics study concluded that the concentrations of nearly 20% of the metabolites in serum samples are impacted by storage temperature (25). Another study showed that prolonged storage of either whole plasma or isolated plasma DNA had a substantial degradation effect on the DNA measured by real-time PCR-based assays (26). Betsou et al. have summarized other various biomolecules in P/S that can be altered *ex vivo* by poor handling and storage, ranging from simple ion concentrations to DNA and protein concentrations (45). Clearly, poor storage and handling can affect all types of molecules in P/S samples.

In vivo, P/S proteins undergo glycation through the conjugation of a reducing sugar monosaccharide (i.e. glucose) to the protein (usually via a lysine residue side chain) (*Fig. 1.2*). This process proceeds through the formation of a reversible Schiff base and later intramolecular rearrangements occur to form a stable, covalently-bonded Amadori product, which eventually leads to the formation of advanced glycation end-products (123). Protein glycation is an unavoidable process of metabolism *in vivo*. The degree to which it occurs is determined by the concentrations of protein and glucose available in P/S and can be measured through various methods, such as glycated hemoglobin (HbA1c) measurements, the fructosamine assay (124), or by measuring glycated albumin (GA) (125, 126). *In vitro*, dissolved oxygen has been shown to contribute to a process known as autoxidative glycation—a phenomenon that drives protein glycation above and beyond that observed in the absence of oxygen and which is likely to be relevant to P/S samples *ex vivo* (23, 127). This *ex vivo* glycation is similar to that observed in the S-Cysteinylation (oxidation) of human serum albumin.

In clinical laboratories, P/S storage time is generally kept to a minimum and therefore tends not to raise some of the potential integrity issues that can be found in research laboratories, where samples may need to be stored indefinitely. Clinicians employ HbA1c to gather an overall picture of what average blood sugar levels have been over a period of a few months in diabetic patients. Little et al. investigated the stability of HbA1c in whole blood samples kept at various storage conditions and determined that HbA1c was stable at -70 °C. However, when samples were stored at -20 °C they were only stable for 3-57 days, depending on the method of analysis (128). Another clinically relevant test to measure blood glucose levels is the fructosamine assay. Fructosamine reflects blood glucose levels over the previous 2-3 weeks and may be used to help a person with diabetes monitor and control their blood sugar. The fructosamine assay has limited clinical usage compared to that of HbA1c; for example, it is not recommended in cases where there are significant abnormalities of plasma protein concentrations (e.g., nephrotic syndrome, liver cirrhosis) (129). However, like the HbA1c test, storage conditions play a role in the stability of fructosamine in P/S. In 1988 a study was completed showing that fructosamine in serum is not stable when samples are stored at -20 °C for long periods of time (130). Since albumin is the most abundant protein in P/S, fructosamine is predominantly a measure of GA—though other circulating proteins such as glycated lipoproteins and glycated globulins do contribute to the total concentration of fructosamine (131). The concentration of GA can be directly measured by several methods, including gel electrophoresis, enzymatic methods, colorimetry, and immunoassays (125, 126, 132, 133). HbA1c remains the primary test for protein glycation that is used to monitor diabetes; however, studies have shown that GA may be

more reliable than HbA1c in certain instances—such as specific clinical conditions in which HbA1c does not work properly (e.g., iron deficiency, pregnancy, and end-stage renal disease) (134).

As mentioned above, when P/S samples are drawn from patients they are exposed to a dramatic increase in dissolved oxygen concentration. Considering that this spike in oxygen concentration may contribute to autoxidative glycation, this creates the potential for substantial increases in protein glycation as P/S samples are exposed to the thawed state. Previous work has analyzed the effect of storage and handling conditions on *ex vivo* protein oxidation, showing that exposure of P/S to temperatures above -30 °C can have a substantial impact on the oxidation status of albumin and apolipoprotein A-I—two of the most abundant proteins in P/S (14). The simple dilute-and-shoot LC-MS method used in this study provided easily interpreted mass spectra for the relative quantification of all intact albumin proteoforms. Here, a simple method to document how albumin glycation changes *ex vivo* under suboptimal storage and handling conditions and evaluate the impact of oxidative processes on the *ex vivo* glycation that takes place within P/S is implemented.

4.2 Materials and Methods

4.2.1 Materials and Reagents

Trifluoroacetic acid (TFA; Cat. No. 299537) and formic acid (06440) were purchased from Sigma-Aldrich (St. Louis, MO). Acetonitrile (L-16923) and HPLC grade water (L16978) were purchased from ThermoFisher Scientific (Waltham, MA). Hands-in-Bag atmospheric chamber (Cat. No. 15552-192) was purchased from VWR. Glucose Colorimetric assay kit (Cat. No. 10009582) was purchased from Cayman Chemical.

Compressed oxygen and nitrogen were obtained from Arizona State University Stores and were 99.999% and 99.99% pure, respectively.

4.2.2 Plasma and Serum

For the poorly controlled type 2 diabetic plasma sample involved in the multi-month time-course study (Fig. 4.1), fasting EDTA blood plasma was collected via venipuncture, under IRB approval at the University of Southern California. The sample was received frozen on dry ice. To avoid potential acidification of the plasma sample, vial headspace was cleared of carbon dioxide prior to thawing for aliquoting (135). Fifty-microliter aliquots were placed into each of three different types of vials for the long-term stability study at -20 °C: a cryogenic storage vial with inner threads and a sealing o-ring, a 1.5-mL snap-cap Eppendorf test tube, and a 1.5-mL snap-cap Eppendorf test tube with a ~2 mm hole punched in the top.

Additional matched, fasting EDTA plasma and serum samples were collected from several healthy volunteers, via venipuncture, under institutional review board approval at Arizona State University. The samples were collected according to the NIH's Early Detection Research Network blood collection standard operating procedures (71, 72). Within 35 minutes of collection, plasma samples were processed, aliquoted, and placed in -80 °C freezer; serum samples were placed at -80 °C within 95 minutes of collection. One or more of these P/S specimens were used for all experiments described below. Unless otherwise noted, aliquot volumes were 50 µL.

4.2.3 Measurement of Plasma Glucose Concentration

Plasma glucose concentrations were measured using the glucose colorimetric assay kit from Cayman Chemical (Product No. 10009582), following the standard

manufacturer-recommended protocol. A Thermo Scientific Multiskan GO Microplate Spectrophotometer was used to record sample absorbance values at 520 nm.

4.2.4 Incubation under Nitrogen or Oxygen

P/S samples were incubated in a chamber filled with either nitrogen or oxygen using the hand-in-a-bag setup. One sample was removed from the chamber at each time point. During removal of the samples from the chamber, a positive pressure was used to ensure that no air was able to enter the chamber. No attempt was made to sparge oxygen from the P/S samples prior to incubating them under the nitrogen atmosphere. This decision was made due to concerns about the overall effectiveness of such a procedure. Thus, a limited amount of oxygen must have been dissolved in these samples prior to their introduction into the nitrogen chamber.

4.2.5 Sample Preparation and Analysis

P/S samples were thawed at room temperature, mixed by vortexing, and then centrifuged at 13,000g for 1.5 min to sediment any particulates. 0.5 µL was removed and diluted into 500 µL of 0.1% (v/v) trifluoroacetic acid. 5 µL of this solution were injected without delay by a Spark Holland Endurance autosampler in microliter pick-up mode and loaded by an Eksigent nanoLC*1D at 10 µL/min using 80% water/20% acetonitrile with 0.1% formic acid onto a protein captrap (Michrom, city/country no longer commercially available) configured for unidirectional flow on a six-port diverter valve. The captrap was then washed for 3 min with this loading solvent. The flow rate over the protein captrap cartridge was then changed to 1 µL/min, and a linear gradient of increasing acetonitrile from 20% to 90% was employed to elute the proteins into the mass spectrometer. The captrap eluent was directed to a Bruker MicrOTOF-Q (Q-TOF) mass spectrometer

operating in positive ion, TOF-only mode, acquiring spectra in the m/z range of 300 to 3000 with a resolving power of ~20,000 m/Δm full width at half-maximum. Electrospray ionization settings for the Agilent G1385A capillary microflow nebulizer ion source were as follows: end plate offset -500 V, capillary -4500 V, nebulizer nitrogen 2 bar, and dry gas nitrogen 3.0 l/min at 225 °C. Notably, this electrospray ionization mass spectrometer has a source design in which the spray needle is kept at ground and the inlet of the instrument is brought to a high negative voltage (in positive ion mode). This design is important because it avoids the possibility of corona discharge and subsequent artifactual protein oxidation (33). Data were acquired in profile mode at a digitizer sampling rate of 2 GHz. Spectra rate control was by summation at 1 Hz.

4.2.6 Data Analysis

As previously described (14), approximately 1 minute of recorded spectra were averaged across the chromatographic peak apex of albumin. The electrospray ionization charge-state envelope was deconvoluted with Bruker DataAnalysis v3.4 software to a mass range of 1000 Da on either side of any identified peak. Deconvoluted spectra were baseline subtracted, and all peak heights were calculated, tabulated and exported to a spreadsheet for further analysis. Peak heights were used for quantification as opposed to peak areas, because of the lack of baseline resolution for some of the peaks. Representative raw mass spectra and their corresponding charge deconvoluted forms are provided in Figures 4.2 and 4.3.

Albumin has multiple glycation sites; thus, each molecule of albumin may contain multiple glycation states, a maximum of four glycation events per albumin molecule was observed—see (Fig. 4.4). The distribution of albumin in each of these four glycation

states can readily be determined via electrospray ionization MS. This degree of analytical clarity facilitates comprehensive molecular analysis of albumin glycation and is expressed here as weighted albumin glycation (WAG). To calculate WAG, the mass spectral peak heights of native (unmodified) albumin and of singly, doubly, triply, and quadruply glycated albumin are multiplied by 0, 1, 2, 3, and 4 respectively, before normalizing by the sum of these peak heights. The glycated *and* (simultaneously) S-cysteinylated albumin proteoform was not considered because at early time points the relative abundance of S-cysteinylated albumin is low, making determination of the glycated form of this oxidized proteoform difficult to distinguish from baseline noise. As S-cysteinylation increases during P/S exposure to the thawed state (14), glycation of the S-cysteinylated form becomes apparent. However, for consistency, only the non-S-cysteinylated form of albumin was considered in all calculations. Since S-cysteinylation does not impact glycation, including information from this proteoform would provide, at best, a duplicate measurement of albumin glycation. All statistical analyses were conducted with GraphPad Prism 7.

4.3 Results

4.3.1 Analytical Reproducibility and Autosampler Stability

The analysis of intact human albumin by LC-MS for relative quantification of its various proteoforms has been previously described (14, 136). However, to verify that this approach to measuring albumin glycation is reproducible, intra- and inter-day precision of the analytical method were evaluated. Plasma samples from three healthy males and three healthy females were analyzed in quadruplicate on three separate days. The average WAG in these samples was 14%. The average intra-day precision of WAG (expressed as

%CV) was 4.6%, and the total inter-day precision was 6.4%. For the studies described herein, samples were injected onto the LC-MS immediately following dilution in 0.1% TFA. Nevertheless, it was thought that it might be useful to evaluate the autosampler stability of the diluted samples. WAG was found to be stable for at least 1100 minutes (~ 18 hrs), which was the time required to run 96 samples (Fig. 4.5).

4.3.2 Impact of Storage Conditions on Albumin Glycation

The charge deconvoluted electrospray ionization mass spectra of albumin from a healthy fasting donor are shown in Fig. 4.6. The black spectrum represents a fresh, never frozen sample in which WAG was 17%. The red spectrum represents an aliquot of the same sample stored at -20°C for 60 days, after which time WAG increased to 23%. Raw spectra corresponding to the charge deconvoluted spectra shown in Fig. 4.6 are provided as Figures 4.2 and 4.3.

An increasing abundance of glycated albumin in plasma can be seen over time when samples are stored at -20°C and at room temperature (25°C)—both in a healthy donor and in a poorly controlled type 2 diabetic (pcT2D) patient (HbA1c > 10 and triglycerides > 1,000 mg/dL, with a history of coronary artery disease and myocardial infarction) (Fig. 4.7A). Both samples were collected and analyzed fresh (i.e., at time 0) prior to storage at -20 °C. Free glucose concentrations (± S.D.) in the healthy and pcT2D donor were determined in triplicate and found to be 78.8 ± 0.63 mg/dL (4.37 ± 0.035 mM) and 194 ± 7.3 mg/dL (10.8 ± 0.41 mM), respectively. Analysis of glycated albumin at time zero revealed 17% WAG for the healthy donor and 28% WAG for the pcT2D donor. Each sample was then aliquoted into three different vial types and stored in a manual-defrost freezer at -20 °C; an additional aliquot from the healthy donor was set

aside for the room temperature time course. When stored at -20 °C, samples from both donors exhibited significant increases in the amount of glycated albumin, reaching 34% WAG for the healthy donor and 66% WAG for the pcT2D donor over a time span of approximately 200 days (Fig. 4.7A). At room temperature, albumin glycation increased within hours, reaching its peak within a week (Fig. 4.7B). Samples stored at -80 °C did not show a significant increase in albumin glycation (Fig. 4.7A).

When the individual data points from the pcT2D sample aliquots stored at -20 °C were separated based on the type of vial in which the specimens were stored, a statistically significant trend emerged in which the aliquot in the snap-cap test tube without a hole exhibited the smallest increase in *ex vivo* glycation, followed by the cryogenic storage vial with inner threads and a sealing o-ring, while the snap-cap test tube with a hole punched in the top exhibited the greatest degree of *ex vivo* glycation (Fig. 4.8A; $p < 0.01$ for all three Wilcoxon matched pairs signed-rank comparisons. A Bonferroni correction for multiple comparisons set α at 0.017). These differences between storage vials were not as pronounced in the plasma specimen from the healthy patient (Fig. 4.8B); in this case the only significant difference observed between the three data series was between the aliquots stored in the snap-cap test tube without a hole and in the snap-cap test tube with a hole punched in the top ($p = 0.0034$).

4.3.3 Matched Plasma vs. Serum

Matched sets of EDTA plasma and serum were collected from two healthy male and two healthy female donors to evaluate potential differences between plasma and serum regarding initial measurements of albumin glycation. Plasma and serum samples were processed and aliquoted within 35 and 95 minutes of collection, respectively, and

then placed in -80 °C freezer until analysis. Average WAG ± S.D. in plasma was 17.7 ± 0.016; in serum it was 18.0 ± 0.015. A Wilcoxon matched pairs signed-rank test comparing plasma vs. serum revealed no significant difference in WAG between the two sample types.

4.3.4 Freeze-Thaw Cycles

To assess the effect of freeze-thaw cycles on albumin glycation, a plasma sample was collected from a healthy donor, measured immediately without ever being frozen (n = 6), then split into two separate vials. Both vials were then submitted to 20 freeze-thaw cycles (going from -80 ºC to room temperature then back to -80 ºC), with one vial subjected to opening and closing during each freeze-thaw cycle (to simulate aliquot withdrawal) and the other vial remaining sealed during each freeze-thaw cycle. There was no significant difference in albumin glycation between the fresh sample and either of the freeze-thawed samples. Opening the vials during the freeze-thaw cycles (to simulate aliquot withdrawal) did not have a significant effect on albumin glycation (Fig. 4.9).

4.3.5 Surface Area-to-Volume Effects

Because oxidation may play a role in *ex vivo* albumin glycation (23, 137), the effects of surface area-to-volume (sa/vol) ratio on albumin glycation were investigated at room temperature for up to 25 days by dividing a fresh plasma sample from a healthy donor into 100-µL, 200-µL, and 400-µL aliquots in cylindrical, 8-mm internal diameter polypropylene screw-cap test tubes. Additional 10-µL aliquots were placed into a 1.5-mL conical-bottom polypropylene snap-cap test tube to represent an extreme case of high sa/vol. The effect of plasma sa/vol ratio on glycated albumin over time is shown in Fig.

4.7. Samples that were stored at a higher sa/vol ratio experienced significantly greater *ex vivo* glycation than those stored at lower sa/vol ratios for the same period. On day 1, the only sample that had a significant difference in WAG was the smallest volume of 10 µL (i.e., largest sa/vol ratio). For days 3 and 18 there were significant differences between all sample volumes. On day 11 there were significant differences between all samples except for between 400 and 200 µL. Day 25 there were significant differences between the 10 µL sample and all other sample volumes (Fig. 4.7A). Significance was determined using ANOVA; for all significant differences indicated, Holm-Sidak's pairwise comparisons $p < 0.05$. As plasma sample sa/vol ratio increases there is an increase in WAG (Fig. 4.7B). Plasma albumin glycation for all days was positively correlated to the sample sa/vol ratio (Pearson correlation, $r \geq 0.9$, $p < 0.05$).

4.3.6 Effect of Atmospheric Oxygen

To investigate the effect of atmospheric oxygen on *ex vivo* albumin glycation, aliquots of plasma from a healthy donor (collected on a different day than the other samples employed in this study) were incubated under nitrogen or oxygen for 16 days. For nearly all time points, the samples incubated under oxygen exhibited higher levels of WAG than the samples incubated under nitrogen (Fig. 4.10). After propagating the error for all measurements (138) the average *difference* between all nitrogen and oxygen data points past time zero was found to be 0.022 ± 0.005 WAG units, which was significantly different from zero (Wilcoxon matched pairs signed-rank test; $p = 0.016$). As a control experiment, data were also collected from samples kept in air; these data points largely fell in between those of the nitrogen and oxygen data points (Fig. 4.10).

4.4 Discussion

Although plasma and serum samples may appear to be frozen at -20 °C, they are not fully frozen or chemically inactive at this temperature. Previously, it has been demonstrated that protein oxidation occurs slowly but inevitably when P/S samples are stored at -20 °C (14). Herein it is shown that glycation of albumin in blood plasma of both healthy and diabetic donors increases substantially over time at temperatures at or above the known plasma freezing point of -30°C (46, 99, 119, 120). It is important to note that when samples were stored at -80 °C there was no significant alteration of WAG *ex vivo* (Fig. 4.1A). This is consistent with the stability of protein glycation observed in other studies (139-141) as well as the stability shown for protein oxidation (14).

Samples shown in Figure 4.1 were collected fresh, at which point WAG in the healthy donor was 17% and WAG in the pcT2D donor was 28%. This difference in initial WAG values was expected based on the higher average concentration of blood glucose that is observed in T2D patients (142, 143) and reported above. Both samples experienced an *ex vivo* increase in albumin glycation: Over a time period of 268 days at -20 °C, the sample from the healthy donor increased to 34% WAG (a relative increase of 100%, Fig. 4.1A). After 229 days, the sample from the pcT2D donor increased to 66% (a relative increase of 136%, Fig. 4.1A). The large difference in the absolute increase in percent WAG can be explained by the fact that fasting plasma glucose in the pcT2D patient was nearly 2.5 times the concentration found in the healthy donor.

Watano et al. showed that GA in diabetics experienced a *relative* increase of 17% after 6 months and 73% after 12 months when serum was stored at -20 °C (141). The albumin-specific enzymatic method employed by Watano et al. accounts for multiple

glycation events per albumin molecule and is thus similar to our WAG metric. Differences in the relative increases in glycated albumin between our study and the Watano study might be accounted for by the concentration of free glucose in the samples when drawn, but these were not reported by Watano et al. (141). Notably, Watano et al. observed the greatest increases in GA between 6 and 12 months of their 12-month study, but the greatest increases in WAG in our study occurred within the first 6 months (Fig. 4.1A). The reason for this discrepancy in the kinetic profiles is unknown.

Though numerous groups have evaluated the stability of protein glycation *ex vivo* (139-141), the mechanism(s) behind observed increases in protein glycation in P/S have not been elucidated. *Ex vivo* increases in protein glycation are likely due to either of two mechanisms: First, the chemical reaction between glucose and protein may not be at chemical equilibrium *in vivo*. This mechanism is most likely to be relevant to proteins with short half-lives, albumin has a half-life of about 20 days (144). At 37 °C the rate constant for the overall rate-limiting formation of the Amadori product from the Schiff based intermediate is 0.026 hr^{-1} (145). As a first-order reaction, the half-life for the Schiff base intermediate is given by the equation $t_{1/2} = \ln 2/k$ and is therefore 26.7 hrs. Thus, the reaction can effectively be considered to be at equilibrium within one week—a time period well within the ~ 20-day half-life of albumin. Considered in conjunction with the fact that blood samples were drawn from fasting subjects, it is rather unlikely that the increase in albumin glycation observed *ex vivo* is simply due to chemical equilibration.

A second possible mechanism behind the *ex vivo* increase in albumin glycation is autoxidative glycation (23, 127). When P/S is exposed to air it takes on a dissolved oxygen concentration as high as 0.25 mM (88, 89)—a concentration far higher than that

found *in vivo* where oxygen in the blood is carried by hemoglobin inside of red blood cells. To begin to ascertain the role of oxidative processes in the *ex vivo* glycation of albumin in P/S, samples were incubated for several days under atmospheres of nitrogen or oxygen (Fig. 4.10). Starting at 18 hours glycation was, on average, elevated under an oxygen atmosphere relative to a nitrogen atmosphere. These results suggest that the mechanism underlying the *ex vivo* increase in albumin glycation involves molecular oxygen—a finding that is further substantiated by the facts that 1) increased plasma surface area-to-volume ratios enhanced the rate of *ex vivo* glycation (Fig. 4.7) and 2) plasma storage at -20 °C in vials with holes in them resulted in significantly greater *ex vivo* glycation than when the same sample was stored in vials without holes (Fig. 4.8).

The precise molecular mechanism of autoxidative glycation is not yet clear. In 1987 Wolff et al. first reported roles for transition metals and oxygen in the autoxidation of glucose (23)—a phenomenon that accounted for up to 45% of the covalent attachment of glucose to bovine serum albumin when the two components were incubated together in air. They postulated that the two-electron oxidation of glucose mediated by transition metals and molecular oxygen produced glucosone, an α-dicarbonyl derivative of glucose that readily reacts with protein amino groups. However, in 1995 Wells-Knecht and colleagues demonstrated that only arabinose and glyoxal (but not glucosone) are produced during the autoxidation of glucose, neither of which would result in a 162 Da mass shift upon attachment to a protein molecule. Moreover, they demonstrated that glucosone is not even an intermediate in the formation of arabinose or glyoxal during the oxidative degradation of glucose (137). This being the case, the only way to reconcile the findings of these two groups with the findings that a 162-Da molecule attaches to

albumin during exposure of P/S to thawed conditions is to propose that the enediol radical anion of glucose that has been postulated to form upon initial one-electron oxidation (23) reacts directly with albumin (rather than a molecule of oxygen or a transition metal atom, which facilitates the second-electron oxidation of glucose in the Wolff mechanism (23)) (Fig. 4.11). Considering that the total concentration of free transition metals in P/S is in the low micromolar range and that the concentration of oxygen in P/S is, at maximum, approximately 0.25 mM (88, 89) but the concentration of albumin is higher—at approximately 0.65 mM (146) (putting the total number of reactive amino-group equivalents with albumin in the millimolar range), this mechanism for the oxidative *ex vivo* glycation of albumin in P/S may be viable—though it has yet to be proven.

4.5 Conclusion

In conclusion, this study demonstrated that albumin glycation increases substantially *ex vivo* when fasting P/S specimens from either healthy subjects or diabetics are stored at -20 °C or otherwise subjected to temperatures above their melting point of -30 °C. The mass spectra employed to quantify albumin glycation revealed the presence of multiple glycation events per albumin molecule (Fig. 4.4), affording the opportunity to account for these events in a metric referred to here as weighted albumin glycation. Furthermore, experiments conducted under atmospheres of nitrogen vs. oxygen in conjunction with studies on the impact of P/S surface area-to-volume ratio strongly suggested a role for autoxidative processes during the *ex vivo* glycation of albumin in human P/S.

Figures

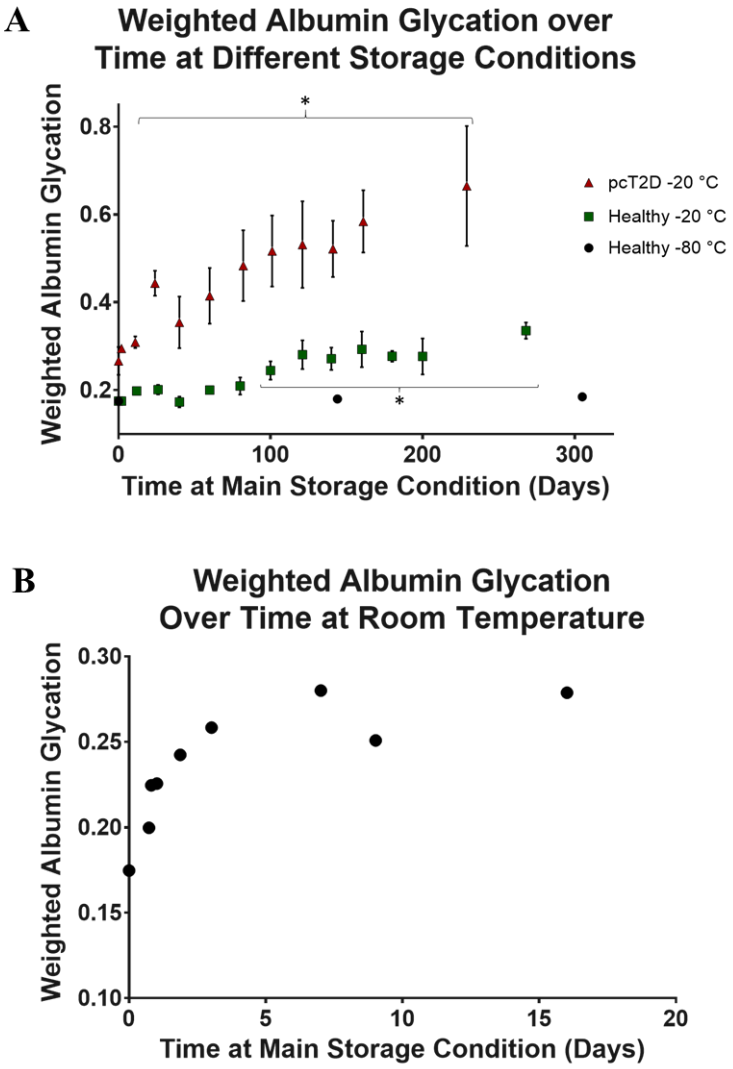

Figure 4.1: WAG in plasma over time at -80°C and -20°C (manual defrost freezers) (A), and at room temperature (25°C) (B). One sample was collected from a healthy donor and a second sample was obtained from a poorly controlled type 2 diabetic (pcT2D) with an HbA1c greater than 10 and a history of coronary artery disease and myocardial infarction. Both samples were collected and analyzed fresh, starting on Day 0—at which time WAG in the healthy and pcT2D samples was 17% and 28%, respectively. At -20°C albumin glycation nearly doubled in both the healthy and pcT2D samples after about 200 days. Samples stored at -80°C did not show an increase in WAG. Shown is the mean ± S.D. of the three aliquots per point. (* Indicates a significant difference from the initial time point; Repeated measures ANOVA, $p < 0.0001$ for all Tukey pairwise comparisons). An additional aliquot from the healthy donor was set aside for the room temperature time course. At room temperature (B), albumin glycation increased within hours, reaching its peak within two weeks.

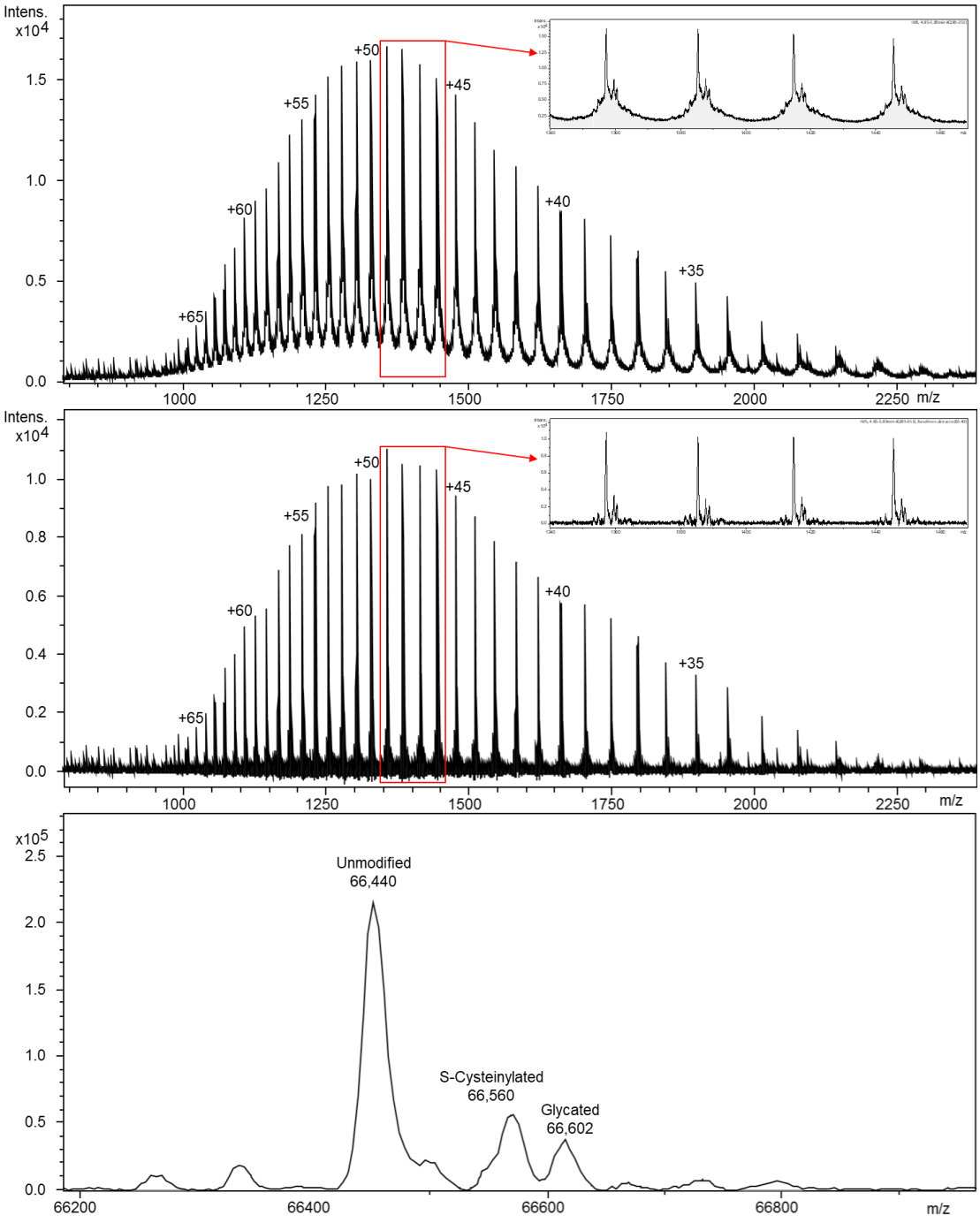

Figure 4.2: Raw (top), baseline subtracted (middle), and charge deconvoluted mass spectra (bottom) of a fresh never frozen plasma sample.

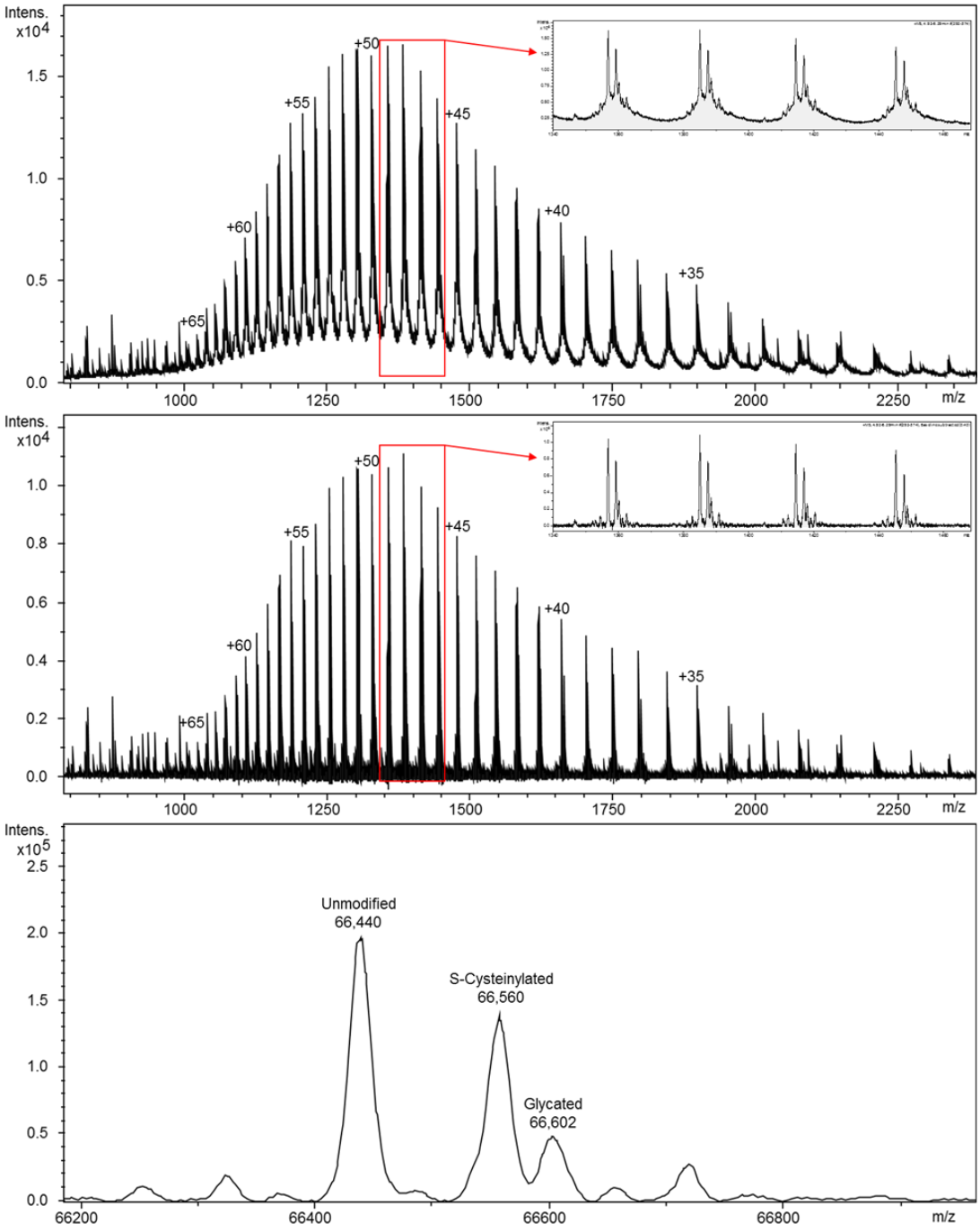

Figure 4.3: Raw (top), baseline subtracted (middle), and charge deconvoluted mass spectra (bottom) of the same sample as in Fig. 4.2 but has been stored for 60 days at -20 °C.

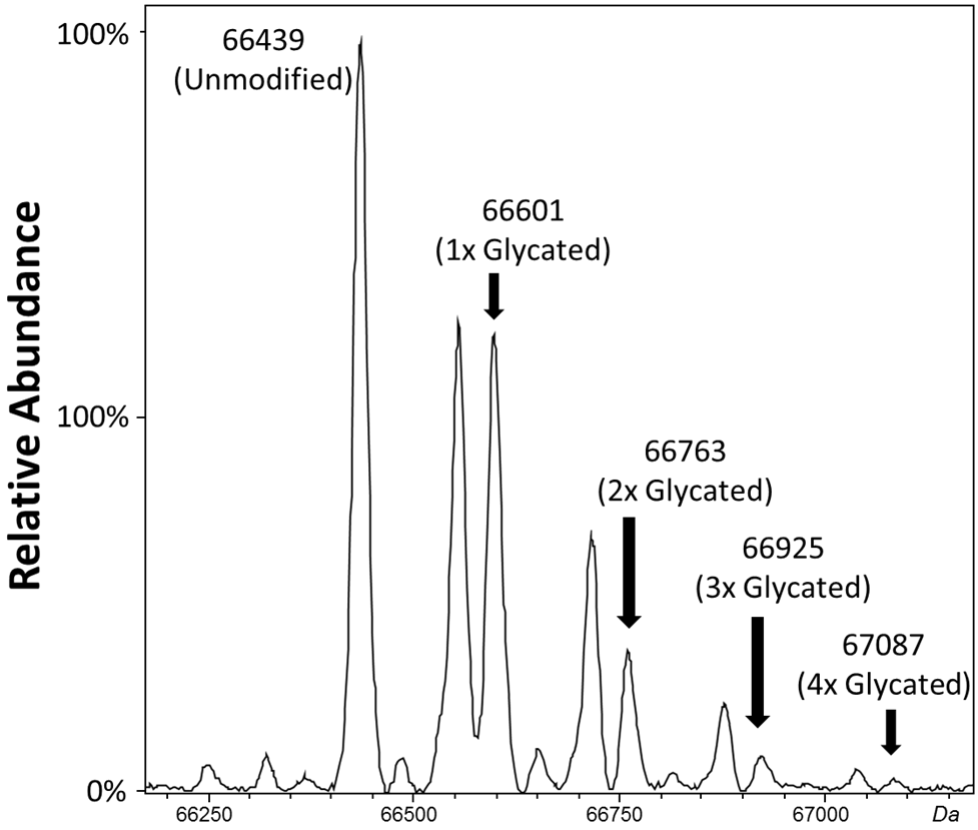

Figure 4.4: Each molecule of albumin may contain multiple glycation states a maximum of four glycation events per albumin molecule was observed in the pcT2D samples.

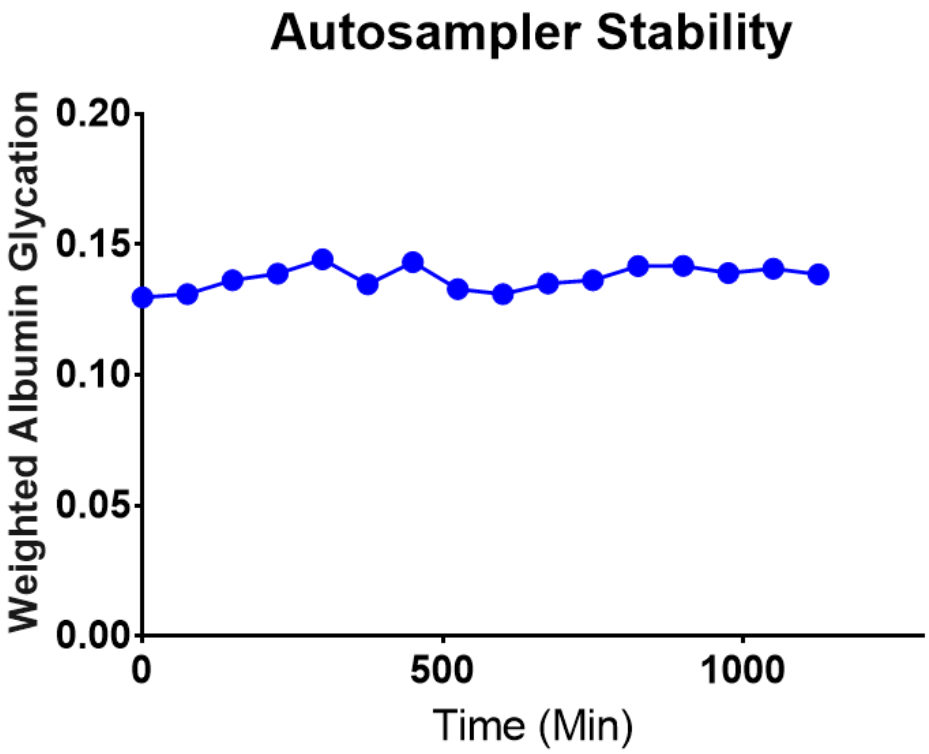

Figure 4.5: Weighted albumin glycation measurements were stable for at least 18 hours when pre-diluted samples were placed on an autosampler held at 8 ºC.

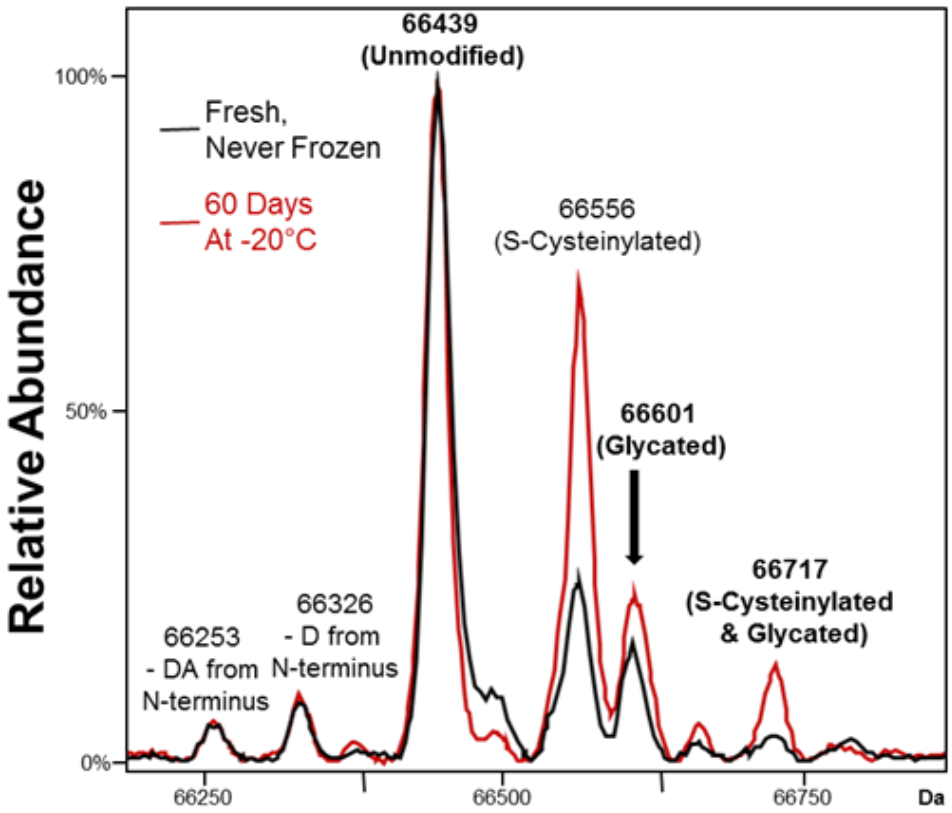

Figure 4.6: Charge deconvoluted electrospray ionization mass spectra of albumin from a healthy donor showing an increase in glycated albumin under less-than-ideal storage conditions. The black spectrum is from a fresh, never frozen sample. The red spectrum is from the same sample stored at -20 °C for 60 days.

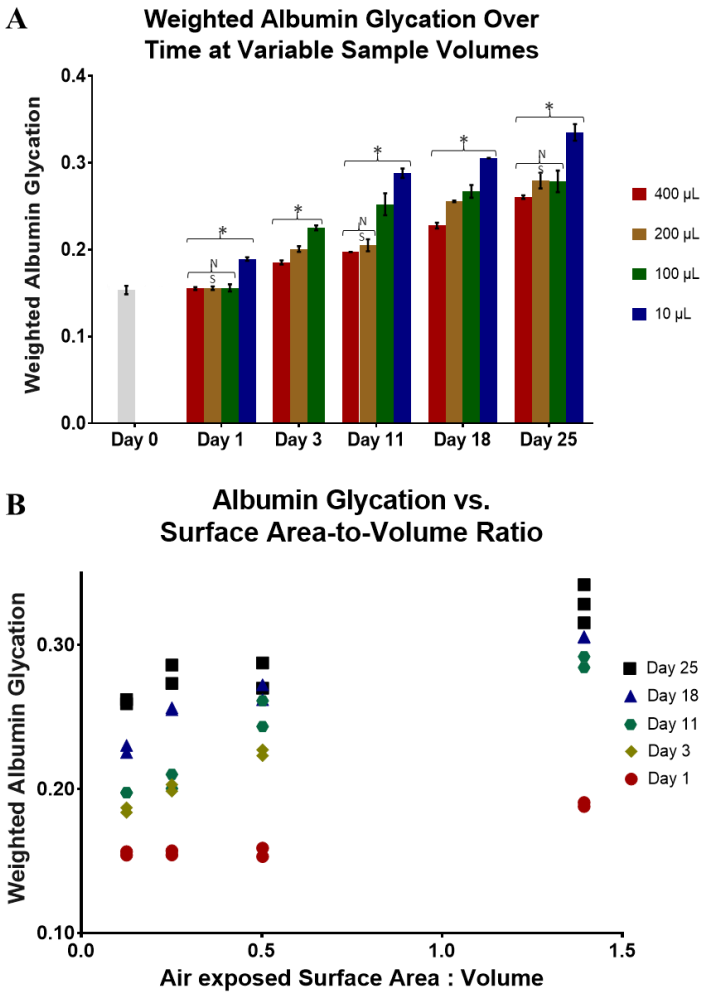

Figure 4.7: Effect of surface area-to-volume ratio on the *ex vivo* increase in plasma albumin glycation at room temperature. WAG in plasma samples of different volumes over time at room temperature (A), each of which had a different surface area-to-volume ratio (B). Bar graphs represent the average of duplicate analyses with the error bars representing the actual points. On day 1 there was a significant difference between the 10 µL sample and all other samples. On day 3 and 18 there was a significant difference between all volumes (i.e., surface area-to-volume ratios). For day 11, there was a significant difference between all volumes except 400 and 200 µL. On day 25 there was a significant difference between the 10 µL sample and all other sample volumes. (* Represents a significant difference between surface area-to-volume ratios as determined by ANOVA; $p < 0.05$ for all Holm-Sidak's pairwise comparisons. "NS" indicates that the bracketed samples were not significantly different.). Individual data points are shown in the scatter plot (B). In this plot, the sample with the highest sa/vol ratio corresponds to the lowest-volume sample (10 µL) shown in (A); accordingly, sa/vol ratios decrease (B) as volume increases (A). For all days sa/vol ratios were positively correlated with albumin glycation (Pearson Correlation, $r \geq 0.9$, $p < 0.05$).

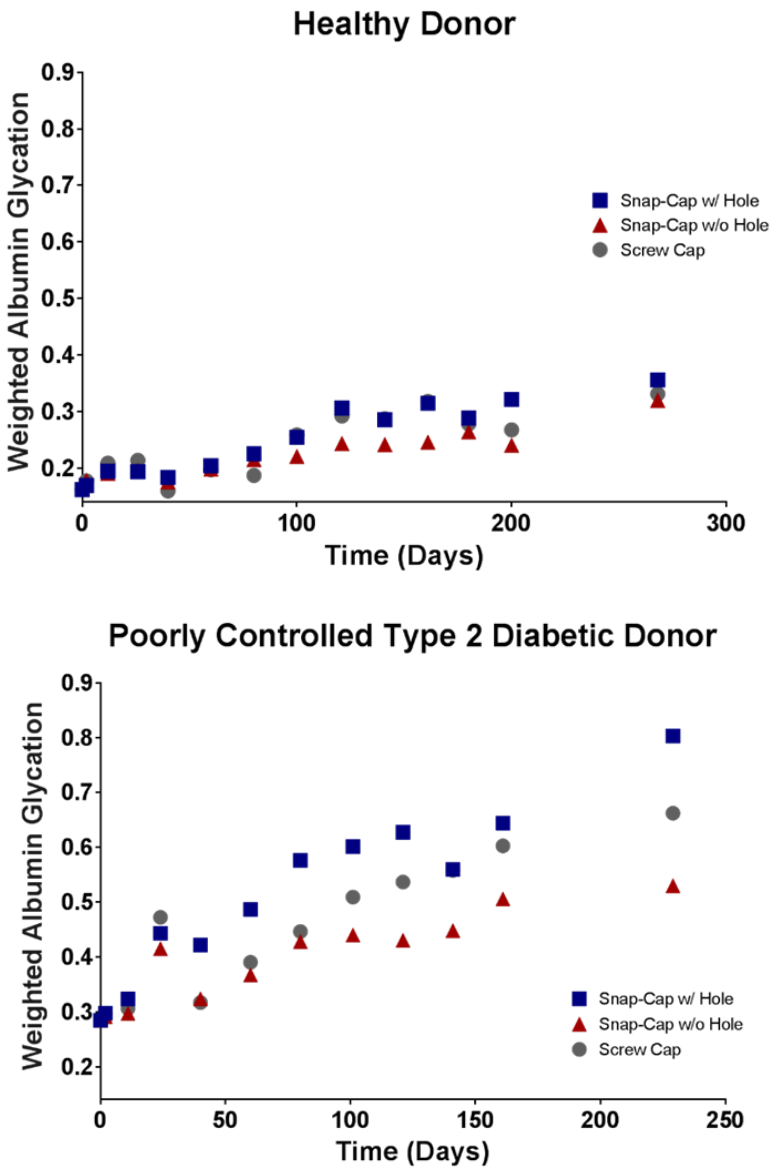

Figure 4.8: Weighted albumin glycation over time in samples stored at -20 °C in different vial types. These data are the same as those shown in Fig. 3 for the pcT2D sample (A) and the healthy donor sample (B), but expanded in detail based on the vial type in which each of the 3 aliquots per patient were stored. (In Fig. 3 each of the three vial types was considered a replicate sample.) For the pcT2D plasma sample (A) statistically significant differences were observed between all 3 vial types ($p < 0.01$ for all three Wilcoxon matched pairs signed-rank comparisons. A Bonferroni correction for multiple comparisons set α at 0.017). The differences between storage vials were not as pronounced in the plasma specimen from the healthy patient (B); in this case the only significant difference observed between the three data series was between the aliquots stored in the snap-cap test tube without a hole and in the snap-cap test tube with a hole punched in the top ($p = 0.0034$).

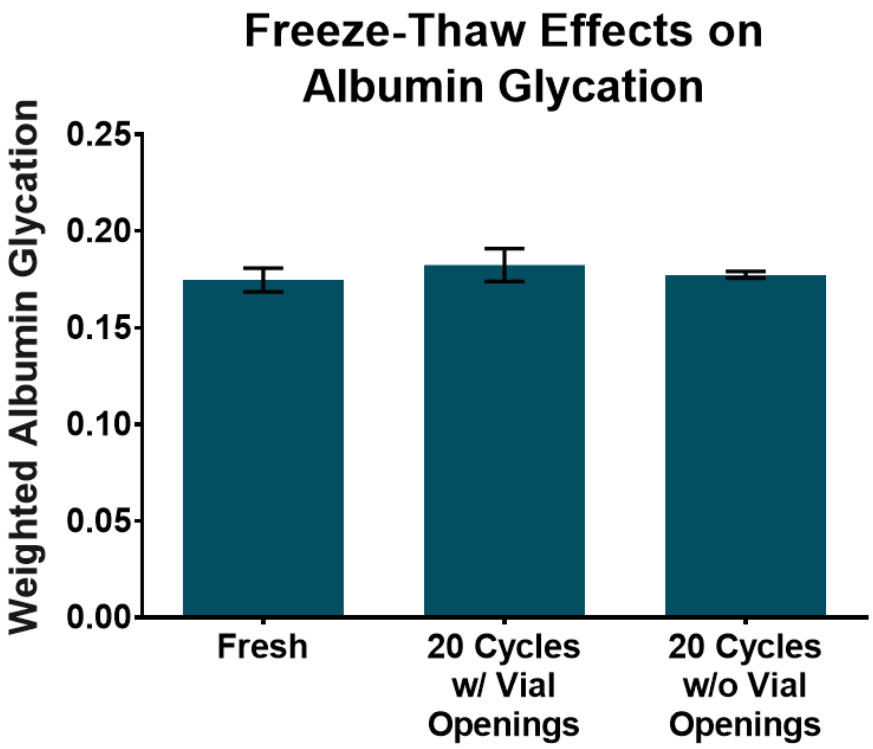

Figure 4.9: Effect of freeze-thaw cycles on weighted albumin glycation. Following initial analysis (n = 6 technical replicates), a fresh plasma sample from a healthy donor was split into two cryogenic storage vials, each of which was subjected to 20 freeze-thaw cycles prior to analysis in triplicate (mean ± S.D. shown). One vial was opened at each thaw cycle, and the other vial was not opened until 20 freeze-thaw cycles were completed. There was no significant difference between the fresh and incubated samples (Repeated measures ANOVA, $p = 0.66$).

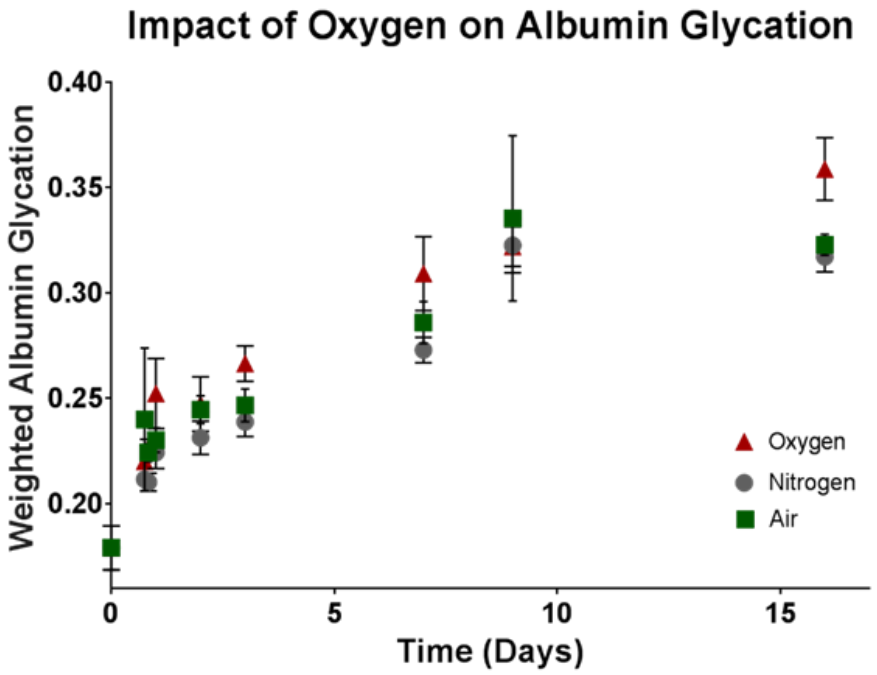

Figure 4.10: Role of atmospheric oxygen on the *ex vivo* glycation of albumin in blood plasma. WAG in healthy-donor plasma kept under pure nitrogen, pure oxygen or air at room temperature (n = 3 aliquots measured per data point). Significant differences were observed between the nitrogen and oxygen series ($p = 0.016$) and the nitrogen and air series ($p = 0.008$), but not between the air and oxygen series (Wilcoxon matched pairs signed-rank test; a Bonferroni correction for multiple comparisons set α at 0.017 instead of 0.05).

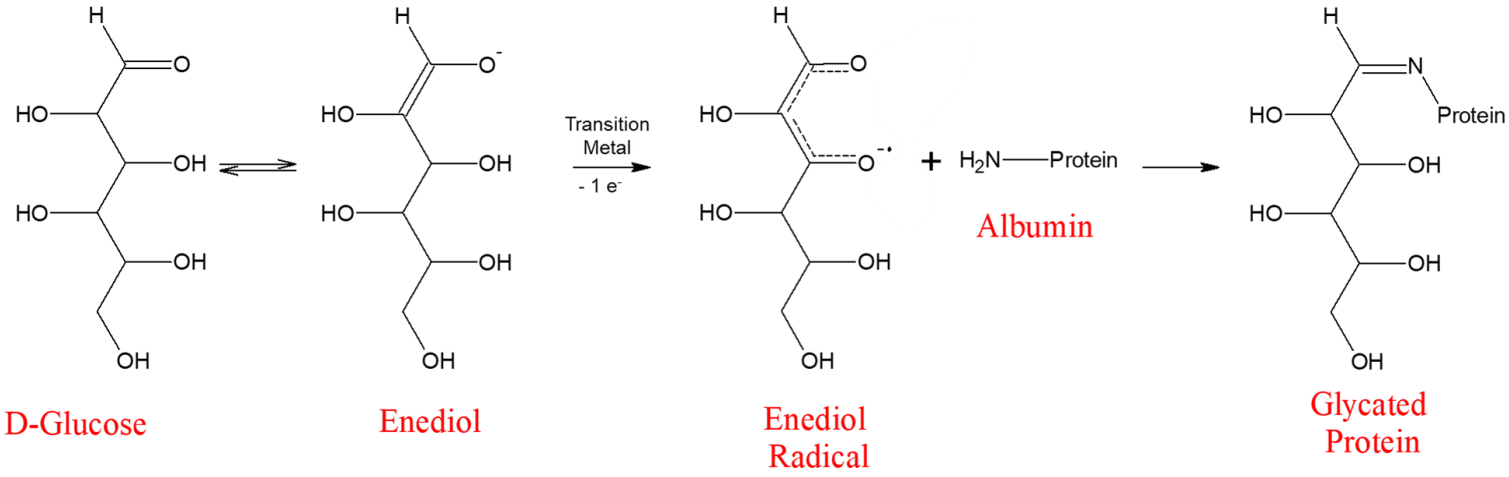

Figure 4.11: Proposed route of albumin *ex* vivo glycation that the enediol radical anion of glucose that has been postulated to form upon initial one-electron oxidation (23) reacts directly with albumin in place of oxygen or transition metals.

CHAPTER 5

CONCLUSIONS AND FUTURE DIRECTIONS

Collection, processing, storage and handling expose biospecimens to pre-analytical variables that have the potential to produce misleading results in downstream clinical research. Most investigators know that P/S should be stored at -80 °C. As it is clearly demonstrated here, simply accepting that SOPs were followed (with or without a detailed paper trail as evidence) or just simply accepting that specimens were stored at -80 °C after initial collection and processing, represents a naïve approach to clinical research.

The rate law for the *ex vivo* formation of S-Cys-Alb at room temperature has been determined. And with the simple, low-consumption, ΔS-Cys-Alb assay, it is now relatively quick and easy to identify archived samples that are not suitable for a particular study. With the proper implementation of this ΔS-Cys-Alb assay, in connection with the determined rate law, research studies that use improperly stored and handled P/S samples will become a thing of the past.

Efforts are underway to develop a comprehensive rate law-based model that considers oxygen and all relevant metals (e.g., copper and iron) within their P/S-liganded context across the range of temperatures likely to be encountered by P/S samples (e.g., 4 °C and -20 °C). While the first critical steps in this direction have been taken, establishing a fully comprehensive rate law will facilitate the most accurate possible linkage of ΔS-Cys-Alb to the stability of clinically important analytes in P/S, merely by defining the stability limitations of the clinical analytes themselves. That is, if proper

analytical assay development guidelines are followed and stability studies are conducted on P/S samples during clinical marker assay development, then every clinical analyte will *automatically* be linked to ΔS-Cys-Alb by virtue of the ΔS-Cys-Alb rate law. This represents a far more efficient approach to establishing a global marker of P/S integrity than any in which an integrity marker is simply empirically measured in parallel with the clinical marker in order to establish a linkage between the two.

For clinical research that employs archived P/S samples, the quality of samples should be of primary concern. While no widely accepted gold standard marker of P/S integrity has been established, this work represents an important step in that direction. The research presented here provides a robust, mechanistically understood tool to assess the integrity of the already innumerable pre-existing P/S specimens—and thus contribute substantially to decrease the large number of false leads produced in biomarker research.

REFERENCES

1. Gros, F., Hiatt, H., Gilbert, W., Kurland, C. G., Risebrough, R. W., and Watson, J. D. (1961) Unstable ribonucleic acid revealed by pulse labelling of Escherichia coli. *Nature* 190, 581-585

2. Brenner, S., Jacob, F., and Meselson, M. (1961) An unstable intermediate carrying information from genes to ribosomes for protein synthesis. *Nature* 190, 576-581

3. Minguez, P., Letunic, I., Parca, L., and Bork, P. (2013) PTMcode: a database of known and predicted functional associations between post-translational modifications in proteins. *Nucleic Acids Res* 41, D306-311

4. Minguez, P., Parca, L., Diella, F., Mende, D. R., Kumar, R., Helmer-Citterich, M., Gavin, A. C., van Noort, V., and Bork, P. (2012) Deciphering a global network of functionally associated post-translational modifications. *Mol Syst Biol* 8, 599

5. Santos, A. L., and Lindner, A. B. (2017) Protein Posttranslational Modifications: Roles in Aging and Age-Related Disease. *Oxid Med Cell Longev* 2017, 5716409

6. Xin, F., and Radivojac, P. (2012) Post-translational modifications induce significant yet not extreme changes to protein structure. *Bioinformatics* 28, 2905-2913

7. Karve, T. M., and Cheema, A. K. (2011) Small changes huge impact: the role of protein posttranslational modifications in cellular homeostasis and disease. *J Amino Acids* 2011, 207691

8. Khoury, G. A., Baliban, R. C., and Floudas, C. A. (2011) Proteome-wide post-translational modification statistics: frequency analysis and curation of the swiss-prot database. *Sci Rep* 1

9. Walsh, C. T., Garneau-Tsodikova, S., and Gatto, G. J., Jr. (2005) Protein posttranslational modifications: the chemistry of proteome diversifications. *Angew Chem Int Ed Engl* 44, 7342-7372

10. Paulsen, C. E., Truong, T. H., Garcia, F. J., Homann, A., Gupta, V., Leonard, S. E., and Carroll, K. S. (2011) Peroxide-dependent sulfenylation of the EGFR catalytic site enhances kinase activity. *Nat Chem Biol* 8, 57-64

11. Moellering, R. E., and Cravatt, B. F. (2013) Functional lysine modification by an intrinsically reactive primary glycolytic metabolite. *Science* 341, 549-553

12. Keller, M. A., Piedrafita, G., and Ralser, M. (2015) The widespread role of non-enzymatic reactions in cellular metabolism. *Curr Opin Biotechnol* 34, 153-161

13. Rehder, D. S., and Borges, C. R. (2010) Cysteine sulfenic acid as an intermediate in disulfide bond formation and nonenzymatic protein folding. *Biochemistry* 49, 7748-7755

14. Borges, C. R., Rehder, D. S., Jensen, S., Schaab, M. R., Sherma, N. D., Yassine, H., Nikolova, B., and Breburda, C. (2014) Elevated Plasma Albumin and Apolipoprotein A-I Oxidation under Suboptimal Specimen Storage Conditions. *Molecular & cellular proteomics : MCP* 13, 1890-1899

15. Turell, L., Radi, R., and Alvarez, B. (2013) The thiol pool in human plasma: the central contribution of albumin to redox processes. *Free Radic Biol Med* 65, 244-253

16. Marino, S. M., and Gladyshev, V. N. (2012) Analysis and functional prediction of reactive cysteine residues. *J Biol Chem* 287, 4419-4425

17. Reddie, K. G., and Carroll, K. S. (2008) Expanding the functional diversity of proteins through cysteine oxidation. *Curr Opin Chem Biol* 12, 746-754

18. Roos, G., and Messens, J. (2011) Protein sulfenic acid formation: from cellular damage to redox regulation. *Free Radic Biol Med* 51, 314-326

19. Paulsen, C. E., and Carroll, K. S. (2013) Cysteine-mediated redox signaling: chemistry, biology, and tools for discovery. *Chem Rev* 113, 4633-4679

20. Kachur, A. V., Koch, C. J., and Biaglow, J. E. (1999) Mechanism of copper-catalyzed autoxidation of cysteine. *Free Radic Res* 31, 23-34

21. Holmgren, A., and Sengupta, R. (2010) The use of thiols by ribonucleotide reductase. *Free Radic Biol Med* 49, 1617-1628

22. Zhao, H. R., Smith, J. B., Jiang, X. Y., and Abraham, E. C. (1996) Sites of glycation of beta B2-crystallin by glucose and fructose. *Biochem Biophys Res Commun* 229, 128-133

23. Wolff, S. P., and Dean, R. T. (1987) Glucose autoxidation and protein modification. The potential role of 'autoxidative glycosylation' in diabetes. *Biochem J* 245, 243-250

24. Pasella, S., Baralla, A., Canu, E., Pinna, S., Vaupel, J., Deiana, M., Franceschi, C., Baggio, G., Zinellu, A., Sotgia, S., Castaldo, G., Carru, C., and Deiana, L. (2013) Pre-analytical stability of the plasma proteomes based on the storage temperature. *Proteome Sci* 11, 10

25. Anton, G., Wilson, R., Yu, Z. H., Prehn, C., Zukunft, S., Adamski, J., Heier, M., Meisinger, C., Romisch-Margl, W., Wang-Sattler, R., Hveem, K., Wolfenbuttel, B., Peters, A., Kastenmuller, G., and Waldenberger, M. (2015) Pre-analytical sample quality: metabolite ratios as an intrinsic marker for prolonged room temperature exposure of serum samples. *PLoS One* 10, e0121495

26. Sozzi, G., Roz, L., Conte, D., Mariani, L., Andriani, F., Verderio, P., and Pastorino, U. (2005) Effects of prolonged storage of whole plasma or isolated plasma DNA on the results of circulating DNA quantification assays. *J Natl Cancer Inst* 97, 1848-1850

27. Buettner, G. R. (1988) In the absence of catalytic metals ascorbate does not autoxidize at pH 7: ascorbate as a test for catalytic metals. *J Biochem Biophys Methods* 16, 27-40

28. Gevantman, L. (1998) *Solubility of selected gases in water*, CRC Press, Boca Raton, Fl

29. Gaza-Bulseco, G., Faldu, S., Hurkmans, K., Chumsae, C., and Liu, H. (2008) Effect of methionine oxidation of a recombinant monoclonal antibody on the binding affinity to protein A and protein G. *J Chromatogr B Analyt Technol Biomed Life Sci* 870, 55-62

30. Bertolotti-Ciarlet, A., Wang, W., Lownes, R., Pristatsky, P., Fang, Y., McKelvey, T., Li, Y., Li, Y., Drummond, J., Prueksaritanont, T., and Vlasak, J. (2009) Impact of methionine oxidation on the binding of human IgG1 to Fc Rn and Fc gamma receptors. *Mol Immunol* 46, 1878-1882

31. Pan, H., Chen, K., Chu, L., Kinderman, F., Apostol, I., and Huang, G. (2009) Methionine oxidation in human IgG2 Fc decreases binding affinities to protein A and FcRn. *Protein Sci* 18, 424-433

32. Gao, J., Yao, Y., and Squier, T. C. (2001) Oxidatively modified calmodulin binds to the plasma membrane Ca-ATPase in a nonproductive and conformationally disordered complex. *Biophys J* 80, 1791-1801

33. Yao, Y., Yin, D., Jas, G. S., Kuczer, K., Williams, T. D., Schoneich, C., and Squier, T. C. (1996) Oxidative modification of a carboxyl-terminal vicinal methionine in calmodulin by hydrogen peroxide inhibits calmodulin-dependent activation of the plasma membrane Ca-ATPase. *Biochemistry* 35, 2767-2787

34. Galceran, T., Lewis-Finch, J., Martin, K. J., and Slatopolsky, E. (1984) Absence of biological effects of oxidized parathyroid hormone-(1-34) in dogs and rats. *Endocrinology* 115, 2375-2378

35. Horiuchi, N. (1988) Effects of oxidation of human parathyroid hormone on its biological activity in continuously infused, thyroparathyroidectomized rats. *J Bone Miner Res* 3, 353-358

36. Nabuchi, Y., Fujiwara, E., Ueno, K., Kuboniwa, H., Asoh, Y., and Ushio, H. (1995) Oxidation of recombinant human parathyroid hormone: effect of oxidized position on the biological activity. *Pharm Res* 12, 2049-2052

37. Hocher, B., Oberthur, D., Slowinski, T., Querfeld, U., Schaefer, F., Doyon, A., Tepel, M., Roth, H. J., Gron, H. J., Reichetzeder, C., Betzel, C., and Armbruster, F. P. (2013) Modeling of oxidized PTH (oxPTH) and non-oxidized PTH (n-oxPTH) receptor binding and relationship of oxidized to non-oxidized PTH in children with chronic renal failure, adult patients on hemodialysis and kidney transplant recipients. *Kidney Blood Press Res* 37, 240-251

38. Weiskopf, D., Schwanninger, A., Weinberger, B., Almanzar, G., Parson, W., Buus, S., Lindner, H., and Grubeck-Loebenstein, B. (2010) Oxidative stress can alter the antigenicity of immunodominant peptides. *J Leukoc Biol* 87, 165-172

39. Thibault, G., Grove, K. L., and Deschepper, C. F. (1995) Reduced affinity of iodinated forms of Tyr0 C-type natriuretic peptide for rat natriuretic peptide receptor B. *Mol Pharmacol* 48, 1046-1053

40. Canello, T., Frid, K., Gabizon, R., Lisa, S., Friedler, A., Moskovitz, J., Gasset, M., and Gabizon, R. (2010) Oxidation of Helix-3 methionines precedes the formation of PK resistant PrP. *PLoS Pathog* 6, e1000977

41. Houde, D., Kauppinen, P., Mhatre, R., and Lyubarskaya, Y. (2006) Determination of protein oxidation by mass spectrometry and method transfer to quality control. *J Chromatogr A* 1123, 189-198

42. Jenkins, N., Murphy, L., and Tyther, R. (2008) Post-translational modifications of recombinant proteins: significance for biopharmaceuticals. *Mol Biotechnol* 39, 113-118

43. Turell, L., Botti, H., Carballal, S., Ferrer-Sueta, G., Souza, J. M., Duran, R., Freeman, B. A., Radi, R., and Alvarez, B. (2008) Reactivity of sulfenic acid in human serum albumin. *Biochemistry* 47, 358-367

44. Cray, C., Rodriguez, M., Zaias, J., and Altman, N. H. (2009) Effects of storage temperature and time on clinical biochemical parameters from rat serum. *J Am Assoc Lab Anim Sci* 48, 202-204

45. Betsou, F., Gunter, E., Clements, J., DeSouza, Y., Goddard, K. A., Guadagni, F., Yan, W., Skubitz, A., Somiari, S., Yeadon, T., and Chuaqui, R. (2013) Identification of evidence-based biospecimen quality-control tools: a report of the International Society for Biological and Environmental Repositories (ISBER) Biospecimen Science Working Group. *J Mol Diagn* 15, 3-16

46. Bravo, M. I., Grancha, S., and Jorquera, J. I. (2006) Effect of temperature on plasma freezing under industrial conditions. *Pharmeur Sci Notes* 2006, 31-35

47. Cagle, P. T. (2005) The proposal to close the armed forces institute of pathology. *Arch Pathol Lab Med* 129, 856-857

48. Global Biobank Directory.

49. Henderson, G. E., Cadigan, R. J., Edwards, T. P., Conlon, I., Nelson, A. G., Evans, J. P., Davis, A. M., Zimmer, C., and Weiner, B. J. (2013) Characterizing biobank organizations in the U.S.: results from a national survey. *Genome Med* 5, 3

50. McGuire, A. L., and Beskow, L. M. (2010) Informed consent in genomics and genetic research. *Annu Rev Genomics Hum Genet* 11, 361-381

51. Harris, J. R., Burton, P., Knoppers, B. M., Lindpaintner, K., Bledsoe, M., Brookes, A. J., Budin-Ljosne, I., Chisholm, R., Cox, D., Deschenes, M., Fortier, I., Hainaut, P., Hewitt, R., Kaye, J., Litton, J. E., Metspalu, A., Ollier, B., Palmer, L. J., Palotie, A., Pasterk, M., Perola, M., Riegman, P. H., van Ommen, G. J., Yuille, M., and Zatloukal, K. (2012) Toward a roadmap in global biobanking for health. *Eur J Hum Genet* 20, 1105-1111

52. Kaiser, J. (2002) Biobanks. Population databases boom, from Iceland to the U.S. *Science* 298, 1158-1161

53. Simeon-Dubach, D., Zeisberger, S. M., and Hoerstrup, S. P. (2016) Quality Assurance in Biobanking for Pre-Clinical Research. *Transfus Med Hemother* 43, 353-357

54. Vaught, J., Rogers, J., Myers, K., Lim, M. D., Lockhart, N., Moore, H., Sawyer, S., Furman, J. L., and Compton, C. (2011) An NCI perspective on creating sustainable biospecimen resources. *J Natl Cancer Inst Monogr* 2011, 1-7

55. Hughes, S. E., Barnes, R. O., and Watson, P. H. (2010) Biospecimen use in cancer research over two decades. *Biopreserv Biobank* 8, 89-97

56. Carraro, P., Zago, T., and Plebani, M. (2012) Exploring the initial steps of the testing process: frequency and nature of pre-preanalytic errors. *Clin Chem* 58, 638-642

57. Lippi, G., Guidi, G. C., Mattiuzzi, C., and Plebani, M. (2006) Preanalytical variability: the dark side of the moon in laboratory testing. *Clin Chem Lab Med* 44, 358-365

58. Bonini, P., Plebani, M., Ceriotti, F., and Rubboli, F. (2002) Errors in laboratory medicine. *Clin Chem* 48, 691-698

59. Rai, A. J., Gelfand, C. A., Haywood, B. C., Warunek, D. J., Yi, J., Schuchard, M. D., Mehigh, R. J., Cockrill, S. L., Scott, G. B., Tammen, H., Schulz-Knappe, P., Speicher, D. W., Vitzthum, F., Haab, B. B., Siest, G., and Chan, D. W. (2005) HUPO Plasma Proteome Project specimen collection and handling: towards the standardization of parameters for plasma proteome samples. *Proteomics* 5, 3262-3277

60. Saleem, S., Mani, V., Chadwick, M. A., Creanor, S., and Ayling, R. M. (2009) A prospective study of causes of haemolysis during venepuncture: tourniquet time should be kept to a minimum. *Ann Clin Biochem* 46, 244-246

61. (2010) BD Diagnostics Tube Guide.

62. Lee, J. E., Kim, J. W., Han, B. G., and Shin, S. Y. (2016) Impact of Whole-Blood Processing Conditions on Plasma and Serum Concentrations of Cytokines. *Biopreserv Biobank* 14, 51-55

63. Skogstrand, K., Ekelund, C. K., Thorsen, P., Vogel, I., Jacobsson, B., Norgaard-Pedersen, B., and Hougaard, D. M. (2008) Effects of blood sample handling procedures on measurable inflammatory markers in plasma, serum and dried blood spot samples. *J Immunol Methods* 336, 78-84

64. Kisand, K., Kerna, I., Kumm, J., Jonsson, H., and Tamm, A. (2011) Impact of cryopreservation on serum concentration of matrix metalloproteinases (MMP)-7, TIMP-1, vascular growth factors (VEGF) and VEGF-R2 in Biobank samples. *Clin Chem Lab Med* 49, 229-235

65. Morgan, A. R., O'Hagan, C., Touchard, S., Lovestone, S., and Morgan, B. P. (2017) Effects of freezer storage time on levels of complement biomarkers. *BMC Res Notes* 10, 559

66. Jung, K., Lein, M., Brux, B., Sinha, P., Schnorr, D., and Loening, S. A. (2000) Different stability of free and complexed prostate-specific antigen in serum in relation to specimen handling and storage conditions. *Clin Chem Lab Med* 38, 1271-1275

67. de Jager, W., Bourcier, K., Rijkers, G. T., Prakken, B. J., and Seyfert-Margolis, V. (2009) Prerequisites for cytokine measurements in clinical trials with multiplex immunoassays. *BMC Immunol* 10, 52

68. Naldi, M., Baldassarre, M., Nati, M., Laggetta, M., Giannone, F. A., Domenicali, M., Bernardi, M., Caraceni, P., and Bertucci, C. (2015) Mass spectrometric characterization of human serum albumin dimer: A new potential biomarker in chronic liver diseases. *J Pharm Biomed Anal* 112, 169-175

69. Watanabe, H., Imafuku, T., Otagiri, M., and Maruyama, T. (2017) Clinical Implications Associated With the Posttranslational Modification-Induced Functional Impairment of Albumin in Oxidative Stress-Related Diseases. *J Pharm Sci* 106, 2195-2203

70. Nagumo, K., Tanaka, M., Chuang, V. T., Setoyama, H., Watanabe, H., Yamada, N., Kubota, K., Tanaka, M., Matsushita, K., Yoshida, A., Jinnouchi, H., Anraku, M., Kadowaki, D., Ishima, Y., Sasaki, Y., Otagiri, M., and Maruyama, T. (2014) Cys34-cysteinylated human serum albumin is a sensitive plasma marker in oxidative stress-related chronic diseases. *PLoS One* 9, e85216

71. The Early Detection Research Network (EDRN) Standard Operating Procedure (SOP) For Collection of EDTA Plasma. Downloaded from http://edrn.nci.nih.gov/resources/standard-operating-procedures/standard-operating-procedures/plasma-sop.pdf August 2013.

72. The Early Detection Research Network (EDRN) Standard Operating Procedure (SOP) For Collection of Serum. Downloaded from http://edrn.nci.nih.gov/resources/standard-operating-procedures/standard-operating-procedures/serum-sop.pdf August 2013.

73. Atkins, P. W. (1994) *Physical Chemistry*, 5th Ed., W. H. Freeman and Company, Chapter 25 - *The rates of chemical reactions*; New York, NY

74. Orsak, T., Smith, T. L., Eckert, D., Lindsley, J. E., Borges, C. R., and Rutter, J. (2012) Revealing the allosterome: systematic identification of metabolite-protein interactions. *Biochemistry* 51, 225-232

75. Johnson, J. M., Strobel, F. H., Reed, M., Pohl, J., and Jones, D. P. (2008) A rapid LC-FTMS method for the analysis of cysteine, cystine and cysteine/cystine steady-state redox potential in human plasma. *Clin Chim Acta* 396, 43-48

76. Ohie, T., Fu, X., Iga, M., Kimura, M., and Yamaguchi, S. (2000) Gas chromatography-mass spectrometry with tert.-butyldimethylsilyl derivation: use of the simplified sample preparations and the automated data system to screen for organic acidemias. *J Chromatogr B Biomed Sci Appl* 746, 63-73

77. Liebisch, G., Lieser, B., Rathenberg, J., Drobnik, W., and Schmitz, G. (2004) High-throughput quantification of phosphatidylcholine and sphingomyelin by electrospray ionization tandem mass spectrometry coupled with isotope correction algorithm. *Biochim Biophys Acta* 1686, 108-117

78. Liebisch, G., Lieser, B., Rathenberg, J., Drobnik, W., and Schmitz, G. (2005) Erratum to "High-throughput quantification of phosphatidylcholine and sphingomyelin by electrospray ionization tandem mass spectrometry coupled with isotope corrections algorithm" [Biochimica et Biophysics Acta, 1686 (2004) 108–117]. *Biochim Biophys Acta* 1734, 86-89

79. Jones, D. P., Mody, V. C., Jr., Carlson, J. L., Lynn, M. J., and Sternberg, P., Jr. (2002) Redox analysis of human plasma allows separation of pro-oxidant events of aging from decline in antioxidant defenses. *Free Radic Biol Med* 33, 1290-1300

80. Blanco, R. A., Ziegler, T. R., Carlson, B. A., Cheng, P. Y., Park, Y., Cotsonis, G. A., Accardi, C. J., and Jones, D. P. (2007) Diurnal variation in glutathione and cysteine redox states in human plasma. *Am J Clin Nutr* 86, 1016-1023

81. Bocedi, A., Cattani, G., Stella, L., Massoud, R., and Ricci, G. (2018) Thiol disulfide exchange reactions in human serum albumin: the apparent paradox of the redox transitions of Cys34. *FEBS J* 285, 3225-3237

82. Berthon, G. (1995) Critical Evalution of the Stability-Constants of Metal-Complexes of Amino-Acids with Polar Side-Chains. *Pure Appl Chem* 67, 1117-1240

83. Atkins, P. W. (1994) Physical Chemistry. 5th Ed., W. H. Freeman and Company, Chapter 9 - *Chemical Equilibrium*; New York, NY

84. Goth, L. (1991) A simple method for determination of serum catalase activity and revision of reference range. *Clin Chim Acta* 196, 143-151

85. Hellman, N. E., and Gitlin, J. D. (2002) Ceruloplasmin metabolism and function. *Annual review of nutrition* 22, 439-458

86. Kasper, C. B., Deutsch, H. F., and Beinert, H. (1963) Studies on the state of copper in native and modified human ceruloplasmin. *J Biol Chem* 238, 2338-2342

87. Kolb, A. M., Smit, N. P. M., Lentz-Ljuboje, R., Osanto, S., and van Pelt, J. (2009) Non-transferrin bound iron measurement is influenced by chelator concentration. *Analytical biochemistry* 385, 13-19

88. Buettner, G. R. (1988) In the absence of catalytic metals ascorbate does not autoxidize at pH 7: ascorbate as a test for catalytic metals. *J Biochem Biophys Methods* 16, 27-40

89. Gevantman, L. H. (2015) Solubility of Selected Gases in Water. In: Haynes, W. M., ed. *CRC Handbook of Chemistry and Physics*, 95th Ed., pp. Section 5, 149-152, CRC Press/Taylor and Francis, Boca Raton, FL

90. Compton, C. (2007) Getting to personalized cancer medicine: taking out the garbage. *Cancer* 110, 1641-1643

91. McLerran, D., Grizzle, W. E., Feng, Z., Bigbee, W. L., Banez, L. L., Cazares, L. H., Chan, D. W., Diaz, J., Izbicka, E., Kagan, J., Malehorn, D. E., Malik, G., Oelschlager, D., Partin, A., Randolph, T., Rosenzweig, N., Srivastava, S., Srivastava, S., Thompson, I. M., Thornquist, M., Troyer, D., Yasui, Y., Zhang, Z., Zhu, L., and Semmes, O. J. (2008) Analytical validation of serum proteomic profiling for diagnosis of prostate cancer: Sources of sample bias. *Clinical Chemistry* 54, 44-52

92. Ransohoff, D. F., and Gourlay, M. L. (2010) Sources of Bias in Specimens for Research About Molecular Markers for Cancer. *Journal of Clinical Oncology* 28, 698-704

93. Poste, G., Compton, C. C., and Barker, A. D. (2015) The national biomarker development alliance: confronting the poor productivity of biomarker research and development. *Expert Rev Mol Diagn* 15, 211-218

94. Tsuchida, S., Satoh, M., Umemura, H., Sogawa, K., Takiwaki, M., Ishige, T., Miyabayashi, Y., Iwasawa, Y., Kobayashi, S., Beppu, M., Nishimura, M., Kodera, Y., Matsushita, K., and Nomura, F. (2018) Assessment by Matrix-Assisted Laser Desorption/Ionization Time-of-Flight Mass Spectrometry of the Effects of Preanalytical Variables on Serum Peptidome Profiles Following Long-Term Sample Storage. *Proteomics. Clinical applications*

95. Betsou, F., Barnes, R., Burke, T., Coppola, D., Desouza, Y., Eliason, J., Glazer, B., Horsfall, D., Kleeberger, C., Lehmann, S., Prasad, A., Skubitz, A., Somiari, S., and Gunter, E. (2009) Human biospecimen research: experimental protocol and quality control tools. *Cancer epidemiology, biomarkers & prevention : a publication of the American Association for Cancer Research, cosponsored by the American Society of Preventive Oncology* 18, 1017-1025

96. Lippi, G., Chance, J. J., Church, S., Dazzi, P., Fontana, R., Giavarina, D., Grankvist, K., Huisman, W., Kouri, T., Palicka, V., Plebani, M., Puro, V., Salvagno, G. L., Sandberg, S., Sikaris, K., Watson, I., Stankovic, A. K., and Simundic, A. M. (2011) Preanalytical quality improvement: from dream to reality. *Clin Chem Lab Med* 49, 1113-1126

97. Ellervik, C., and Vaught, J. (2015) Preanalytical Variables Affecting the Integrity of Human Biospecimens in Biobanking. *Clin Chem*

98. Salvagno, G. L., Danese, E., and Lippi, G. (2017) Preanalytical variables for liquid chromatography-mass spectrometry (LC-MS) analysis of human blood specimens. *Clinical biochemistry* 50, 582-586

99. (2005) *Human plasma for fractionation, monograph 0853. Ph. Eur. Suppl 5.3 Strasbourg, France: Council of Europe*

100. Carrick, D. M., Mette, E., Hoyle, B., Rogers, S. D., Gillanders, E. M., Schully, S. D., and Mechanic, L. E. (2014) The use of biospecimens in population-based research: a review of the National Cancer Institute's Division of Cancer Control and Population Sciences grant portfolio. *Biopreserv Biobank* 12, 240-245

101. Rifai, N., Annesley, T. M., Berg, J. P., Brugnara, C., Delvin, E., Lamb, E. J., Ness, P. M., Plebani, M., Wick, M. R., Wu, A., and Delanghe, J. (2012) An appeal to medical journal editors: the need for a full description of laboratory methods and specimen handling in clinical study reports. *Clin Chem* 58, 483-485

102. Rifai, N., Annesley, T. M., Berg, J. P., Brugnara, C., Delvin, E., Lamb, E. J., Ness, P. M., Plebani, M., Wick, M. R., Wu, A., and Delanghe, J. (2012) An appeal to medical journal editors: the need for a full description of laboratory methods and specimen handling in clinical study reports. *Clin Chem Lab Med* 50, 411-413

103. Rifai, N., Annesley, T. M., Berg, J. P., Brugnara, C., Delvin, E., Lamb, E. J., Ness, P. M., Plebani, M., Wick, M. R., Wu, A., and Delanghe, J. (2012) An appeal to medical journal editors: the need for a full description of laboratory methods and specimen handling in clinical study reports. *American journal of hematology* 87, 347-348

104. United States Center for Disease Control and Prevention, National Health and Nutrition Examination Survey (NHANES), 2015-2016.

105. Weaving, G., Batstone, G. F., and Jones, R. G. (2016) Age and sex variation in serum albumin concentration: an observational study. *Annals of clinical biochemistry* 53, 106-111

106. Borges, C. R., Rehder, D. S., and Boffetta, P. (2013) Multiplexed surrogate analysis of glycotransferase activity in whole biospecimens. *Analytical chemistry* 85, 2927-2936

107. Zaare, S., Aguilar, J. S., Hu, Y., Ferdosi, S., and Borges, C. R. (2016) Glycan Node Analysis: A Bottom-up Approach to Glycomics. *J Vis Exp* 111, e53961

108. Hu, Y., and Borges, C. R. (2017) A spin column-free approach to sodium hydroxide-based glycan permethylation. *Analyst* 142, 2748-2759

109. Ferdosi, S., Rehder, D. S., Maranian, P., Castle, E. P., Ho, T. H., Pass, H. I., Cramer, D. W., Anderson, K. S., Fu, L., Cole, D. E. C., Le, T., Wu, X., and Borges, C. R. (2018) Stage Dependence, Cell-Origin Independence, and Prognostic Capacity of Serum Glycan Fucosylation, beta1-4 Branching, beta1-6 Branching, and alpha2-6 Sialylation in Cancer. *Journal of proteome research* 17, 543-558

110. Ferdosi, S., Ho, T. H., Castle, E. P., Stanton, M. L., and Borges, C. R. (2018) Behavior of blood plasma glycan features in bladder cancer. *PloS one* 13, e0201208

111. Kolarich, D., Weber, A., Turecek, P. L., Schwarz, H. P., and Altmann, F. (2006) Comprehensive glyco-proteomic analysis of human alpha1-antitrypsin and its charge isoforms. *Proteomics* 6, 3369-3380

112. Nakanishi, T., Hasuike, Y., Otaki, Y., Hama, Y., Nanami, M., Miyagawa, K., Moriguchi, R., Nishikage, H., Izumi, M., and Takamitsu, Y. (2003) Free cysteine is increased in plasma from hemodialysis patients. *Kidney Int* 63, 1137-1140

113. Soejima, A., Matsuzawa, N., Hayashi, T., Kimura, R., Ootsuka, T., Fukuoka, K., Yamada, A., Nagasawa, T., and Era, S. (2004) Alteration of redox state of human serum albumin before and after hemodialysis. *Blood Purificat* 22, 525-529

114. Terawaki, H., Yoshimura, K., Hasegawa, T., Matsuyama, Y., Negawa, T., Yamada, K., Matsushima, M., Nakayama, M., Hosoya, T., and Era, S. (2004) Oxidative stress is enhanced in correlation with renal dysfunction: Examination with the redox state of albumin. *Kidney International* 66, 1988-1993

115. Terawaki, H., Nakayama, K., Matsuyama, Y., Nakayama, M., Sato, T., Hosoya, T., Era, S., and Ito, S. (2007) Dialyzable uremic solutes contribute to enhanced oxidation of serum albumin in regular hemodialysis patients. *Blood Purif* 25, 274-279

116. Regazzoni, L., Del Vecchio, L., Altomare, A., Yeum, K. J., Cusi, D., Locatelli, F., Carini, M., and Aldini, G. (2013) Human serum albumin cysteinylation is increased in end stage renal disease patients and reduced by hemodialysis: mass spectrometry studies. *Free Radical Res* 47, 172-180

117. Galliano, M., Minchiotti, L., Porta, F., Rossi, A., Ferri, G., Madison, J., Watkins, S., and Putnam, F. W. (1990) Mutations in Genetic-Variants of Human Serum-Albumin Found in Italy. *P Natl Acad Sci USA* 87, 8721-8725

118. Exley, C., and Mold, M. J. (2015) The binding, transport and fate of aluminium in biological cells. *J Trace Elem Med Biol* 30, 90-95

119. Farrugia, A., Hill, R., Douglas, S., Karabagias, K., and Kleinig, A. (1992) Factor VIII/von Willebrand factor levels in plasma frozen to-30 degrees C in air or halogenated hydrocarbons. *Thromb Res* 68, 97-102

120. MacKenzie, A. P. (1980, June 8-12) First and second order transitions during the freezing and thawing of source plasma (human). *American Institute of Chemical Engineers Symposium: Processing and fractionation of blood plasma*, Philadelphia

121. McIntosh, R. V., Dickson, A. J., Smith, D., and Foster, P. R. (1990) Freezing and thawing of plasma. In: Sibinga, C. T. S., Das, P.C., Meryman, H. T., ed. *Cryopreservation and low temperature biology*, pp. 11-24, Kluwer Academic Publishers, Norwell, MA

122. van den Besselaar, A. M., Witteveen, E., and van der Meer, F. J. (2013) Long-term stability of frozen pooled plasmas stored at -70 degrees C, -40 degrees C, and -20 degrees C for prothrombin time and International Normalized Ratio (INR) assessment. *Thromb Res* 131, 349-351

123. Brownlee, M. (1995) Advanced protein glycosylation in diabetes and aging. *Annu Rev Med* 46, 34

124. Baker, J., Metcalf, P., Scragg, R., and Johnson, R. (1991) Fructosamine Test-Plus, a modified fructosamine assay evaluated. *Clin Chem* 37, 552-556

125. Kouzuma, T., Usami, T., Yamakoshi, M., Takahashi, M., and Imamura, S. (2002) An enzymatic method for the measurement of glycated albumin in biological samples. *Clin Chim Acta* 324, 61-71

126. Kouzuma, T., Uemastu, Y., Usami, T., and Imamura, S. (2004) Study of glycated amino acid elimination reaction for an improved enzymatic glycated albumin measurement method. *Clin Chim Acta* 346, 135-143

127. Hunt, J. V., Dean, R. T., and Wolff, S. P. (1988) Hydroxyl radical production and autoxidative glycosylation. Glucose autoxidation as the cause of protein damage in the experimental glycation model of diabetes mellitus and ageing. *Biochem J* 256, 205-212

128. Little, R. R., Rohlfing, C. L., Tennill, A. L., Connolly, S., and Hanson, S. (2007) Effects of sample storage conditions on glycated hemoglobin measurement: evaluation of five different high performance liquid chromatography methods. *Diabetes Technol Ther* 9, 36-42

129. Constanti, C., Simo, J. M., Joven, J., and Camps, J. (1992) Serum fructosamine concentration in patients with nephrotic syndrome and with cirrhosis of the liver: the influence of hypoalbuminaemia and hypergammaglobulinaemia. *Ann Clin Biochem* 29 (Pt 4), 437-442

130. Koskinen, P., and Irjala, K. (1988) Stability of serum fructosamine during storage. *Clin Chem* 34, 2545-2546

131. Beck, R., Steffes, M., Xing, D., Ruedy, K., Mauras, N., Wilson, D. M., Kollman, C., and Diabetes Research in Children Network Study, G. (2011) The interrelationships of glycemic control measures: HbA1c, glycated albumin, fructosamine, 1,5-anhydroglucitrol, and continuous glucose monitoring. *Pediatr Diabetes* 12, 690-695

132. Morais, M. P., Mackay, J. D., Bhamra, S. K., Buchanan, J. G., James, T. D., Fossey, J. S., and van den Elsen, J. M. (2010) Analysis of protein glycation using phenylboronate acrylamide gel electrophoresis. *Proteomics* 10, 48-58

133. Mashiba, S., Uchida, K., Okuda, S., and Tomita, S. (1992) Measurement of glycated albumin by the nitroblue tetrazolium colorimetric method. *Clin Chim Acta* 212, 3-15

134. Dozio, E., Di Gaetano, N., Findeisen, P., and Corsi Romanelli, M. M. (2017) Glycated albumin: from biochemistry and laboratory medicine to clinical practice. *Endocrine* 55, 682-690

135. Murphy, B. M., Swarts, S., Mueller, B. M., van der Geer, P., Manning, M. C., and Fitchmun, M. I. (2013) Protein instability following transport or storage on dry ice. *Nat Methods* 10, 278-279

136. Bar-Or, D., Heyborne, K. D., Bar-Or, R., Rael, L. T., Winkler, J. V., and Navot, D. (2005) Cysteinylation of maternal plasma albumin and its association with intrauterine growth restriction. *Prenatal Diag* 25, 245-249

137. Wells-Knecht, K. J., Zyzak, D. V., Litchfield, J. E., Thorpe, S. R., and Baynes, J. W. (1995) Mechanism of autoxidative glycosylation: identification of glyoxal and arabinose as intermediates in the autoxidative modification of proteins by glucose. *Biochemistry* 34, 3702-3709

138. Skoog, D. A., West, D. M., Holler, F. J., and Crouch, S. R. (2014) *Fundamentals of analytical chemistry*, 9th Ed., Cengage - Brooks/Cole, Chapter 6 - *Random errors in chemical analysis*; Belmont, CA

139. Rolandsson, O., Marklund, S. L., Norberg, M., Agren, A., and Hagg, E. (2004) Hemoglobin A1c can be analyzed in blood kept frozen at -80 degrees C and is not commonly affected by hemolysis in the general population. *Metabolism* 53, 1496-1499

140. Jones, W., Scott, J., Leary, S., Stratton, F., Smith, S., Jones, R., Day, A., Ness, A., and Team, A. S. (2004) Stability of whole blood at -70 degrees C for measurement of hemoglobin A(1c) in healthy individuals. *Clin Chem* 50, 2460-2461

141. Watano, T., Sasaki, K., Omoto, K., and Kawano, M. (2013) Stability of stored samples for assays of glycated albumin. *Diabetes Res Clin Pract* 101, e1-2

142. Anguizola, J., Matsuda, R., Barnaby, O. S., Hoy, K. S., Wa, C., DeBolt, E., Koke, M., and Hage, D. S. (2013) Review: Glycation of human serum albumin. *Clin Chim Acta* 425, 64-76

143. Roohk, H. V., and Zaidi, A. R. (2008) A review of glycated albumin as an intermediate glycation index for controlling diabetes. *J Diabetes Sci Technol* 2, 1114-1121

144. Peters, T., Jr. (1985) Serum albumin. *Adv Protein Chem* 37, 161-245

145. Baynes, J. W., Thorpe, S. R., and Murtiashaw, M. H. (1984) Nonenzymatic glucosylation of lysine residues in albumin. *Methods Enzymol* 106, 88-98

146. United States Center for Disease Control and Prevention, National Health and Nutrition Examination Survey (NHANES), 2006.

147. Seibig, S., and vanEldik, R. (1997) Kinetics of [Fe-II(edta)] oxidation by molecular oxygen revisited. New evidence for a multistep mechanism. *Inorg Chem* 36, 4115-4120

APPENDIX A

ILLUSTRATED MODELS OF ALBUMIN OXIDATION

Kinetics simulations in which the Reaction 2 (see *Section 2.3.1.1*) rate law constants k_3, K_y and K_z are individually changed to their 37 °C values or 10x below these values. a-b) Serum and plasma, respectively, where $k_3 = 0.32\ M^{-1}\ s^{-1}$, the value established by Kachur et al. (20) at 37 °C; c-d) $k_3 = 0.032\ M^{-1}\ s^{-1}$; e-f) $K_y = 5.1 \times 10^{-6}$ M, the value established by Kachur et al. (20) at 37 °C; g-h) $K_y = 5.1 \times 10^{-7}$ M; i-j) $K_z = 8.8 \times 10^{-4}$ M, the value established by Kachur et al. (20) at 37 °C; k-l) $K_z = 8.8 \times 10^{-5}$ M. Cys-Cys is abbreviated as CSSC in the legends.

a) Serum: $k_3 = 0.32\ M^{-1}\ s^{-1}$

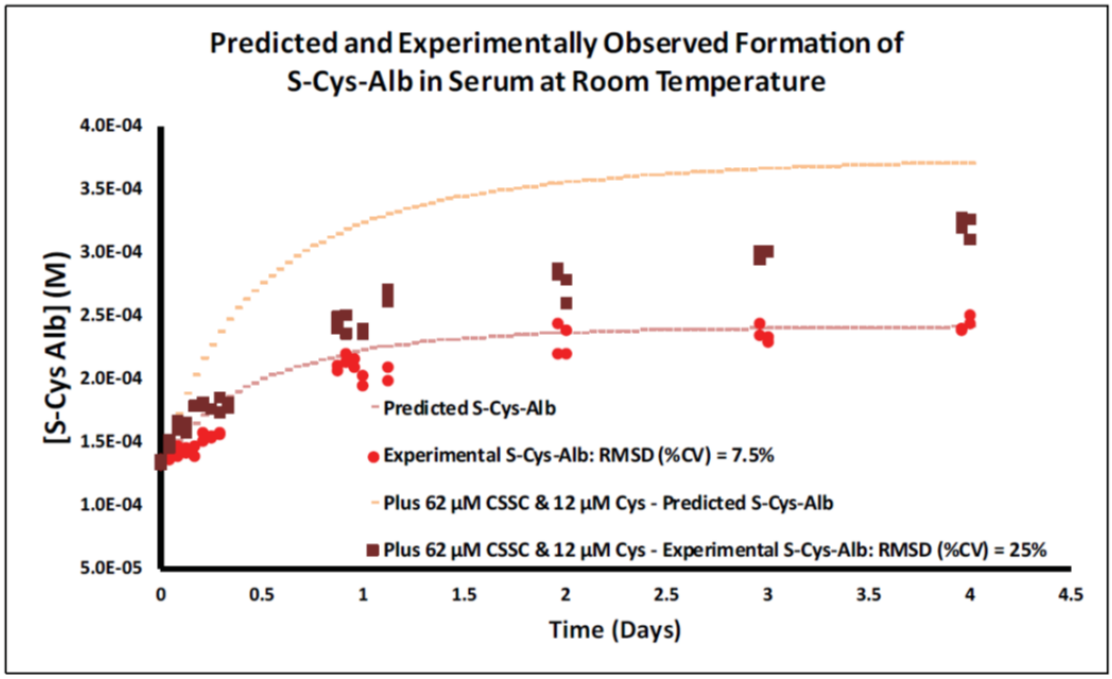

b) Plasma: $k_3 = 0.32\ M^{-1}\ s^{-1}$

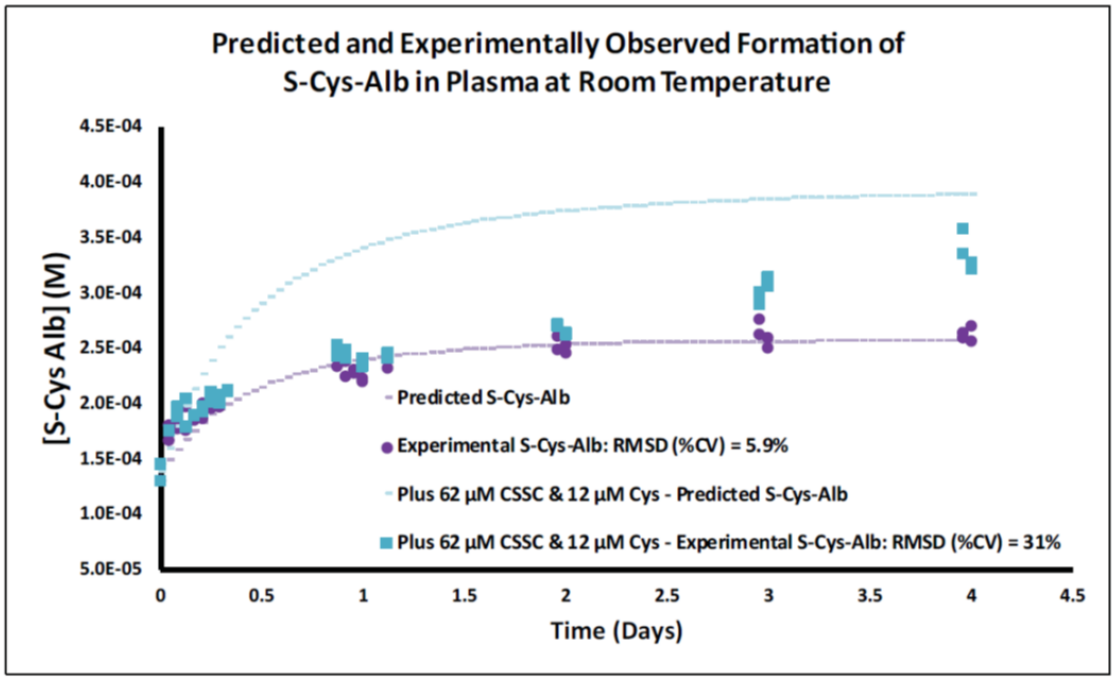

c) Serum: $k_3 = 0.032\ M^{-1}\ s^{-1}$

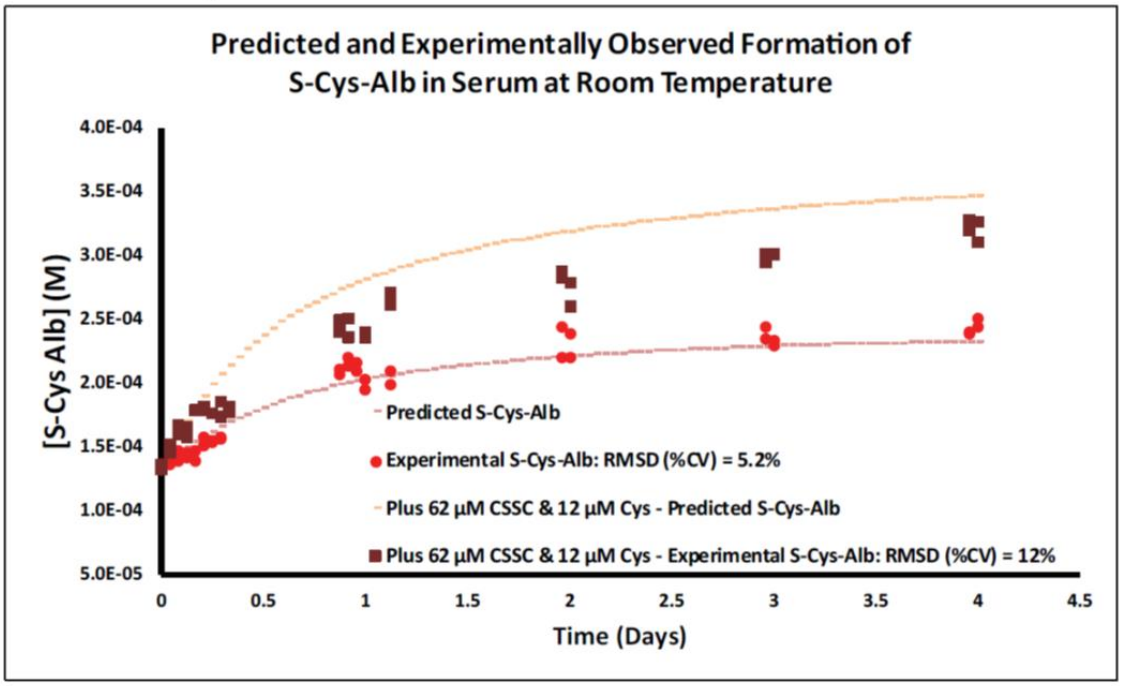

d) Plasma: $k_3 = 0.032\ M^{-1}\ s^{-1}$

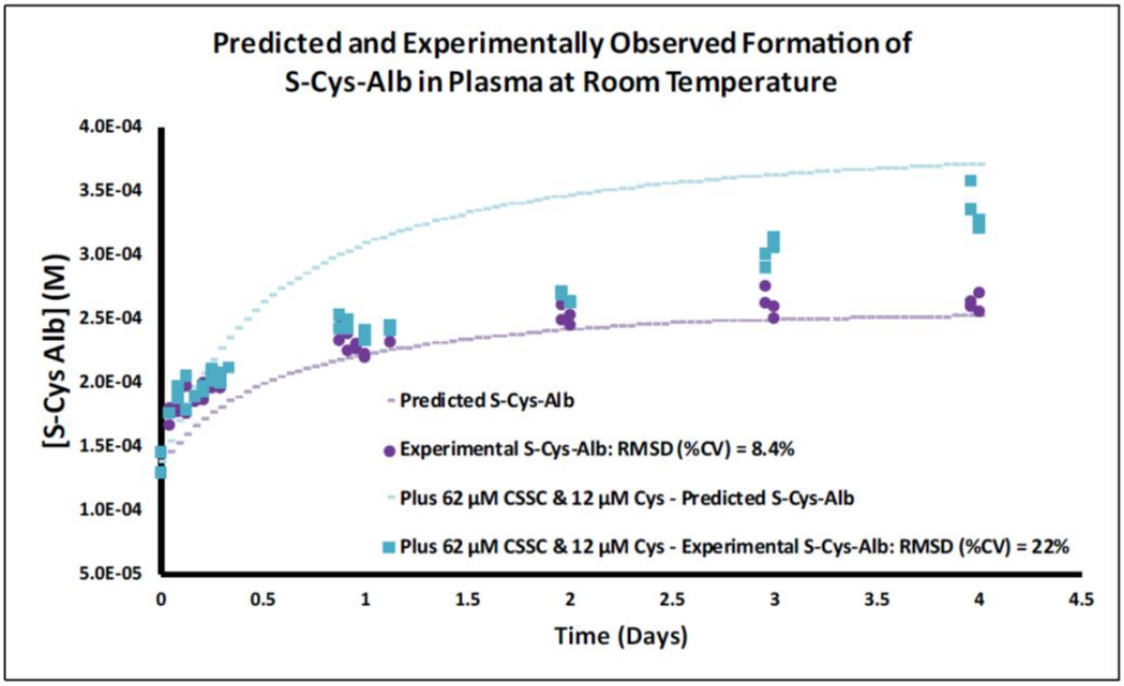

e) Serum: $K_y = 5.1 \times 10^{-6}$

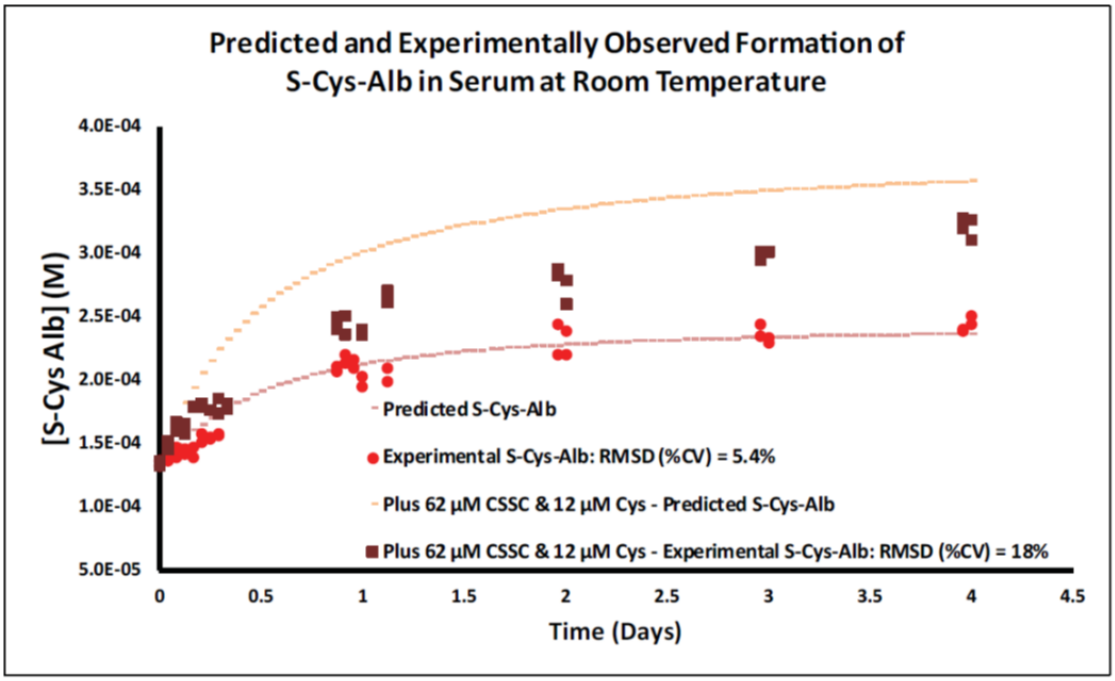

f) Plasma: $K_y = 5.1 \times 10^{-6}$

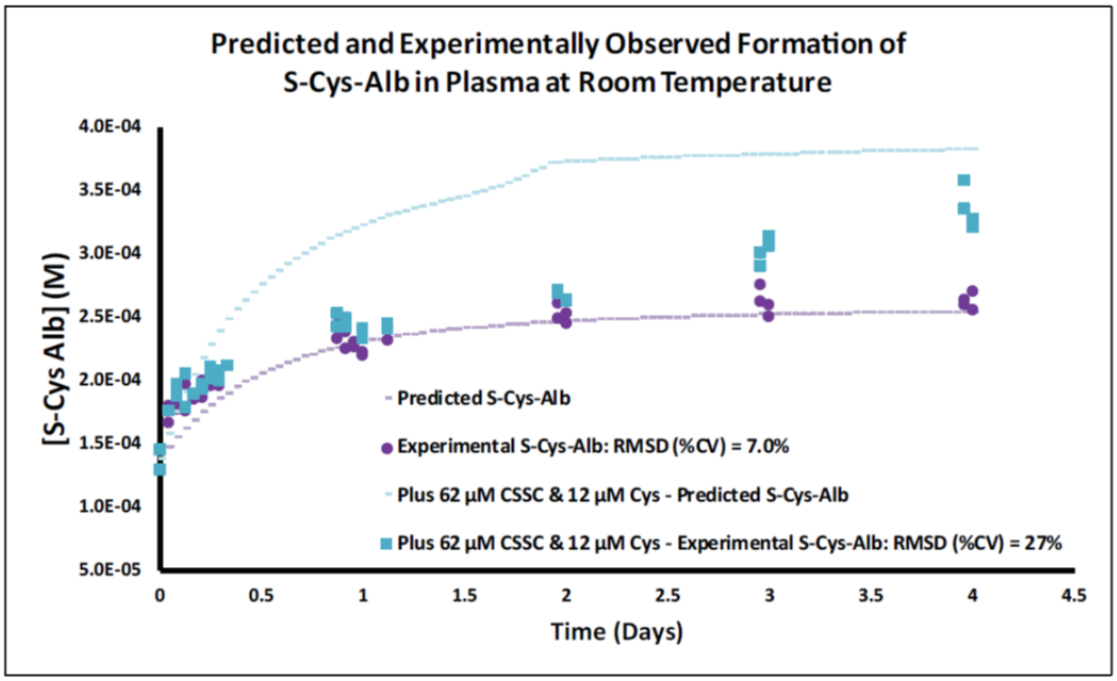

g) Serum: $K_y = 5.1 \times 10^{-7}$

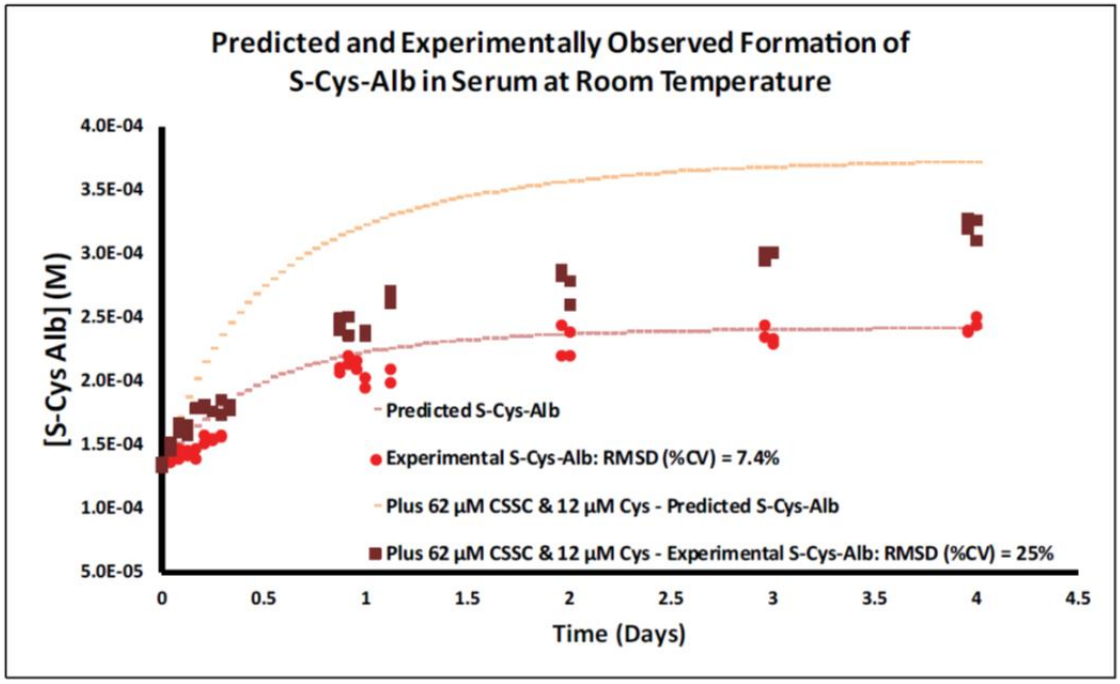

h) Plasma: $K_y = 5.1 \times 10^{-7}$

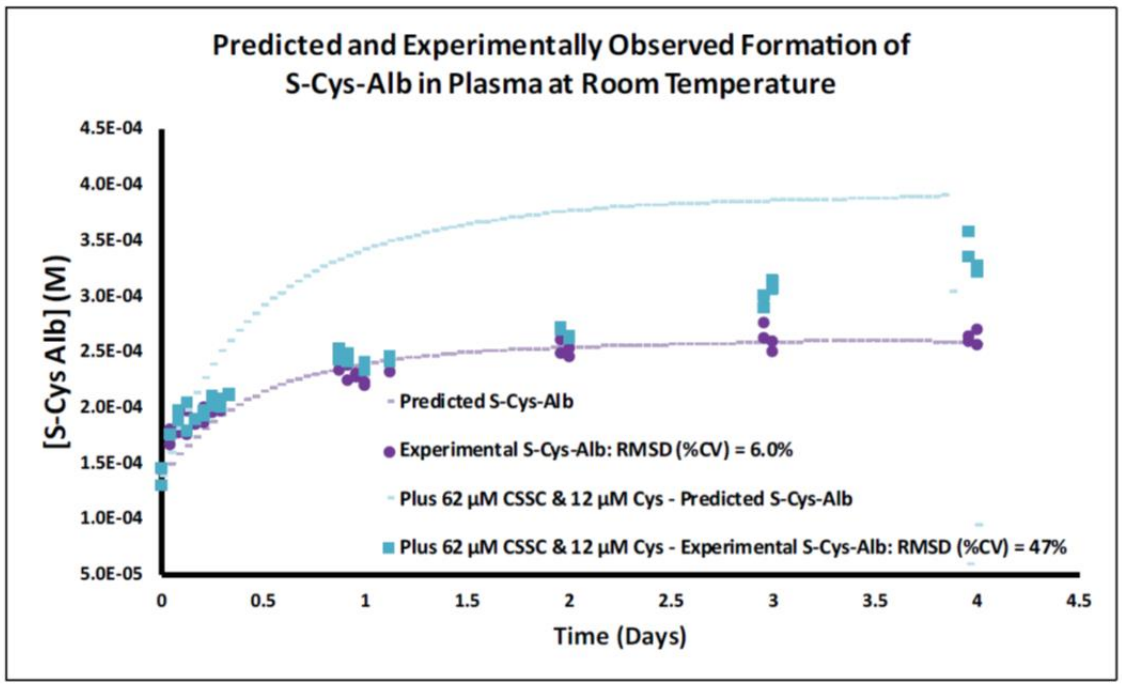

i) Serum: $K_z = 8.8 \times 10^{-4}$

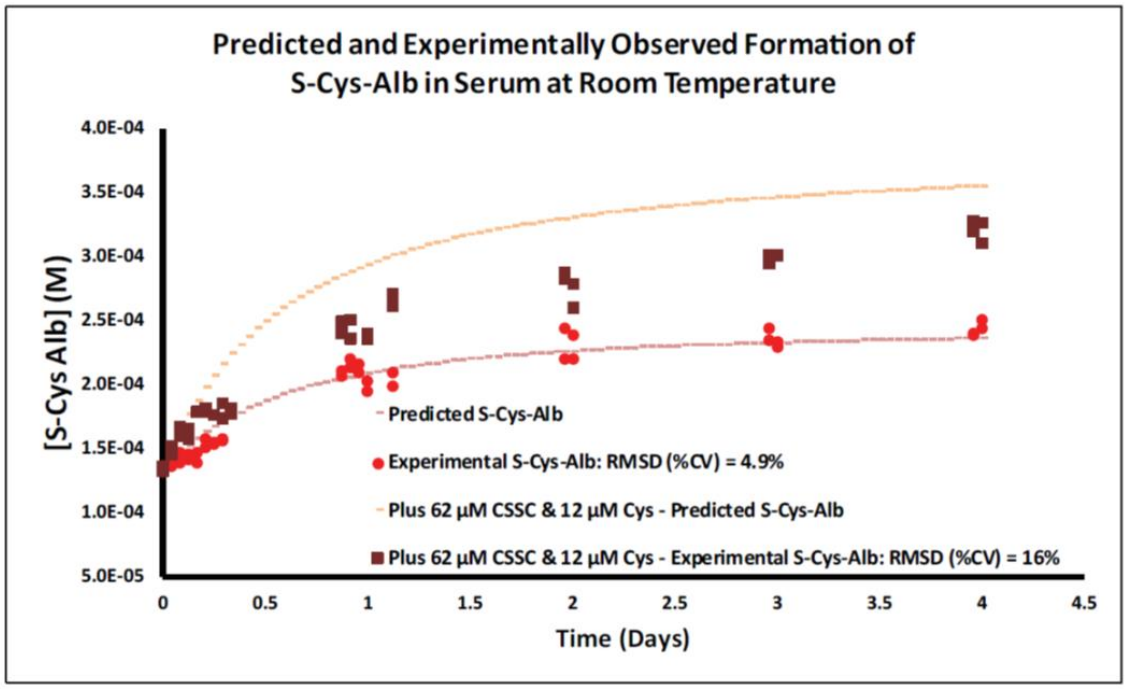

j) Plasma: $K_z = 8.8 \times 10^{-4}$

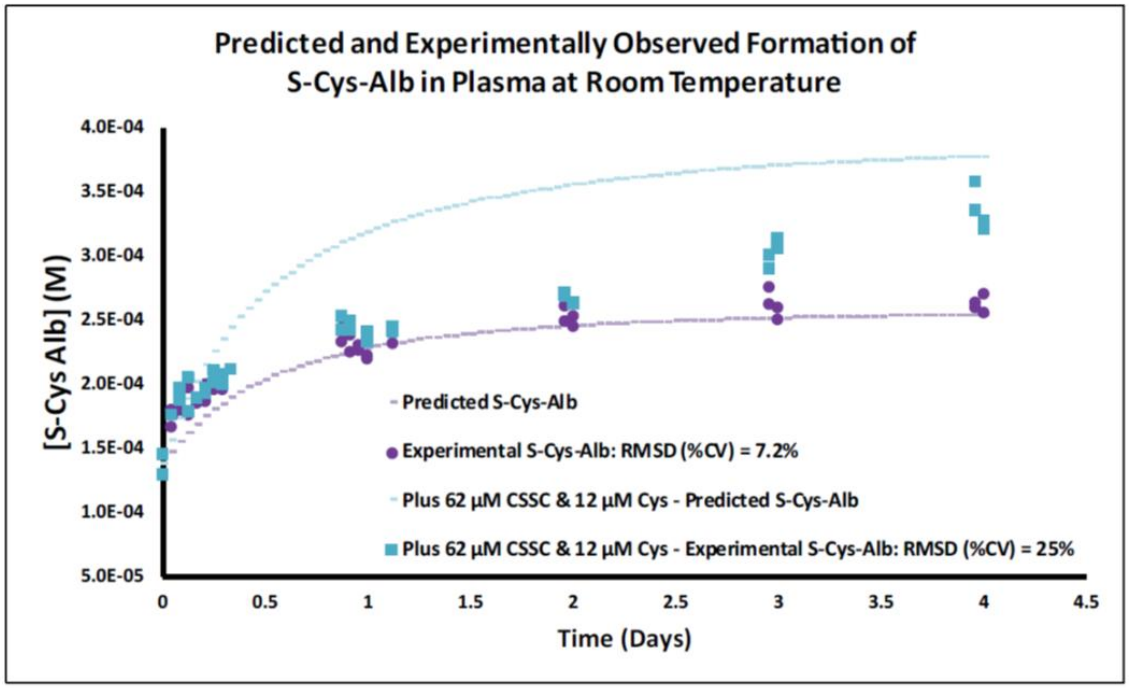

k) Serum: $K_z = 8.8 \times 10^{-5}$

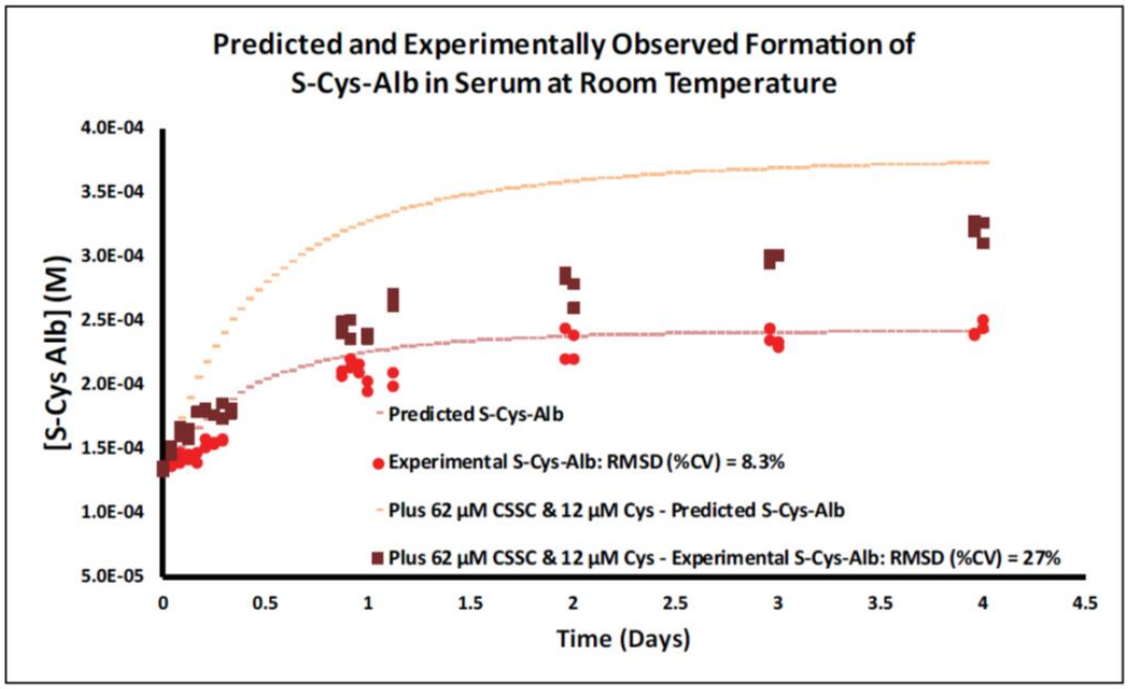

l) Plasma: $K_z = 8.8 \times 10^{-5}$

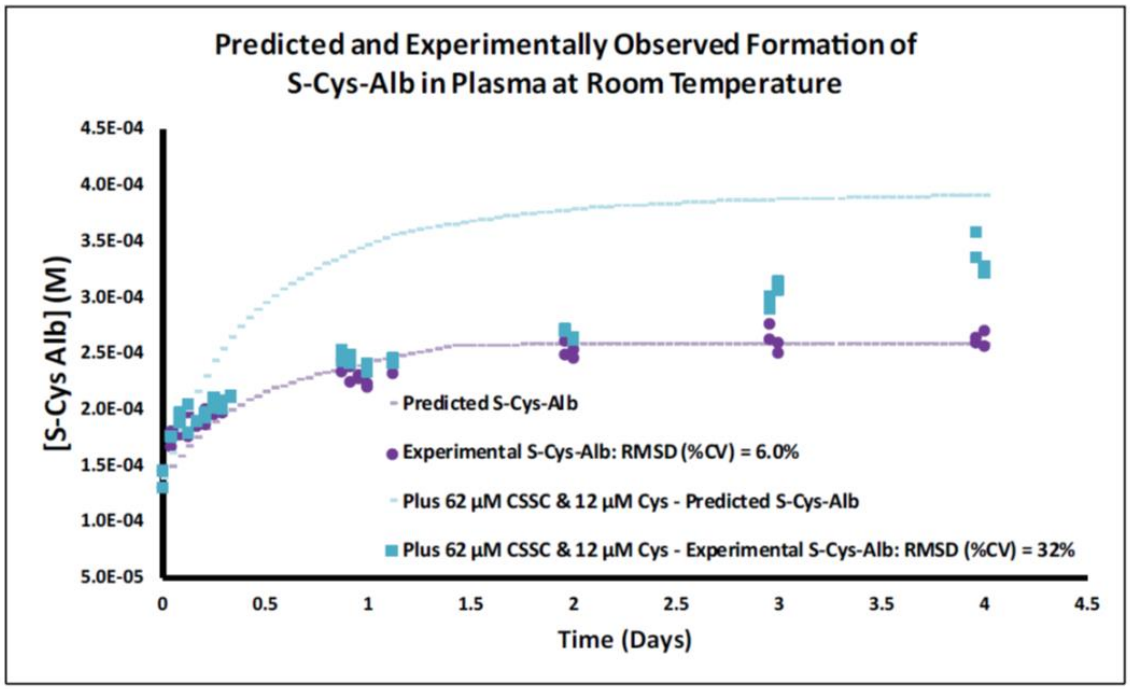

APPENDIX B

HYPOTHETICAL KINETIC MODEL AND SIMULATIONS THAT CONSIDER OXYGEN AS RATE LIMITING

Part A) Chemical and mathematical equations. Reactions 10 and 11 break apart Reaction 2 (see *Section 2.3.1.*1) to show how $O_{2(aq)}$ recycles Cu(I) into Cu(II) and allows Cu(II) to serve as the reaction catalyst. The rate law described by Kachur et al. (20) for Reaction 2 omits O_2 (i.e., assumes it is not rate limiting) and takes into account the equilibrium binding affinities for the first and second Cys liganding to Cu(II). Thus, strictly speaking, it is actually the rate law for Reaction 10—but one in which the Cu(I) produced is assumed to be immediately recycled back to Cu(II). When $O_{2(aq)}$ is in short supply, Reaction 11 can become rate limiting and must be taken into account in the model.

Taking $O_{2(aq)}$ into account requires three additional differential equations (Equations 12-14), two additional reaction components ($O_{2(aq)}$ and Cu(I)) and two additional rate constants (k_4 and k_{O_2}). Simulations based on this model (*Part b*) should be considered speculative because not all parameters are known: $O_{2(aq)}$ was estimated at 30% saturation (70 µM) and Cu(I) was assumed to initially exist only in trace quantities (i.e., < 1% of total Cu or 0.1 µM). k_4 will vary depending on how Cu(II) is bound in P/S. A value of 200 M^{-1} s^{-1} was employed based on the known rate constant for the reaction of $O_{2(aq)}$ with the Fe(II)-EDTA complex (147) (that for the Cu(I)-EDTA complex is unknown). k_{O_2} is a constant that describes the rate at which $O_{2(g)}$ from the headspace above the P/S sample dissolves, becoming how $O_{2(aq)}$. It was estimated at 1 x 10^{-10} M/s.

Chemical Reactions

$$AlbSH + Cys\text{-}Cys \underset{k_2}{\overset{k_1}{\rightleftharpoons}} SCysAlb + Cys \quad (1)$$

$$2Cys + O_2 \xrightarrow[k_3]{Cu(II)} Cys\text{-}Cys + H_2O_2 \quad (2)$$

$$\left\{ \begin{array}{l} Cys + Cu(II) \xrightarrow{k_x} 1/2\, Cys\text{-}Cys + Cu(I) \quad (10) \\ \\ Cu(I) + O_2 \xrightarrow{k_4} Cu(II) + O_2^{\cdot -} \quad (11) \end{array} \right\}$$

Rate Equations

$$\frac{d[AlbSH]}{dt} = -k_1[AlbSH][Cys\text{-}Cys] + k_2[SCysAlb][Cys] \quad (5)$$

$$\frac{d[Cys\text{-}Cys]}{dt} = -k_1[AlbSH][Cys\text{-}Cys] + k_2[SCysAlb][Cys] + \frac{k_3[Cu(II)][Cys]}{K_z\left(1 + \frac{K_y}{[Cys]}\right) + [Cys]} \quad (6)$$

$$\frac{d[SCysAlb]}{dt} = k_1[AlbSH][Cys\text{-}Cys] - k_2[SCysAlb][Cys] \quad (7)$$

$$\frac{d[Cys]}{dt} = k_1[AlbSH][Cys\text{-}Cys] - k_2[SCysAlb][Cys] - 2\left(\frac{k_3[Cu(II)][Cys]}{K_z\left(1 + \frac{K_y}{[Cys]}\right) + [Cys]}\right) \quad (8)$$

$$\frac{d[Cu(II)]}{dt} = -2\left(\frac{k_3[Cu(II)][Cys]}{K_z\left(1 + \frac{K_y}{[Cys]}\right) + [Cys]}\right) + k_4[Cu(I)][O_2] \quad (12)$$

$$\frac{d[Cu(I)]}{dt} = 2\left(\frac{k_3[Cu(II)][Cys]}{K_z\left(1 + \frac{K_y}{[Cys]}\right) + [Cys]}\right) - k_4[Cu(I)][O_2] \quad (13)$$

$$\frac{d[O_2]}{dt} = k_{O_2} - k_4[Cu(I)][O_2] \quad (14)$$

Part B) Model predictions (lines), overlaid on actual results (symbols), that take into account best estimates for the additional parameters (reaction components and rate constants) required for an $O_{2(aq)}$–dependent model as described in the preceding paragraph (panels a-b, corresponding to serum and K_2EDTA plasma, respectively). All other parameters in the model exist as described in Fig. 2.5. Additional panels vary the starting concentration of one reaction component or one rate constant at a time (generally -10x or +10x unless physically unreasonable) to evaluate its effect on the model. c-d) Starting $O_{2(aq)}$ = 250 µM (saturation); e-f) Starting $O_{2(aq)}$ = 7 µM; g-h) k_4 = 2,000 M^{-1} s^{-1} ; i-j) k_4 = 20 M^{-1} s^{-1} ; k-l) k_{O_2} = 1 x 10^{-9} M/s; m-n) k_{O_2} = 1 x 10^{-11} M/s (This simulates placing P/S into a nitrogen (low $O_{2(g)}$) atmosphere following initial processing (which permits an modest initial concentration of $O_{2(aq)}$ to develop in the sample—i.e., ~ 70 µM). The trajectory difference between the predicted and observed formation of S-Cys-Alb matches, approximately, the difference between the unfortified plasma sample incubated under N_2 and the one incubated under air in *Fig. 2.7*). Cys-Cys is abbreviated as CSSC in the legends.

a) Serum: Base [$O_{2(aq)}$]-dependent model

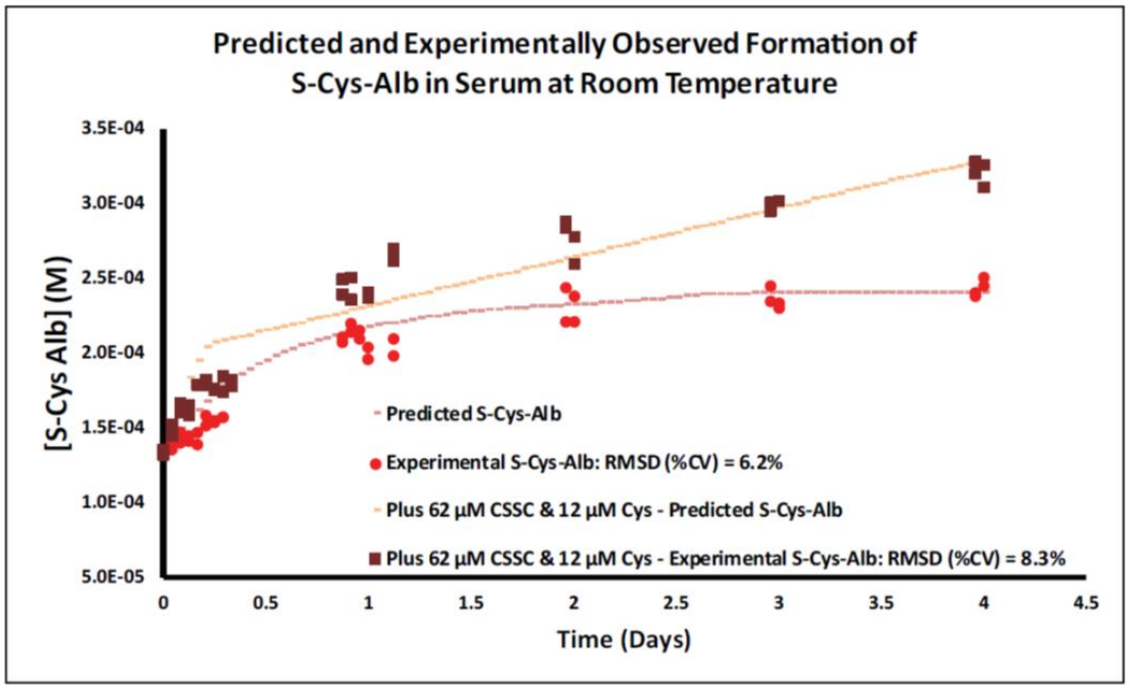

b) Plasma: Base [$O_{2(aq)}$]-dependent model

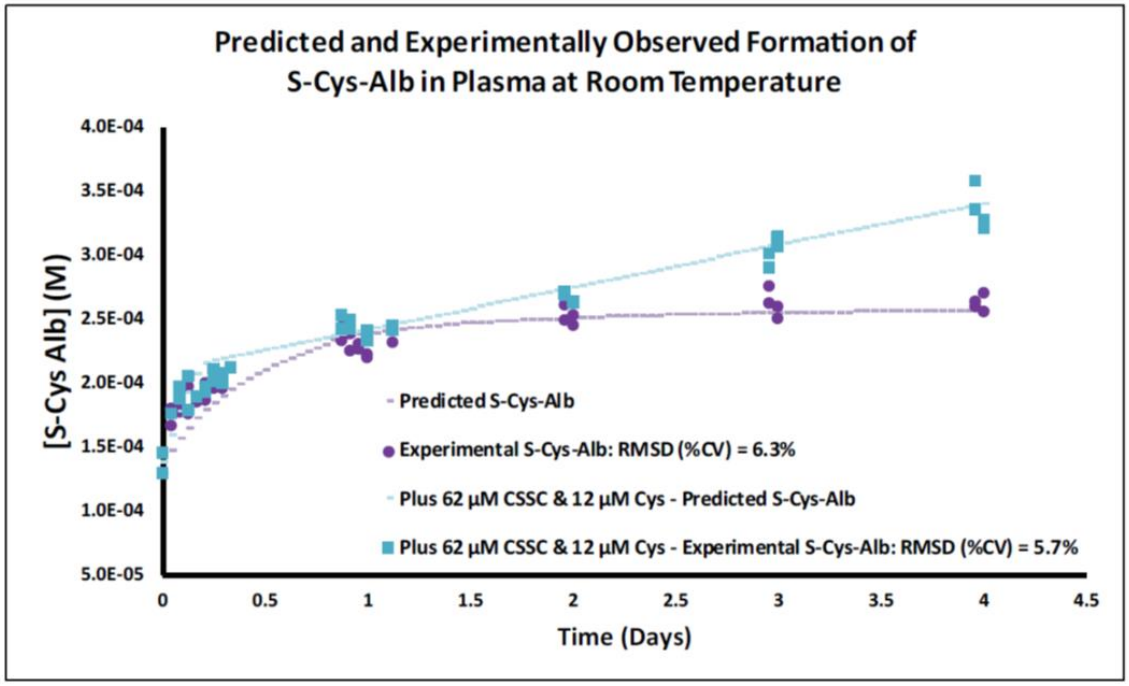

c) Serum: Starting [$O_{2(aq)}$] = 250 µM (saturated)

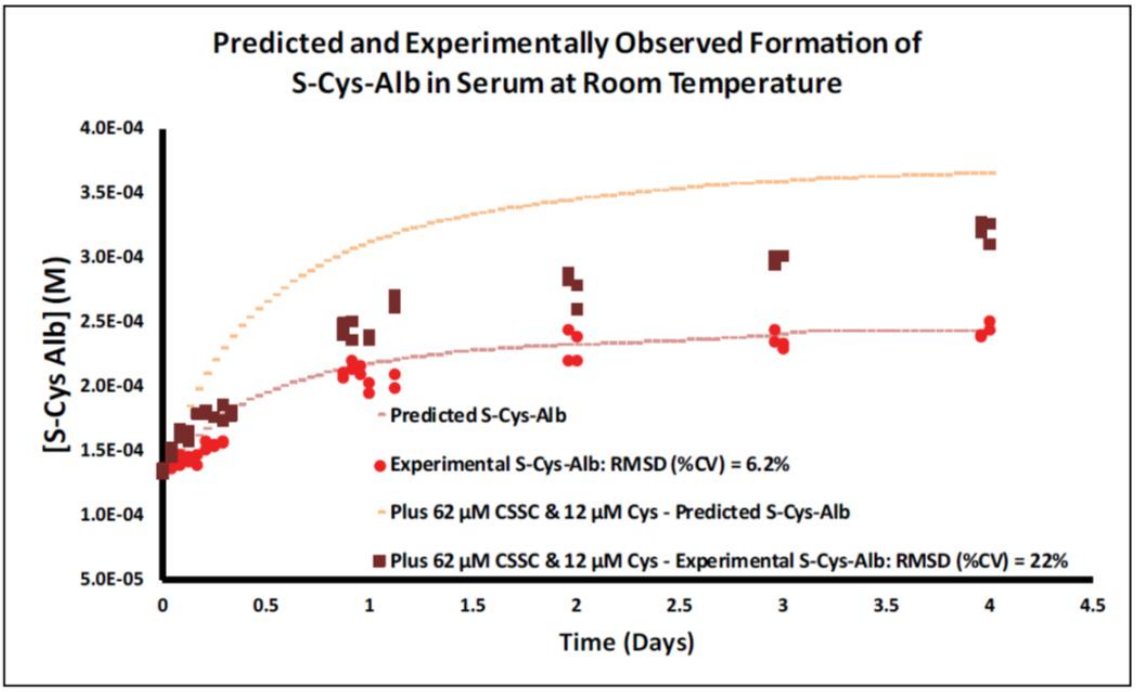

d) Plasma: Starting [$O_{2(aq)}$] = 250 µM (saturated)

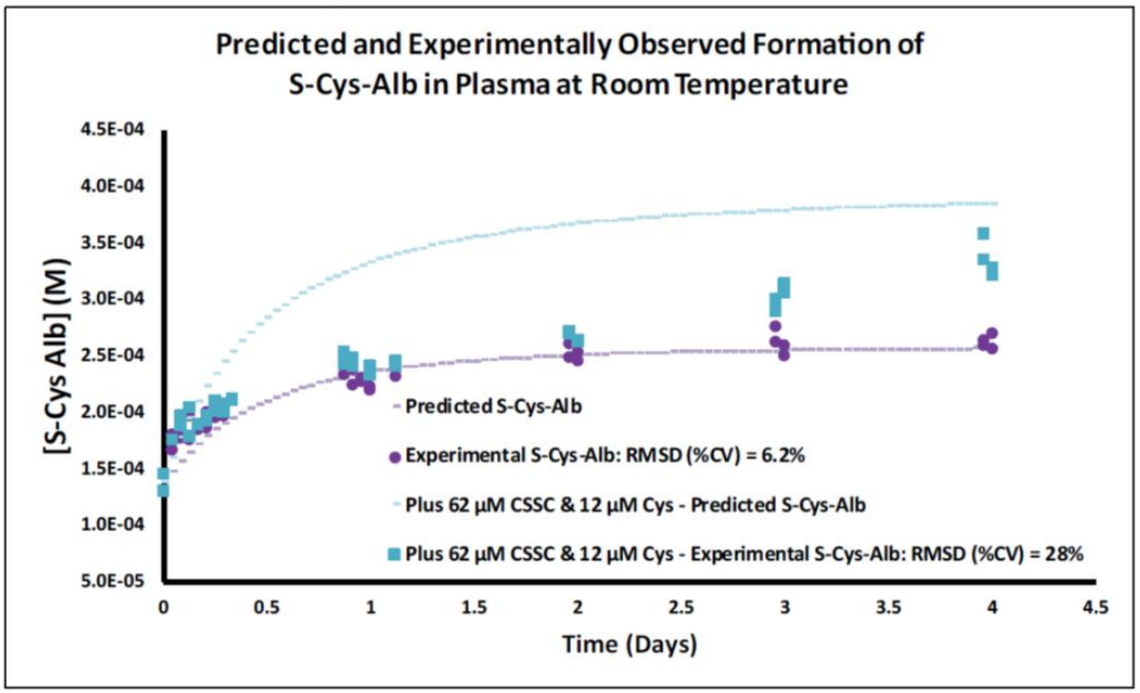

e) Serum: Starting $[O_{2(aq)}] = 7\ \mu M$

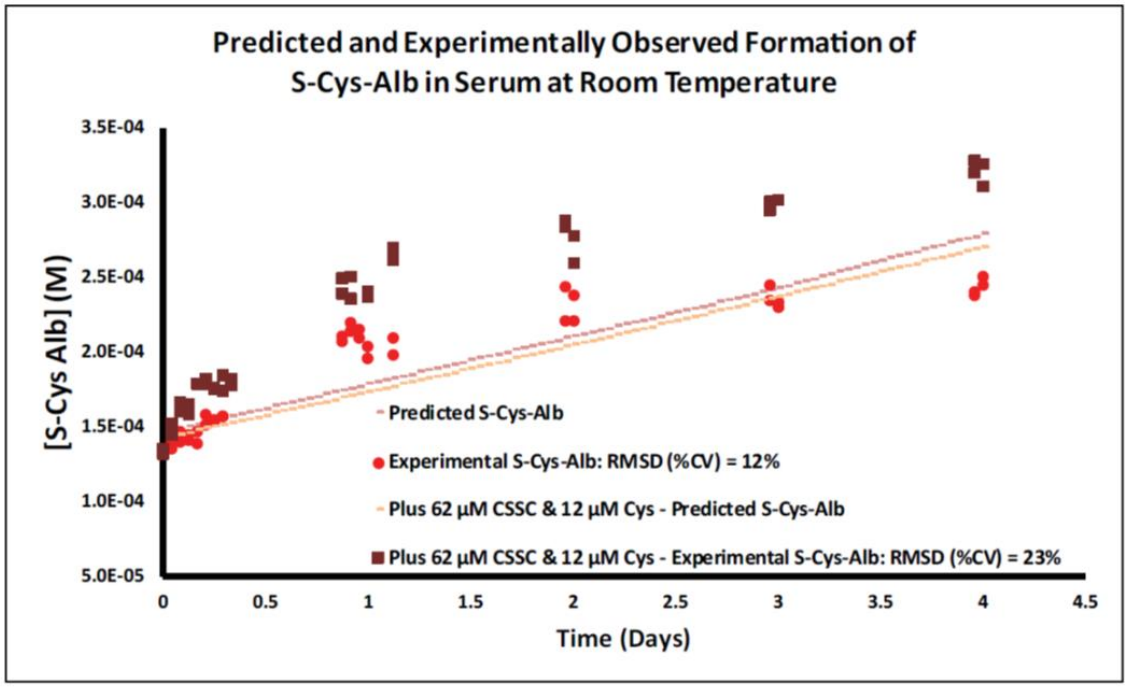

f) Plasma: Starting $[O_{2(aq)}] = 7\ \mu M$

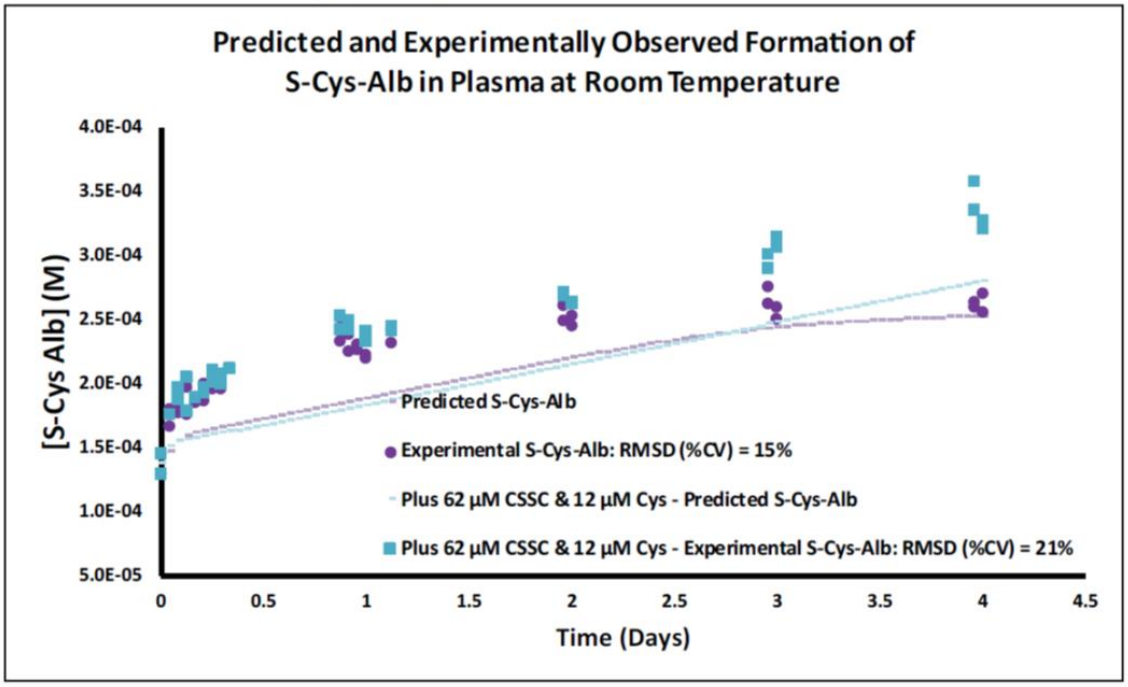

g) Serum: k_4 = 2,000 M^{-1} s^{-1}

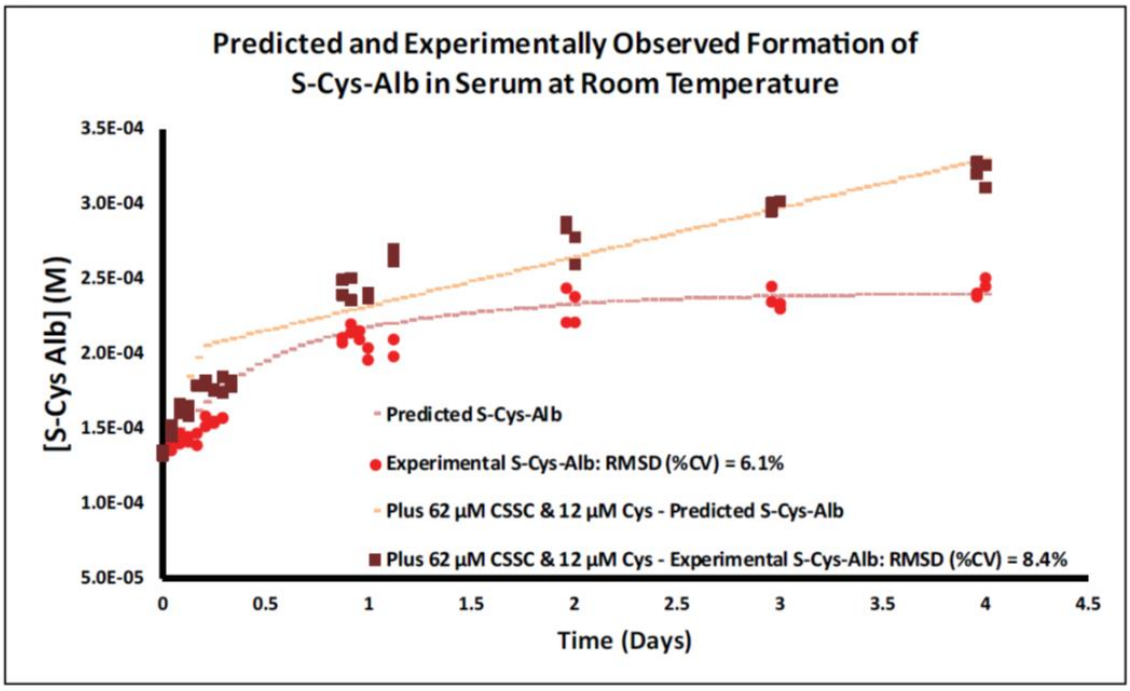

h) Plasma: k_4 = 2,000 M^{-1} s^{-1}

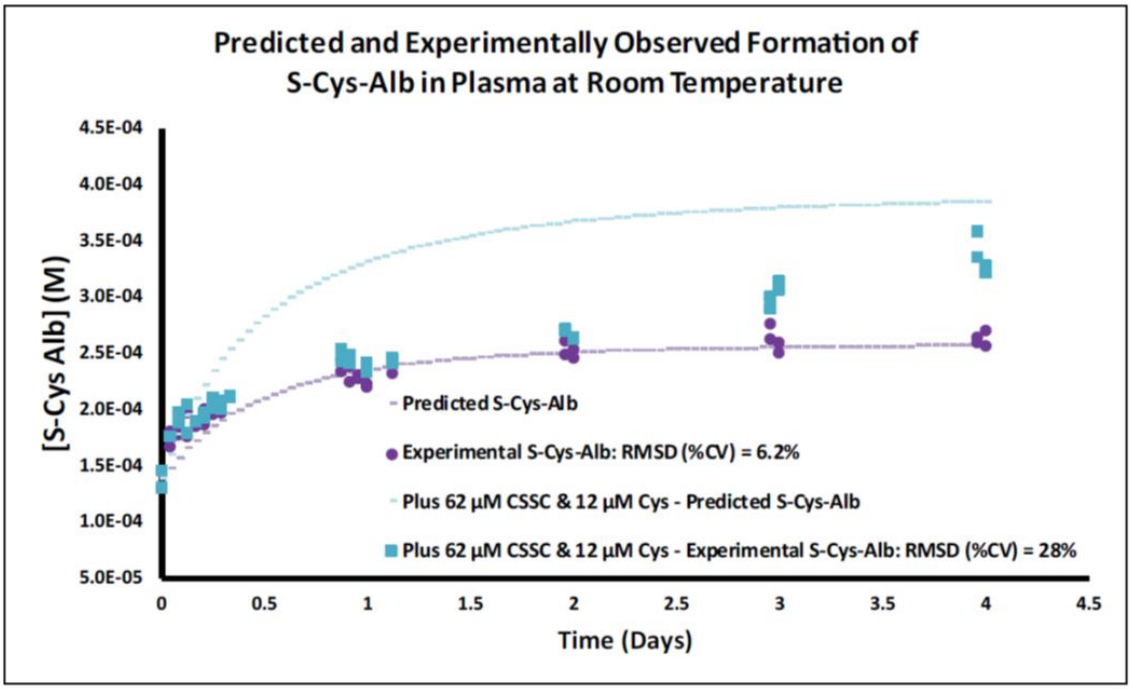

i) Serum: $k_4 = 20\ M^{-1}\ s^{-1}$

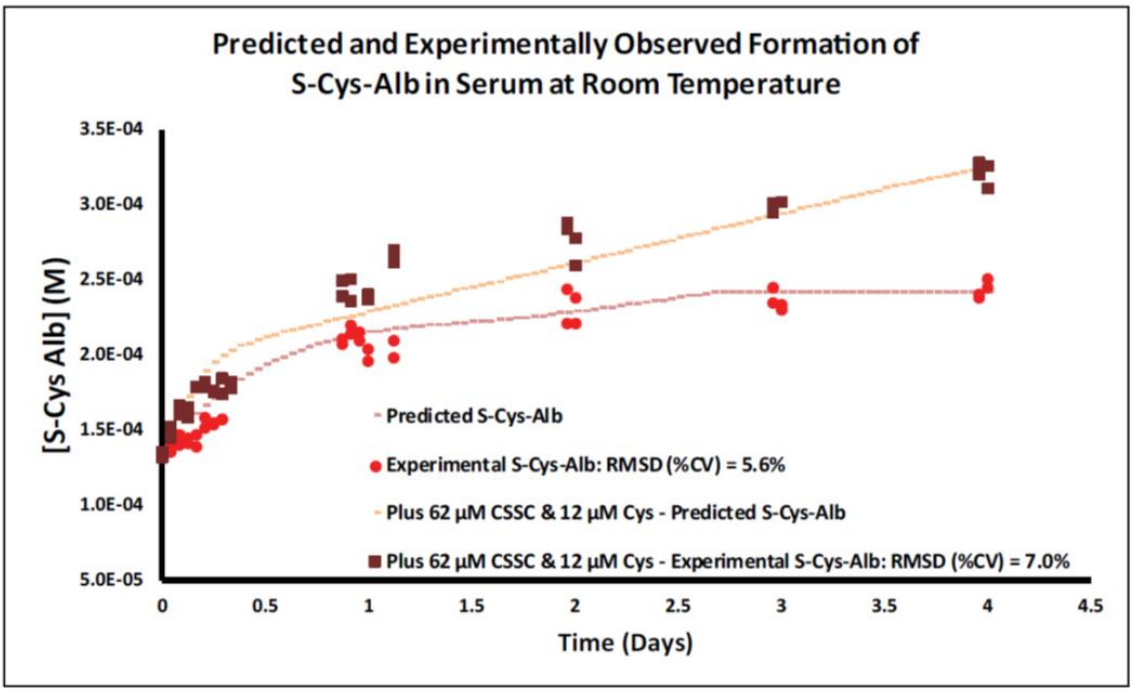

j) Plasma: $k_4 = 20\ M^{-1}\ s^{-1}$

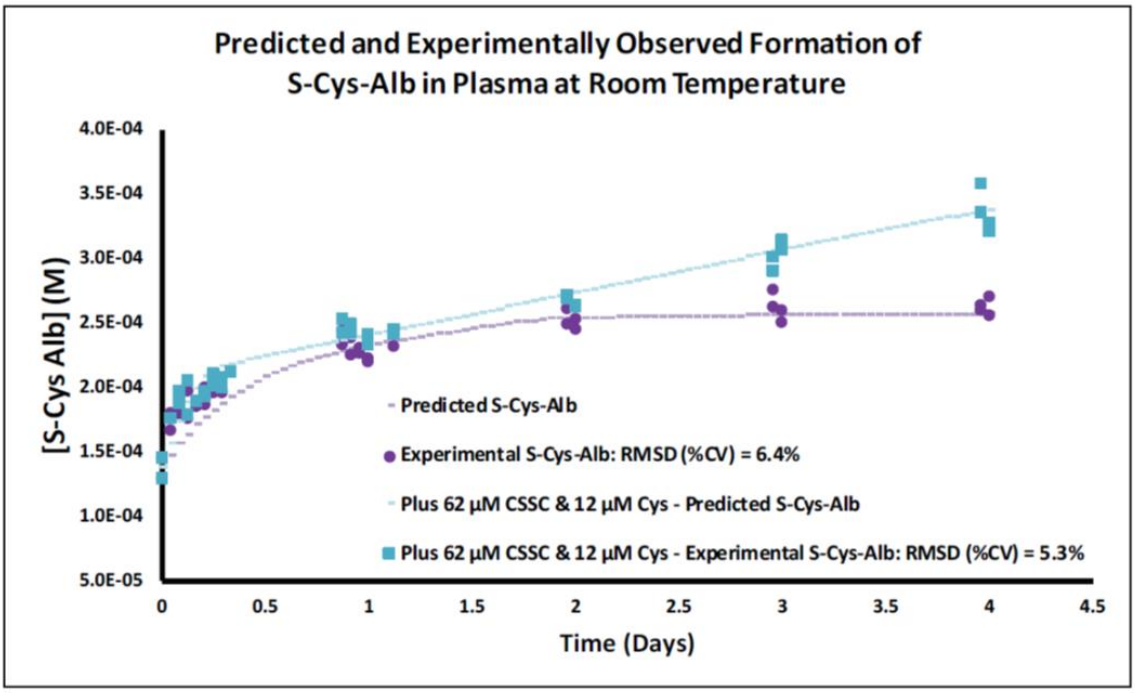

k) Serum: k_{O_2} = 1 x 10^{-9} M/s

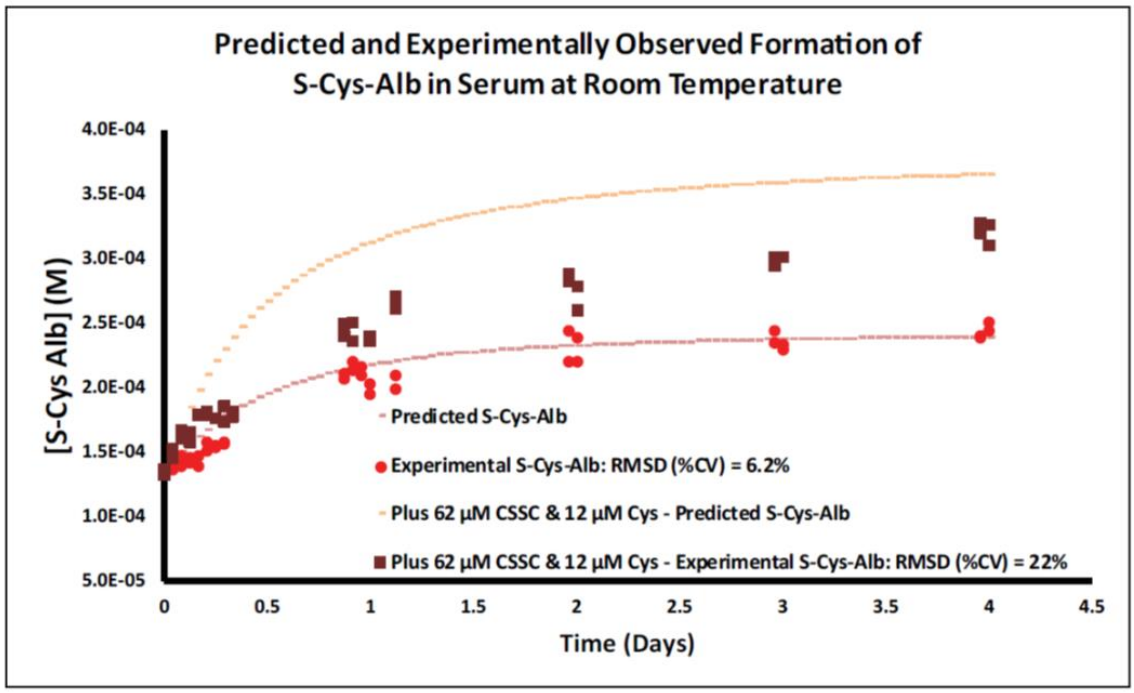

l) Plasma: k_{O_2} = 1 x 10^{-9} M/s

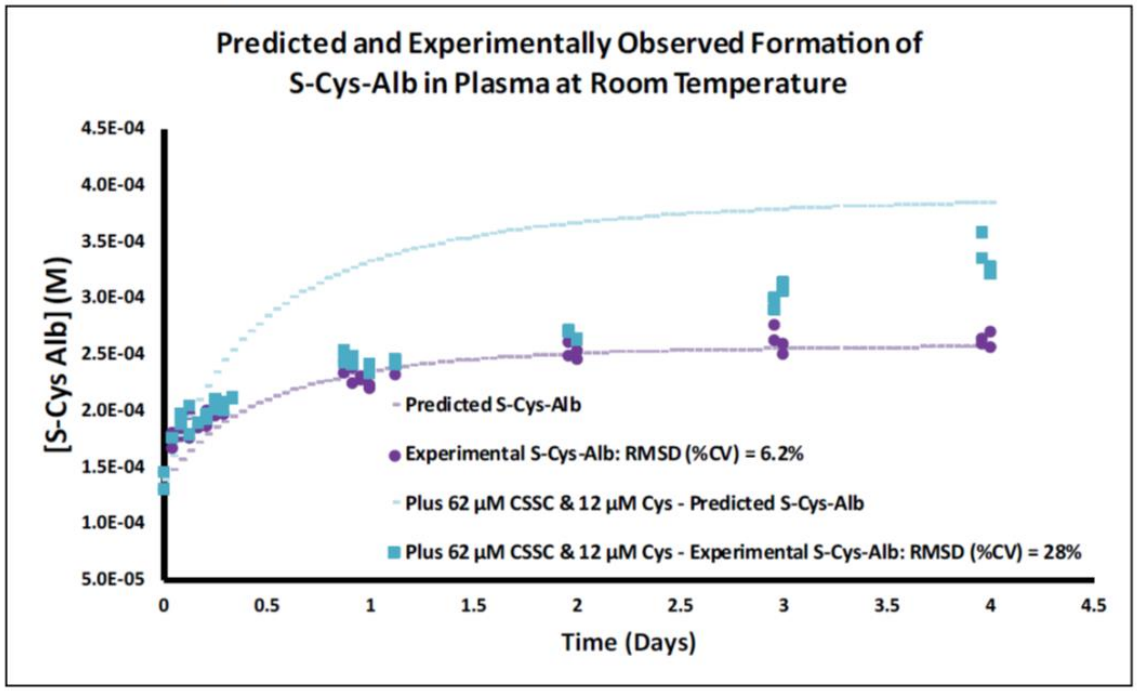

m) Serum: $k_{O_2} = 1 \times 10^{-11}$ M/s

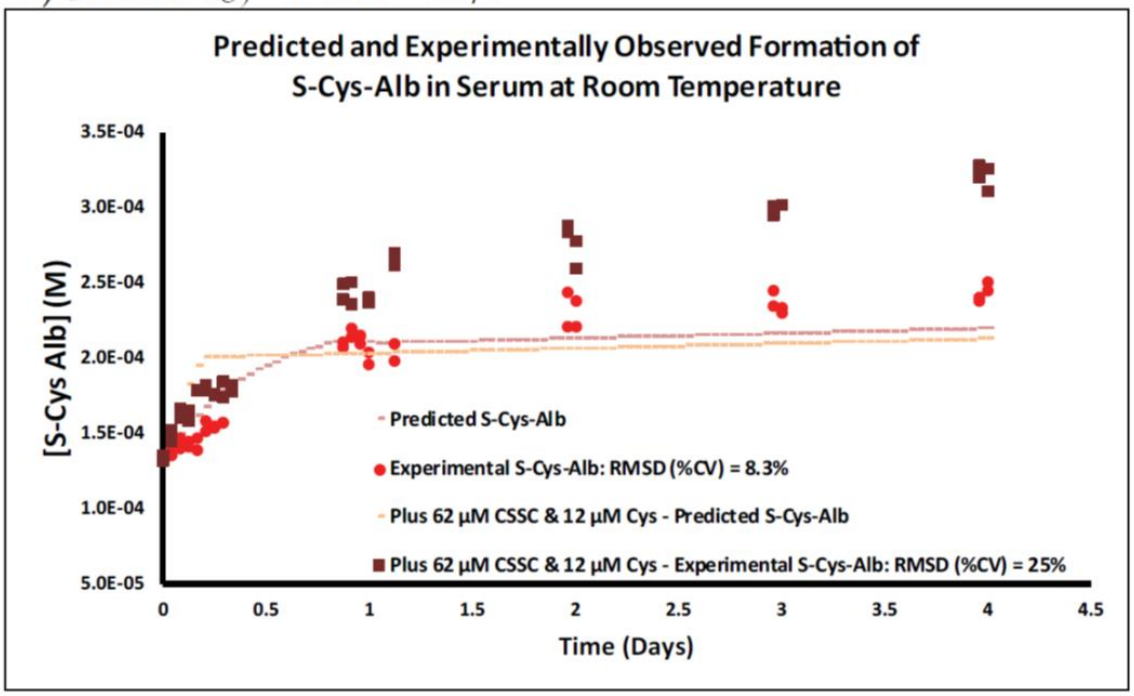

n) Plasma: $k_{O_2} = 1 \times 10^{-11}$ M/s